NUMERICAL STUDIES OF NANOFLUID BOUNDARY LAYER FLOWS USING SPECTRAL METHODS

A THESIS SUBMITTED TO THE UNIVERSITY OF KWAZULU-NATAL
FOR THE DEGREE OF DOCTOR OF PHILOSOPHY
IN THE COLLEGE OF AGRICULTURE, ENGINEERING & SCIENCE

By
Mangwiro Magodora
School of Mathematics, Statistics & Computer Science
August 2021

Contents

Abstract

This thesis is focused on numerical studies of heat and mass transport processes that occur in nanofluid boundary layer flows. We investigate heat and mass transfer mechanisms in the flow of a micropolar nanofluid above a stretching sheet, the squeezed nanofluid flow between two parallel plates and the impact of activation energy and binary chemical reaction on nanofluid flow past a rotating disk. We present an analysis of entropy generation in nanofluid flow past a rotating disk and nanofluid flow past a stretching surface under the influence of an inclined magnetic field. This study aims to numerically determine to a high degree of accuracy, how nanoparticles can be utilized to alter heat and transport properties of base fluids in order to enhance or achieve desirable properties for thermal systems. The heat and mass transfer processes that feature in nanofluid boundary layer flow are described by complex nonlinear transport equations which are difficult to solve. Because of the complex nature of the constitutive equations describing the flow of nanofluids, finding analytic solutions has often proved intractable.

In this study, the model equations are solved using the spectral quasilinearization method. This method is relatively recent and has not been adequately utilized by researchers in solving related problems. The accuracy and reliability of the method are tested through convergence error and residual error analyses. The accuracy is further tested through a comparison of results for limiting cases with those in the literature. The results confirm the spectral quasilinearization method as being accurate, efficient, rapidly convergent and suited for solving boundary value problems. In addition, among other findings, we show that nanofluid concentration enhances heat and mass transfer rates while the magnetic field reduces the velocity distribution. The fluid flows considered in this study have significant applications in science, engineering and technology. The findings will contribute to expanding the existing knowledge on nanofluid flow.

Declaration 1: Plagiarism

I, Mangwiro Magodora, declare that the research reported in this thesis, except where otherwise indicated, is my original research. This thesis has not been submitted for any other degree or examination at this or any other university. This thesis does not contain other persons' writing, pictures, graphs, or other information unless expressly acknowledged as being sourced from those persons. Where other sources have been quoted, the words have been rewritten, while attributing the general information to the authors as referenced, or, where their exact words have been used, then the quotation appears in quotation marks and has been referenced. This thesis does not contain information, graphics or tables copied and pasted from the internet unless specifically acknowledged. The sources are detailed in the thesis and the reference sections.

Signature:.[redacted] 14-03-2022

Mangwiro Magodora Date

Signature:[redacted]. 15-March-2022

Prof. P. Sibanda Date

Declaration 2: Publications

1. **M. Magodora**, H. Mondal, P. Sibanda and, S. Motsa, "Dual solutions of a micropolar nanofluid flow with radiative heat mass transfer over stretching/ shrinking sheet using spectral quasilinearization method". *Multidiscipline modeling in materials and structures*, vol. 16, no. 2, pp. 238-255, 2020.

2. **M. Magodora**, H. Mondal and P. Sibanda, "Effect of Cattaneo-Christov heat flux on radiative hydromagnetic nanofluid flow between parallel plates using spectral quasilinearization method". *Journal of Applied and Computational Mathematics*, 2020.
   DOI: 10.22055/JACM.2020.33298.2195

3. **M. Magodora**, H. Mondal, S. Motsa and P. Sibanda, "Numerical studies on gold-water chemical reacting nanofluid with activation energy past a rotating disk". *International Journal of Applied and Computational Mathematics*, accepted 5 January 2022.

4. **M. Magodora**, H. Mondal, S. Motsa and S. Sibanda, "Effect on entropy generation analysis for heat transfer nanofluid near a rotating disk using quasilinearization method". *Journal of nanofluids*, accepted 7 October 2021.

   In all the above publications, I formulated the flow problems, obtained numerical solutions, analyzed the results and prepared the manuscripts.

Signature: [redacted] 14-03-2022 ....

Mangwiro Magodora Date

This work is dedicated to:

- *my late father, Mr. Jonas Petros Magodora. You were an educationist par excellence. You are fondly remembered,*
- *my mother Mrs. Chemedzai Magodora. You are my pillar of strength and your unconditional love and support is dearly cherished,*
- *my daughters Diana and Jade. Your love, support, patience and understanding makes all the difference. Love you so much.*

Acknowledgements

I give all glory to Almighty God for the opportunity to study for a PhD. I would like to express my heartfelt gratitude to my supervisors Professor Precious Sibanda and Professor Sandile Motsa for their support, guidance, advice, patience, encouragement and inspiration during the course of my studies. Without them my dream of attaining this qualification would not have been realized. Let me also hasten to convey my thanks to my mentor Professor Hiranmoy Mondal who encouraged me consistently in every way possible to soldier on. Also deserving recognition and gratitude are current and former UKZN postgraduate students Dr. Mlamuli Mavuso Dhlamini, Shina D. Oloniiju, Tichaona Mapuwei, Dr. Mohammed Almakki, Munyaradzi Rudziva and Dr. Joseph Masanganise who offered me encouragement and support during the course of my studies. The support of Messrs Michael Magama and Thandolwethu Silongwe from Bindura University of Science Education (Zimbabwe) and National University of Science and Technology (Zimbabwe) respectively, is also greatly appreciated. I also extend my thanks to the administrative staff in the School of Mathematics, Statistics and Computer Science for making my student life comfortable and enjoyable and by assisting in every way possible. The support of my family, relatives and friends is highly regarded and cherished. Last but not least, I would like to extend my gratitude to the DSI-NRF Centre of Excellence for Mathematical and Statistical Sciences (CoE-MaSS) for their generous financial support as well as the research seminars and workshops which they provided in support of my studies. May Good Lord bless you all.

Chapter 1

Introduction

1.1 Background

Fluid dynamics is primarily concerned with the behaviour and structure of fluids in motion. Fluid dynamics finds wide applications in construction engineering, wheezing, ventilation, nuclear power plants, biotechnology, heat exchanger devices, food processing industry and pumps among numerous others [1]. Fluids are intricately connected with and indispensable to all facets of human endevour [2, 3].

This study is concerned with the numerical solution of boundary layer equations that describe the transport of mass and heat in nanofluid flows in a variety of geometrical settings. The boundary layer theory was first presented in 1904 by Prandtl [4]. Since then, numerous studies have been conducted on boundary layers and this has led to many inventions and improvements in the design and manufacture of marine vessels, space shuttles, sports cars, buildings, dams, biotechnology, aeroplanes, etc [5]. The geometries of interest for this study include a stretching sheet, a rotating disk and flow between parallel plates. The problems are solved utilizing the spectral quasilinearization technique.

In recent years, a heightened research interest has been directed towards an emerging and innovative category of fluids termed nanofluids. The reason for this interest could be explained by the fact that nanofluids significantly alter the thermal conductivity, electrical conductivity and viscosity of base fluids [6, 7]. Apart from enhancing the thermo-physical properties of base fluids, nanoparticles have also found widespread application in other areas. For instance, silver nanoparticles have been used in wound treatment [8] while gold nanoparticles are utilized in water treatment [9].

1.2 Newtonian versus non-Newtonian fluids

Fluids can be classified as being either Newtonian or non-Newtonian. The former comprises fluids that obey Newton's law of viscosity, namely that the shear stress is directly proportional to the strain rate. In mathematical terms, this is written as $\tau = \mu(du/dy)$ where τ, μ and du/dy denote the shear stress, viscosity and the rate of strain, respectively. Fluids that do not conform to Newton's law are termed non-Newtonian fluids [10]. A viscoelastic fluid, which belongs to the category of non-Newtonian fluids, will deform after a certain threshold stress is reached. However, upon removing the stress, the stresses inside the fluid will not vanish instantaneously. This flow behaviour is attributable to the intermolecular forces that continue to hold for some time after the withdrawal of stress. This period of maintained molecular configuration after the removal of stress is referred to as the relaxation time [11].

Another notable distinction between Newtonian and non-Newtonian fluids is the Weissenberg effect as described by Morrison [12]. When a Newtonian fluid is spun at high speed in a bowl, the fluid is flung away from the blades towards the walls as a consequence of Newton's first law. In stark contrast, a non-Newtonian fluid such as a dough of flour climbs the mixing blades. This is the Weissenberg effect and is due to the elasticity of the viscous fluid [13, 14]. Non-Newtonian fluids can also be classified into various sub-classes, namely pseudo-plastics, bingham plastics, dilatants, thixotropic, elastic, rheopectic, viscoelastic, shear-thinning or shear-thickening fluids [15].

The Navier-Stokes equations cannot adequately describe the flow of many non-Newtonian fluids [16]. Furthermore, no single constitutive model effectively describes the flow dynamics of all non-Newtonian fluids and as a consequence, there is a variety of models with different rheological properties that have been proposed in the literature. Examples of such non-Newtonian fluids include the Carreau-Yasuda, Ellis, Maxwell, Oldroyd-B, Powell Eyring, Williamson, Carreau, Jeffrey, Casson, couple stress and micropolar models [17].

In this study we investigate the flow and behaviour of both non-Newtonian and Newtonian fluids. Studying the flow and behaviour of non-Newtonian fluids is important, for instance, in order to understand problems that may arise in the operation of machinery. For example, the Weissenberg effect would need to be taken into account in the operation and design of food processing and other industrial equipment. Correct rheological constitutive equations that describe the fluid flow are important in predicting non-Newtonian fluids behaviours to reduce damage to equipment, loss of resources and energy. In manufacturing, the quality of the end product is dependent on the thermal energy transfer rate, hence the study of fluid flow is vital for the manufacturing and engineering processes.

1.3 Mechanisms for Heat and Mass Transport

The transport of heat and mass transfer usually occurs simultaneously in engineering and industrial processes [18]. Heat and mass transport are concerned with the rates of transfer of thermal energy and mass which occur naturally in the environment and in diverse applications in engineering ranging from the cooling of electronic devices, food processing, refrigeration and so on [19, 20].

1.3.1 Heat transfer

If a temperature gradient exists in a system, some thermal energy will transfer from a hotter region to the cooler region [21]. The transfer of heat occurs through convection, conduction and radiation. A firm understanding of heat transport processes is vital in the operation as well as the design of thermal systems. Poor management of heat and heat transfer may result in thermal runaways that could lead to accidents and energy losses through entropy generation and inefficiency [22, 23].

The transport of heat through molecular interaction is called conduction [24]. Conduction may take place in gases, solids and liquids. However, transport of heat by conduction occurs predominantly in solids due to vibrations of constituent molecules coupled with energy transfer by free electrons.

In stationary fluids, conduction is due to the collision of molecules at higher temperatures with those at lower temperatures during random motion [25]. Fourier's law models the transfer of heat by conduction and is expressed in one-dimension as

$$q''_x = -k\frac{dT}{dx} \tag{1.1}$$

where q''_x is the heat flux (Wm^{-2}) in the x-direction, k the thermal conductivity $(Wm^{-1}K^{-1})$ and dT/dx denotes the temperature gradient in the x-direction [1]. Thermal conductivity measures the ability of a material to transport heat by conduction [19]. Metals possess higher thermal conductivity than non-metals, hence they are often used as nanoparticles to enhance the thermal conductivity of base fluids.

Thermal diffusivity is a property that is closely related to thermal conductivity and is defined mathematically as $\alpha = k/\rho c_p$ where ρ is the fluid density, k thermal conductivity while c_p denotes the heat capacity of the material. The thermal diffusivity measures how fast heat diffuses through a substance or material.

The heat transfer between a fluid and a solid surface is predominantly through convection. Convection is a result of a combination of random molecular motion the bulk fluid motion also known as advection [20]. For a fluid flow over a bounding surface, the heat transfer by convection is represented by Newton's law of cooling

$$q'' = h(T_s - T_\infty) \tag{1.2}$$

where q'' denotes the convective heat flux (Wm^{-2}), h is the coefficient of convective heat transfer $(Wm^{-2}K^{-1})$, T_∞ and T_s are the ambient and surface temperatures respectively.

Convection in a fluid can be classified as forced, natural or mixed. Forced convection is defined as energy transfer that is induced by an external agent such as a blower, pump or fan. In natural convection, energy transport is induced by buoyancy forces due to non-uniform density distribution as a result of fluid temperature differences [26]. Mixed convection occurs if both forced and free convection are present.

Energy transfer may also occur through radiation. Radiation refers to the thermal energy released by objects as electromagnetic waves as a consequence of their temperature. Radiation does not require the presence of an intervening medium to transfer heat [19] and can take place in a vacuum.

For a surface that is at a temperature T_s and has surface area A_s, the maximum radiation that is emitted by the surface is given by

$$\dot{Q} = \sigma A_s T_s^4 \tag{1.3}$$

where $\sigma = 5.670 \times 10^{-8}$ is the Stefan-Boltzmann constant. Equation (1.3) is referred to as the Stefan-Boltzmann law [20]. For real surfaces, the radiation transfer rate is represented by

$$\dot{Q} = \varepsilon \sigma A_s T_s^4 \tag{1.4}$$

where ε is the emissivity of the surface and $0 \leq \varepsilon \leq 1$.

Thermal radiation finds significant applications in industry and engineering processes that occur at elevated temperatures such as in solar power technology, astrophysical flows, combustion engines, gas turbines, space vehicles and missile launches [27, 28]. In addition to knowledge of convective processes in fluids, knowledge of thermal radiation is crucial in the design of thermal equipment and advanced energy conversion systems as this greatly assists in the production of goods with superior and desirable characteristics [28].

In order to control the rate of cooling and achieve an output of a desired quality, a magnetic field is often added to the flow configuration of an electrically conductive nanofluid [28]. Such a flow is termed hydromagnetic or magnetohydrodynamic (MHD) flow and has applications in industry and engineering which include annealing of copper wires, metal extrusion, polymer extrusion, hot rolling, etc [28, 29]. In this thesis we consider the magnetic field influence and significance on nanofluid flows in Chapters 3 and 5.

1.3.2 Mass transfer

Mass transfer occurs when the density of a substance in a system is non-homogeneous. This implies that when concentration gradients are present, momentum exchanges and diffusion processes occur from regions of higher concentration to regions of lower concentration.

For a chemical species in a stationary medium, the rate of the mass diffusion $\dot{m}$ is proportional to the concentration gradient dC/dx. This relationship is modelled by Fick's law

$$\dot{m} = -D_m A \frac{dC}{dx} \tag{1.5}$$

where A is the surface area through which the mass transfer takes place, C is the solute concentration and D_m is the mass diffusivity of the chemical species [19].

Mass transfer occurs in many physical processes where convective and diffusive transport of chemical species are present [18]. Mass transport finds application in separation engineering, chemical engineering and sub-disciplines such as ceramic engineering, materials engineering, petroleum engineering, process engineering etc [26]. Equation (1.5) is used in the conservation of mass equations in Chapters 2-4.

1.4 Boundary layer flow

The boundary layer concept was proposed in 1904 by Ludwig Prandtl [30], who is the father of boundary layer theory and aerodynamics [31] . A boundary layer is a thin fluid layer adjacent to a solid surface [32]. The fluid on the surface has zero velocity or moves with the same velocity as the surface and this condition is known as the no-slip condition. The velocity rapidly changes in the free stream far from the surface [33].

Boundary layer theory has wide industrial and engineering applications such as in aeronautics, meteorology, space missions, power generation, high-speed flight, bridge construction, bio-medicine, turbomachinery, cooling of thermal systems, vehicle design and so on [32, 34]. Knowledge of boundary layer theory is important to scientists and engineers as it enhances the understanding of key fluid dynamic processes.

In this study we investigate the flow of nanofluids past stretching sheets, squeezing plates and rotating disk surfaces. Kameswaran et al. [35] studied the flow of nanofluid over a shrinking or stretching sheet with viscous dissipation and a chemical reaction. Their results showed that a magnetic field had the effect of lowering the mass and heat transfer rates. The influence of viscous dissipation on nanofluid flow above a stretched or shrunk sheet was reported by Dero et al. [36]. Their findings indicated that increases in the Biot number, Eckert number, thermo-diffusion parameters caused a rise in the rate of heat transfer. The Biot number is the ratio of the heat conduction resistance inside a body to the external heat convection resistance at the surface of the body [37]. A small value of the Biot number indicates low resistance to heat transfer by conduction whereas a high value implies the dominance of heat convection over heat conduction. The Eckert number is a measure of the effect of a fluid's self-heating due to viscous dissipation [38]. Further studies on nanofluid flows over shrunk or stretched sheets are available in the references [39–43] and so on.

The study of viscous fluid flows emanating from two squeezed parallel plates was pioneered by Stefan [44]. Since then, extensive research has been directed at parallel plates due to their significant industrial and engineering applications [45]. Ullah et al. [46] examined MHD squeezing flow of nanofluids with a chemical reaction and heat radiation. They observed that increasing radiation and the Brownian motion parameters elevated the temperature. Brownian motion is the random movement of particles that occur in liquids and gases [47]. Further studies focusing on the flow between squeezing parallel plates are available in the references [48–55]

The study of flow over a rotating disk was pioneered by Von Kármán [56] who introduced the von Kármán transformations that convert the associated constitutive equations from partial to ordinary differential equations. Due to industrial and engineering use of such flows [57], many investigators have shown keen interest in studying rotating disk flows. Among these studies, Hayat et al. [58] presented a study of nanofluid flow past a rotational disk with heterogeneous-homogeneous reactions and variable thickness while Awais et al. [59] analyzed the flow of a nanofluid past a spinning disk with a heat source/sink. More research on nanofluid flow over rotating disks can be found in the references [60–63] among many others.

1.5 Studies of Nanofluids

The term nanofluid was first introduced by Choi and Eastman in 1995 [64–66]. Nanofluids are made from metals, metal oxides, carbides or non-metals [67]. The research on nanofluids is important due to their diverse and significant applications in engineering, thermal and industrial processes. The use of nanofluids is prevalent in cooling systems, drug delivery, nuclear reactors, wire rolling, radiators etc [68–74].

Nanoparticles are used as a strategy to enhance the performance of regular fluids such as ethylene glycol, water and oil [75]. Nanoparticles alter the viscosities and diffusivities of base fluids because of the ultrafine nanosolids with increased surface area [66]. The specific heat capacities of nanoliquids are generally higher than that of base fluids.

Numerous nanofluid models have been reported in the literature [76, 77]. In this study, we consider the models proposed by Buongiorno [78] and Tiwari and Das [79] respectively. The Buongiorno model assumes that for nanofluids, convective heat transfer is predominantly caused by Brownian motion and thermophoresis [80]. The Tiwari and Das model is a single-phase model in which the suspended nanoparticles and the liquid phase are in thermal equilibrium with the same velocity [79]. The former model has been used by several researchers that include [80–83] while the latter model has been used by researchers such as [84–88].

The conductivity and viscosity of nanofluids depend on the concentration as well as the particle size, shape and the properties of nanosolids and base fluids [89]. The thermal conductivity of nanofluids tends to increase while viscosity reduces as the size of the nanoparticles increases [7, 90]. Minakov et al. [89] also showed that a Newtonian nanofluid transitions from Newtonian behaviour to non-Newtonian behaviour on raising the nanoparticle volume fraction and reducing the nanoparticle size.

The flow of nanofluids is an expanding research area with numerous questions that remain to be answered. These questions range from the efficacy of nanofluids as well as the environmental impact and long term sustainability of associated technologies. In this study, we considered both non-Newtonian and Newtonian nanofluids. The major distinction between the two is that the former consists of a non-Newtonian fluid as the base fluid while the latter has a base fluid that is Newtonian. This study seeks to gain more insight into heat and mass transfer processes in industrial and engineering systems that involve nanofluid flows.

1.6 Methods of solution

The methods used in solving the complex nonlinear transport equations for nanofluid flow can be classified as analytic, semi-analytic or numerical methods. The advantages of analytic methods include that closed form solutions give an instant insight of the problem and that they are less costly in terms of time and computational resources. The pitfalls of using analytic methods are that for highly nonlinear systems that occur in engineering and science, such methods may be cumbersome, difficult to use and possess slow rates of convergence [91, 92].

In order to mitigate the disadvantages of using analytic methods, semi-analytic methods have been developed over the years. Examples of semi-analytic methods that have been used in recent years include the homotopy perturbation method, Adomian decomposition method, differential transformation method and the variational iteration method [93, 94]. The Adomian decomposition method was used by Turkilmazoglu [95] in his 2018 study on heat transfer through extended surfaces while implemented the variational iteration method in their 2016 investigation of squeezing nanofluid flow in a rotating channel [96]. In 2017, Eldabe and Abou-Zeid [97] used the homotopy pertubation method to study hydromagnetic nanofluid flow through a non-Darcy porous medium. The differential transform method was used by Usman et al [98] to study nanofluid heat transfer.

Due to the complexities that emanate from their highly nonlinear nature, model equations for nanofluid flows are difficult to solve explicitly [99]. To address this, several numerical algorithms have been developed to obtain approximate solutions. As shown by Motsa [100], numerical methods play a pivotal role in finding solutions to highly nonlinear transport equations for fluid flow. Examples of numerical methods that have been used to solve fluid flow problems include the finite element, the Keller-box, finite difference, Runge-Kutta, linearization, spectral and element free Galerkin methods among many others. Numerical methods, however, have their weaknesses such as difficulties in handling singularities, convergence and stability issues [101]. The finite difference method, though a simple and well established numerical method, yields low accuracy for few grid points. The accuracy improves with increased number of grid points, which has cost implications in terms of resources and time. In addition, it becomes increasingly difficult to use the finite differences method to solve problems that involve complex geometries [102].

The finite element method divides the domain into smaller sub-domains termed elements. The finite element method is easy to use and works well for complex geometries. It captures the local effects and gives sparse matrices which are easier to solve, leading to reduced cost [103]. Some drawbacks of the finite element method include difficulties in handling singularities and the existence of some inherent errors that could be fatal [104].

Spectral methods provide a way of discretizing differential equations based on Chebyshev or Fourier series that provide low approximation errors [26, 105]. The error of approximation is of order $O(1/N^r)$, where r relates to the number of continuous derivatives and N refers to the truncation [106]. The principal objective of using the spectral method is to approximate a function as an expansion of some basis functions [107].

Spectral methods have become popular in recent years due to many advantages when compared and contrasted with other numerical schemes such as the finite difference, Runge-Kutta and finite element methods. Spectral methods are easy to use, possess high accuracy and are also less expensive to use as they require fewer grid points in comparison with established numerical methods such as the finite element method and the finite difference method [106]. A notable feature of the spectral methods is spectral accuracy where an increased number of grid points is associated with an exponential increase in accuracy. In contrast, for the finite difference method, doubling the number of grid points only leads to reduction of truncation error by a factor of four [105, 107]. In recent years several investigators have applied spectral methods coupled with other techniques such as in the spectral local linearization method [101], bivariate spectral relaxation method [26], bivariate spectral quasilinearization method [106], spectral relaxation method [16], etc.

In order to benefit from the strengths of spectral methods and to mitigate the weaknesses of other common methods such as the finite difference method, researchers have combined spectral methods with other methods. Oyelakin et al. [108] utilized a combination of the implicit finite difference and spectral quasilinearization methods to analyze unsteady nanofluid flow in a porous medium. Kefayat [109] utilized the finite difference lattice Boltzmann method (FDLBM) in which finite difference and lattice Boltzmann methods were combined to solve the equations for entropy generation in non-Newtonian nanofluids. Dehghan and Fakhar-Izadi [110] and Javidi [111] combined the fourth-order Runge-Kutta method with the Chebyshev spectral collocation to solve the Fitzhugh-Nagumo and the Burgers-Huxley equations.

In this study, the spectral quasilinearization method is used to solve the equations that model various nanofluid flows in various geometries. The spectral quasilinearization method is recent and possesses desirable attributes such as robustness and fast convergence to a solution in only a few iterations [28, 112].

1.6.1 The Chebyshev collocation method

In using the spectral collocation, we search for an approximate solution $U^*(x)$ that satisfies the differential equation

$$L[u(x)] = f(x),\ B_a[u(a)] = \tau_a,\ B_b[u(b)] = \tau_b, \tag{1.6}$$

where $L,\ B_a, B_b$ are differential operators, $\tau_a,\ \tau_b$ are real constants and $x \in (a,b)$. In the collocation technique, the differential equations are satisfied at certain discrete points termed collocation or nodal points.

The Chebyshev spectral collocation method can be summarized as follows:

Let $x_0, x_1, \cdots, x_N$ be $N+1$ collocation points. We find an approximate solution $U^*(x)$ such that

$$L[U^*(x_j)] = f(x_j),\ B_a[U^*(x_0)] = \tau_a,\ B_b[U^*(x_N)] = \tau_b,\ j = 1,2,\cdots N-1,\ \text{and } x_j \in (a,b). \tag{1.7}$$

Examples of collocation points are Gauss-Chebyshev, Gauss-Radau and Gauss-Lobatto collocation points which are respectively defined as

$$x_j = \cos\frac{[2j+1]\pi}{2N+2},\ x_j = \cos\frac{2j\pi}{2N+1},\ x_j = \cos\frac{j\pi}{N} \text{ for } j = 1,2,\cdots N. \tag{1.8}$$

In Chebyshev collocation, the differential equation (1.6) requires that the derivatives are determined at the collocation points. As shown by Canuto et al. [105] and Trefethen [113] , the first derivative is written as

$$\left(\frac{du}{dx}\right)_{j,m} = \sum_{i=0}^{N} D_{m,i} u_{j,i} \tag{1.9}$$

where $D_{m,i}$ represents entries of the Chebyshev collocation differential matrix $\mathbf{D}$ defined by

$$D_{m,i} = \begin{cases} \frac{c_m(-1)^{m+1}}{c_i(x_m - x_i)}, & m \neq i, \text{ and } m,i = 0,1,\cdots,N \\ -\frac{x_i}{2(1-x_i^2)}, & 1 \leq m = i \leq N-1 \\ \frac{2N^2+1}{6}, & m = i = 0 \\ -\frac{2N^2+1}{6}, & m = i = N \end{cases}$$

where

$$c_m = \begin{cases} 2, & m = 0,N \\ 1, & -1 \leq j \leq N-1. \end{cases}$$

In matrix form, the first, second and third derivatives can therefore be written as

$$\begin{bmatrix} \frac{\partial u_0}{\partial x} \\ \frac{\partial u_1}{\partial x} \\ \vdots \\ \frac{\partial u_N}{\partial x} \end{bmatrix} = \mathbf{D} \begin{bmatrix} u_0 \\ u_1 \\ \vdots \\ u_N \end{bmatrix},\ \begin{bmatrix} \frac{\partial^2 u_0}{\partial x} \\ \frac{\partial^2 u_1}{\partial x} \\ \vdots \\ \frac{\partial^2 u_N}{\partial x} \end{bmatrix} = \mathbf{D}^2 \begin{bmatrix} u_0 \\ u_1 \\ \vdots \\ u_N \end{bmatrix},\ \begin{bmatrix} \frac{\partial^3 u_0}{\partial x} \\ \frac{\partial^3 u_1}{\partial x} \\ \vdots \\ \frac{\partial^3 u_N}{\partial x} \end{bmatrix} = \mathbf{D}^3 \begin{bmatrix} u_0 \\ u_1 \\ \vdots \\ u_N \end{bmatrix}$$

where $\mathbf{D}^2$ and $\mathbf{D}^3$ are evaluated by squaring and cubing $\mathbf{D}$ respectively. Higher orders can be defined similarly. Further details of the Chebyshev differential matrices can be found in [105] and [113].

1.6.2 The spectral quasilinearization method

The quasilinearization method is a Newton-based method where nonlinear terms are first linearized by employing Taylor series expansions. The method works on the assumption that differences between successive iterations is negligibly small. The spectral quasilinearization method is a combination of linear approximation techniques coupled with the advanced capabilities of the computer. Detailed descriptions of the method can be found in the reference [101].

The attributes of rapid convergence and elevated levels of accuracy have led a number of researchers to use spectral quasilinearization as the method of choice in recent studies. RamReddy et al. [114] used the spectral quasilinearization method in their investigation of heterogeneous-homogeneous chemical reactions on convective flow of micropolar fluid while Pal et al. [115] utilized the same numerical technique in their analysis of entropy generation on flow of Jeffery nanofluid above a stretchable sheet. Further works which utilize the quasilinearization method, include but are not limited to [116–121].

1.7 Problem statement

Real fluids, be they Newtonian and Non-Newtonian, possess highly nonlinear and complex partial differential equations that describe their flow behaviour. It is often difficult to solve the constitutive equations analytically. Numerical methods play a pivotal role in resolving such impediments. However, some numerical methods have limitations such as instability of solutions and slow rate of convergence. Furthermore, some numerical methods are resource-intensive which culminates in high cost in terms of computer memory and time.

The diverse range of constitutive models describing non-Newtonian fluid flows and the challenges emanating from their highly nonlinear nature, implies that there is a great need to develop accurate numerical algorithms to solve the flow equations. However, the drawbacks associated with numerical methods imply that there is a need for researchers to develop numerical methods that are accurate, computationally efficient, less costly, rapidly convergent, robust and stable. This will ensure the accurate and efficient depiction of the boundary layer flow dynamics for nanofluids.

The main aim of this study is to investigate nanofluid boundary layer flows over different geometries that are subject to diverse boundary conditions, and to test the efficacy of spectral methods in solving the flow models.

The specific objectives are:

- to formulate model equations for nanofluid flow over various surfaces or geometries and to compute solutions of the model equations numerically using the spectral quasilinearization method,
- to test the validity and accuracy of the method by comparison of results with limiting cases in the literature and through convergence and residual error analysis and to establish the impact of certain parameters on nanofluid flows.

The remaining portion of this thesis is structured as follows: in Chapter 2 we investigate the flow of a micropolar nanofluid above a stretchable surface with thermo-diffusion and radiation. The impact of radiation on nanofluid flow is further studied in Chapter 3 where the squeezed nanofluid flow between parallel plates is considered. The Cattaneo-Christov heat flux model is adopted in the study, instead of the conventional Fourier's law of heat conduction. The effects of a homogeneous chemical reaction and thermal radiation are analysed and presented. Chapters 4 and 5 deal with nanofluid flow over rotating disks. In Chapter 4 we investigate the rotational disk flow of nanofluids where the effects of chemical reaction and activation energy are discussed. In Chapter 5 we study the steady nanofluid flow over a spinning disk with suction and prescribed heat flux. The measure of disorder or irreversibility referred to as entropy, is presented. The thesis concludes with Chapter 6 in which a general discussion, conclusions and recommendations for future work are presented.

Chapter 2

Dual solutions of a micropolar nanofluid flow with heat mass transfer past a stretching or shrinking sheet

In this chapter, the flow of a micropolar nanofluid over a nonlinearly stretching or shrinking sheet is studied and the equations solved using the spectral quasilinearization method. The study of micropolar fluids was pioneered by Eringen [122]. Micropolar nanofluids are those fluids that are composed of rigid, randomly oriented particles with their specific microrotations in a viscous medium [123, 124]. Micropolar nanofluids find wide application in industry, meteorology and engineering among many others. Common examples of micropolar nanofluids include blood, colloids, dust in the air, silt carried by rivers, paints, lubricants and so on [125]. In the study, the effects of nanofluid particle concentration, thermophoresis and Brownian motion are discussed.

Received 28 January 2019
Revised 13 June 2019
Accepted 12 August 2019

Dual solutions of a micropolar nanofluid flow with radiative heat mass transfer over stretching/shrinking sheet using spectral quasilinearization method

Mangwiro Magodora, Hiranmoy Mondal and Precious Sibanda
University of KwaZulu-Natal – Pietermaritzburg Campus, Pietermaritzburg, South Africa

Abstract

Purpose – The purpose of this paper is to focus on the application of Chebyshev spectral collocation methodology with Gauss Lobatto grid points to micropolar fluid over a stretching or shrinking surface. Radiation, thermophoresis and nanoparticle Brownian motion are considered. The results have attainable scientific and technological applications in systems involving stretchable materials.

Design/methodology/approach – The model equations governing the flow are transformed into non-linear ordinary differential equations which are then reworked into linear form using the Newton-based quasilinearization method (SQLM). Spectral collocation is then used to solve the resulting linearised system of equations.

Findings – The validity of the model is established using error analysis. The velocity, temperature, micro-rotation, skin friction and couple stress parameters are conferred diagrammatically and analysed in detail.

Originality/value – The study obtains numerical explanations for rapidly convergent solutions using the spectral quasilinearization method. Convergence of the numerical solutions was monitored using the residual error analysis. The influence of radiation, heat and mass parameters on the flow are depicted graphically and analysed. The study is an extension on the work by Zheng *et al.* (2012) and therefore the novelty is that the authors tend to take into account nanoparticles, Brownian motion and thermophoresis in the flow of a micropolar fluid.

Keywords Thermophoresis, Micropolar fluid, Boundary layer flow, Brownian motion, Quasilinearization

Paper type Research paper

Nomenclature

$a > 0$	stretching constant
$a < 0$	shrinking constant
c	volumetric volume expansion coefficient
C	concentration of diffusing species in the boundary layer
C_∞	concentration of the diffusing species far away from the wall
C_w	concentration at the sheet surface
C_f	skin-friction coefficient
C_p	specific heat capacity at constant pressure
D_B	Brownian diffusion coefficient
D_T	thermophoretic diffusion coefficient
h	gyration parameter
H	micro-inertia density parameter
j	micro-inertia density
k	vortex viscosity
k_1	mean absorption coefficient
K	viscosity ratio
Le	Lewis number
m	stretching or shrinking parameter
N	micro-rotation velocity
Nb	Brownian motion parameter
Nt	thermophoresis parameter
Nu_x	local Nusselt number

Multidiscipline Modeling in Materials and Structures
Vol. 16 No. 2, 2020
pp. 238-255

1573-6105
DOI 10.1108/MMMS-01-2019-0028

The authors are grateful to acknowledge the financial support received from the CoE-MaSS (Centre of Excellence in Mathematical and Statistical Sciences) and the University of KwaZulu-Natal.

Pr	Prandtl number	u,v	velocities in the $x-$ and $y-$ direction respectively
Pr_n	radiative Prandtl number	U	stretching velocity
q_w	heat flux per unit area of the sheet	U_0	reference velocity
q_r	radiative heat flux	*Greek symbols*	
Re_x	local Reynolds number	α	thermal diffusivity
R_d	radiation parameter	γ	spin gradient of fluid
Sh_x	local Sherwood number	σ	Stephan-Boltzmann constant
S	suction or injection parameter	η	transformed variable
T	temperature in the boundary layer	ρ	density of the fluid
T_∞	temperature of the fluid far away from the wall	μ	dynamic viscosity of the fluid
T_w	temperature at the sheet	ν	kinematic viscosity
T_0	reference temperature	λ	velocity slip parameter

1. Introduction

Micropolar fluids are fluids in which the local micro-structure and intrinsic motion of fluid particles are considered in the flow regimen. The theory of micropolar fluids, which was championed by Eringen (1966) and Eringen (1964), deals with fluids that are composed of rigid and randomly oriented particles suspended in a viscous medium (Chen *et al.*, 2010; Liao, 2005; Maripala and Naikoti, 2016). The particles of this category of fluids exhibit both rotational and translational motion.

Non-Newtonian fluids, a category of fluids to which micropolar fluids belong, find many applications in engineering, agriculture, meteorology, industry and so on. Increased research interest in micropolar fluids has manifested through numerous studies in recent years as this category of fluids represents many industrially important fluid products such as industrial colloidal fluids, polymeric suspensions, liquid crystals, paints, colloids, ferro-liquids, polymeric fluids and lubricants. The presence of dust in air and blood flow in veins, arteries and capillaries may also be studied using micropolar fluid dynamics. The momentum equations of fluid flow termed Navier–Stokes equations are inadequate to totally describe flow of fluids at the nano and micro scale (Chen *et al.*, 2010) and are used in conjunction with an additional model equation that accounts for angular momentum (Zheng *et al.*, 2012).

Ishak *et al.* (2009) considered dual solutions in the flow of micropolar fluids whereas De *et al.* (2016) analysed dual solutions on heat and mass transfer for nanofluid on a stretching/shrinking sheet with thermal radiation. Kameswaran *et al.* (2014) investigated dual solutions of Casson fluid as it flows over shrinking or streching surface. Maripala and Naikoti (2016) considered the magnetohydrodynamic flow of micropolar nanofluid flow over a radiative stretching sheet and solved their problem by employing the implicit difference method with Thomas' algorithm. RamReddy *et al.* (2015) studied mixed convection on micropolar fluid over a porous vertical plate with convective boundary condition and they solved the system using the spectral quasilinearization method. Their findings disclosed that dual solutions exist for certain values of mixed convection parameter.

A new branch of solutions over an impermeable plate was reported by Liao (2005) that was followed by an investigation of a new branch of solutions over a permeable plate surface two years later (Liao, 2007). In both studies, they reported the existence of two branches of solution and features of the flow phenomena were discussed in detail. Ever since, much interest by researchers has been exhibited by focusing more attention on dual solutions. Sulochana *et al.* (2016) have reported a transpiration effect on the stagnation-point flow of a Carreau nanofluid on micropolar fluids. Multiple solutions were also reported by Dhanai *et al.* (2015) when they studied the hydromagnetic flow of nanofluid over stretching/shrinking permeable sheet with viscous dissipation.

Uddin *et al.* (2016) have reported on the existence of dual solutions that emanate from mass and heat transfer of micropolar fluid over an exponentially permeable shrinking sheet. In their findings, the researchers found that dual solutions for temperature, micro-rotation and velocity were obtained when the amount of applied suction had reached a certain threshold. Dual solutions on steady double diffusive boundary layer flow over a vertical surface immersed in an incompressible micropolar fluid were reported by Ishak *et al.* (2009). Rehman and Nadeem (2012) examined the mixed convection transport in micropolar nanofluid over a vertical slender cylinder.

A nanofluid is formed when nanoparticles are suspended in a base fluid. Examples of base fluids can be water, ethylene glycol or oil. Nanoparticles, whose diameters range between 1 and 100 nm, can significantly alter thermal properties of base fluids by increasing their thermal conductivities (De *et al.*, 2016; Goqo *et al.*, 2016; Nadeem, Rehman, Vajravelu, Lee and Lee, 2012; Prasad *et al.*, 2014). Nanoparticles can be made of metal oxides (e.g. titanium oxide), metals (e.g. copper) or non-metals (e.g. graphite). Recently, micropolar nanofluids have received a considerable interest due to their wide application in industry. Nadeem *et al.* have considered the axisymmetric stagnation flow of a micropolar nanofluid flow in a moving cylinder. They applied the Homotopy analysis method to characterize the flow. The study of micropolar nanofluid flow with MHD and viscous dissipation effects towards a stretching sheet was done by Hsiao (2017). Noor *et al.* (2015) investigated micropolar nanofluid fluid flow and they applied the shooting method coupled with the Runga–Kutta Fehlberg scheme to solve the flow model. The effect of nanoparticles on micropolar fluid flow was considered by Hussain *et al.* (2014).

Mondal *et al.* (2019) reported on dual solutions for the magnetohydromagnetic flow of nanofluid with entropy generation. They solved their problem by applying the spectral quasilinearization method and showed that this method produced residual errors than those achieved by applying the fifth-order Runge–Kutta–Fehlberg method. De *et al.* (2016) applied the fifth-order Runge–Kutta–Fehlberg method with shooting technique on dual solutions of heat and mass transfer of nanofluid over a stretching or shrinking sheet with thermal radiation. Goqo *et al.* (2016) utilised spectral quasilinearization to analyse combined effects of convective boundary condition and magnetic field on the unsteady flow of Jeffery nanofluid over a shrinking sheet with heat generation and thermal radiation. Sithole *et al.* (2018) studied couple stress nanofluid flow in a magneto-porous medium by means of spectral quazilinearization.

Radiation as a mode of heat transfer has also caught the attention of researchers in the recent past. This trend can be attributed to the grand importance of radiation in numerous technological and engineering processes such as solar power harvesting, missile launches, satellite navigation and space travel. Pal and Mondal (2011) presented the effects of thermal radiation, Dufour, Soret and chemical reaction on hydromagnetic non-Darcy convective flow over a stretching sheet. In recent times, many studies have been devoted to investigating radiation effects in heat and mass transfer processes of fluids. Studies involving radiative heat flux include those performed by Subhashini *et al.* (2013), Raptis (1998), Hamid *et al.* (2018), De *et al.* (2015, 2016), Bidin and Nazar (2009), Sithole *et al.* (2018) and so on.

Many researchers have focused attention on boundary layer flow. Boundary layer theory has undoubtedly led to modern advances in space flight, air travel, motor sports, irrigation systems, biomedical technologies, etc. (Schlichting and Gersten, 2016). Boundary layer flow over stretching/shrinking surfaces has extensive engineering applications like the cooling of metallic plates, the aerodynamic extrusion of plastic sheets, hot rolling, metal spinning, boundary layer along liquid film condensation process, artificial fibres, glass-fibre production, paper production, and drawing of plastic films and so on (Subhashini *et al.*, 2013; Tan *et al.*, 2008; Uddin *et al.*, 2016).

Pioneering studies on boundary layer flow over solid surfaces were done by Sakiadis (1961). His studies were followed up later by Liao (2005, 2007) who focused attention on flow over stretching permeable and impermeable walls. Liao solved the model equations by means of the

Homotopy analysis method, which is classified as an analytic method. The Homotopy analysis method was also utilised by Nadeem, Rehman, Lee and Lee (2012) to investigate the flow of second grade fluid in a cylinder with heat transfer. Siddheshwar *et al.* (2014) analysed magnetohydrodynamic flow and heat transfer of an exponentially stretching sheet in a Boussinesq–Stokes suspension.

Most real-life phenomena such as heat and mass transfer, fluid flow, biological and engineering processes are modelled by non-linear partial and ordinary differential equations. By their nature such equations are complex and very tough to solve exactly (Ames, 2014; Motsa *et al.*, 2014; Schlichting and Gersten, 2016). Numerical methods have been found useful in solving such complex phenomena to a high degree of accuracy. Examples of such numerical methods include the spectral quasilinearization method, finite difference method, Runge–Kutta method and so on.

Other numerical methods often employed by researchers include the finite element method, the Runge–Kutta–Fehlberg method (Hamid *et al.*, 2018; Siddheshwar *et al.*, 2014), the Keller-box technique (Mishra *et al.*, 2016) and the shooting method (Dhanai *et al.*, 2015). In this work, we apply the Chebyshev spectral quasilinearization method to solve a problem involving the flow of a micropolar nanofluid, for the rationale that spectral methods have been shown to produce high accuracy and precision (Mondal *et al.*, 2019). Furthermore, the method has several advantages in the recent past (Sithole *et al.*, 2018).

2. Mathematical formulations

In this study, a two-dimensional incompressible flow of a micropolar nanofluid is considered. The fluid flows steadily over an impervious stretching/sheeting sheet. On the surface of the sheet, we have $u_w = a(x+b)^m$, $T_w = T_\infty + e(x+b)^\lambda$ and $C_w = C_\infty + d(x+b)^\beta$, where the parameters a, b and m are associated with the shrinking or stretching speed of the surface while e, b and λ are related to the temperature of the surface (Zheng *et al.*, 2012) whilst d, b and β are related to the concentration of the surface. The x-axis lies in the direction parallel to the surface of the sheet, the y-axis is perpendicular thereto, u and v are the velocities in the x and y directions, respectively.

The model equations emanate from the principles of mass, linear momentum, angular momentum and energy conservation and are given as (refer to De *et al.*, 2016; Sithole *et al.*, 2018; Zheng *et al.*, 2012):

$$\frac{\partial u}{\partial x}+\frac{\partial v}{\partial y}=0, \tag{1}$$

$$\bar{u}\,\frac{\partial u}{\partial x}+v\,\frac{\partial u}{\partial y}=\left(\frac{\mu+k}{\rho}\right)\frac{\partial^2 u}{\partial y^2}+\frac{k}{\rho}\frac{\partial N}{\partial y}, \tag{2}$$

$$\rho j\left(u\,\frac{\partial N}{\partial x}+v\,\frac{\partial N}{\partial y}\right)=\frac{\partial}{\partial y}\left(\gamma\,\frac{\partial N}{\partial y}\right)-k\left(2N+\frac{\partial u}{\partial y}\right), \tag{3}$$

$$u\,\frac{\partial j}{\partial x}+v\,\frac{\partial j}{\partial y}=0, \tag{4}$$

$$u\,\frac{\partial T}{\partial x}+v\,\frac{\partial T}{\partial y}=\alpha\,\frac{\partial^2 T}{\partial y^2}-\frac{1}{\rho C_p}\frac{\partial q_r}{\partial y}+\tau\left(D_B\,\frac{\partial C}{\partial y}\frac{\partial T}{\partial y}+\frac{D_T}{T_\infty}\left\{\frac{\partial T}{\partial y}\right\}^2\right), \tag{5}$$

$$u\frac{\partial C}{\partial x}+v\frac{\partial C}{\partial y}=D_B\frac{\partial^2 C}{\partial y^2}+\frac{D_T}{T_\infty}\left(\frac{\partial^2 T}{\partial y^2}\right). \tag{6}$$

The associated boundary conditions are as follows:

$$u=u_w,\ \ v=j=0,\ \ T=T_w,\ \ C=C_w,\ \ N=-\frac{1}{2}\frac{\partial u}{\partial y}\ \text{ at } y=0,$$

$$u\to 0,\ \ N\to 0,\ \ T\to T_\infty,\ \ C\to C_\infty\ \text{ as } y\to+\infty, \tag{7}$$

where N is the angular velocity (also termed the micro-rotation), D_T and D_B denote the thermophoretic diffusion and the Brownian diffusion coefficients, respectively, q_r is the radiative heat flux while j and γ are the micro-inertia density and spin gradient of the fluid, respectively. The parameters μ, ρ, C_p, α and k are the viscosity, the density, the specific heat capacity at constant pressure, the thermal conductivity and the vortex viscosity of the fluid, respectively, $\tau=(\rho c)_p/(\rho c)_f$ is the ratio of effective heat capacity of nanoparticles to that of the micropolar fluid, $H=\mu/\rho ja$ represents the micro-inertia parameter, where $a>0$ and $a<0$ are the stretching and shrinking constants, respectively.

Let $\gamma=\mu(1+(K/2))j$ where the material parameter $K=k/\mu$ represents the viscosity ratio (Zheng *et al.*, 2012). We note here that $K=0$ depicts the flow of a viscous and incompressible Newtonian fluid.

The parameter q_r is modelled by the Rosseland approximation as $q_r=-(4\sigma/3k_1)(\partial(T^4)/\partial y)$ (Raptis, 1998). Here, k_1 is the mean absorption coefficient and σ the Stefan–Boltzmann constant. In the Rosseland approximation, we have $T^4=4T_\infty^3T-3T_\infty^4$ (Bidin and Nazar, 2009). This implies that $(\partial q_r/\partial y)=-(16/3)(\sigma T_\infty^3/k_1)(\partial T/\partial y)$, hence (5) becomes:

$$u\frac{\partial T}{\partial x}+v\frac{\partial T}{\partial y}=\alpha\frac{\partial^2 T}{\partial y^2}+\frac{16\sigma T_\infty^3}{3\rho C_p k_1}\frac{\partial^2 T}{\partial y^2}+\tau\left(D_B\frac{\partial C}{\partial y}\frac{\partial T}{\partial y}+\frac{D_T}{T_\infty}\left\{\frac{\partial T}{\partial y}\right\}^2\right). \tag{8}$$

Let ψ denote the stream function such that $u=\partial\psi/\partial y$ and $v=-(\partial\psi/\partial x)$. The dimensionless similarity variables are introduced as follows:

$$\eta=\sqrt{\frac{a(1+m)}{2v}}(x+b)^{\frac{m-1}{2}}y,\ \ \theta(\eta)=\frac{T-T_\infty}{c(x+b)^\lambda},\ \ \psi=a\sqrt{\frac{2v}{a(1+m)}}(x+b)^{\frac{m-1}{2}}F(\eta),$$

$$j=\frac{2v}{a(1+m)}(x+b)^{1-m}i(\eta),\ \ N=a\sqrt{\frac{a(1+m)}{2v}}(x+b)^{\frac{3m-1}{2}}h(\eta),\ \ \phi(\eta)=\frac{C-C_\infty}{d(x+b)^\beta}. \tag{9}$$

where v denotes the kinematic viscosity of the fluid and $a\neq 0$ and $a(m+1)>0$.

Applying the similarity variables (9) in Equations (2)–(4), (6) and (8), the system becomes:

$$\kappa_1F'''+FF''+\kappa_2h'-\kappa_3(F')^2=0, \tag{10}$$

$$\kappa_4(ih')'+(Fh'-\kappa_4F'h)-\kappa_2(2h+F'')=0, \tag{11}$$

$$\kappa_5F'i-\kappa_6Fi'=0, \tag{12}$$

$$\theta'' + \Pr_n\left\{F\theta' - \kappa_7 F'\theta + \mathrm{Nb}\theta'\phi' + \mathrm{Nt}(\phi')^2\right\} = 0, \tag{13}$$

$$\phi'' + \frac{\mathrm{Nt}}{\mathrm{Nb}}\theta'' + Le\left(\phi' F - \frac{2}{m+1}F'\phi\right) = 0, \tag{14}$$

where:

$$\kappa_1 = (1+K),\ \ \kappa_2 = K,\ \ \kappa_3 = \frac{2m}{1+m},\ \ \kappa_4 = \left(1+\frac{K}{2}\right),\ \ \kappa_5 = 1-m, \tag{15}$$

$$\kappa_6 = \frac{1+m}{2},\ \ \kappa_7 = \frac{2\lambda}{1+m},\ \ \Pr_n = \frac{\Pr}{1+(4R_d/3)},\ \ \Pr = \frac{\nu}{\alpha},\ \ R_d = \frac{4\sigma T_\infty^3}{k_1\alpha\rho C_p}, \tag{16}$$

where Pr is the Prandtl number, $\Pr_n$ is the radiative Prandtl number, R_d is the radiation parameter, $\mathrm{Nb} = \tau D_B(C_w - C_\infty)/\nu$ is the Brownian motion parameter, $\mathrm{Nt} = \tau D_T(T_w - T_\infty)/\nu T_\infty$ denotes the thermophoresis parameter and $\mathrm{Le} = \nu/D_B$ is the Lewis number.

The boundary conditions for Equations (10)–(14) are:

$$F(0) = 0,\ \ \theta(0) = 1,\ \ i(0) = 0,\ \ h(0) = -\frac{1}{2}F''(0),\ \ \phi(0) = 1,$$
$$F'(0) = 1,\ \ \theta(\infty) = 0,\ \ F'(\infty) = 0,\ \ h(\infty) = 0,\ \ \phi(\infty) = 0. \tag{17}$$

Equation (12) is integrated by parts to give $i(\eta) = \varepsilon F(\eta)^\delta$ where $\delta = (\kappa_5/\kappa_6)$ and ε is a constant of integration. If $K \neq 0$ and $\varepsilon = 0$, this implies that $i(\eta) = 0$, and yields the equation $h(\eta) = (1/2)F''(\eta)$, where $h(0) = -(1/2)F''(0)$, $h(\infty) = 0$ meaning that the gyration equals the angular velocity.

Consequently, Equations (10)–(14) are transformed to the equations:

$$\kappa_4 F''' + FF'' - \kappa_3(F')^2 = 0, \tag{18}$$

$$\theta'' + \Pr_n\left\{F\theta' - \kappa_7 F'\theta + \mathrm{Nb}\theta'\phi' + \mathrm{Nt}(\phi')^2\right\} = 0, \tag{19}$$

$$\phi'' + \frac{\mathrm{Nt}}{\mathrm{Nb}}\theta'' + Le(\phi' F - \kappa_8 F'\phi) = 0, \tag{20}$$

where $\kappa_8 = 2/(m+1)$.

The associated boundary conditions are:

$$F(0) = 0,\ \ \theta(0) = 1,\ \ \phi(0) = 1,\ \ F'(0) = 1,\ \ \theta(\infty) = 0,\ \ F'(\infty) = 0,\ \ \phi(\infty) = 0. \tag{21}$$

3. Local skin friction, heat and mass transfer coefficients, wall couple stress

The physical quantities of interest are C_f, Nu_x, M_w which denote the local skin friction coefficient, the local Nusselt number and the local couple stress at the surface, respectively. They are defined as:

$$C_f = \frac{2\tau_w}{\rho u_w^2},\ \ \mathrm{Nu}_x = \frac{(x+b)q_w}{k(T_w - T_\infty)},\ \ M_w = \gamma\left(\frac{\partial N}{\partial y}\right)_{y=0}. \tag{22}$$

Here, τ_w and q_w represent the surface shear stress and the surface heat flux, respectively, and are given by:

$$\tau_w = \left[(\mu+k)\frac{\partial u}{\partial y}+kN\right]_{y=0}, \quad q_w = -k\left(\frac{\partial T}{\partial y}\right)_{y=0}. \tag{23}$$

Using the similarity variables (9), we obtain:

$$0.5C_f\mathrm{Re}_x^{0.5} = \pm\sqrt{0.5|1+m|}(1+0.5K)F''(0) \tag{24}$$

$$\mathrm{Nu}_x\mathrm{Re}_x^{0.5} = -\sqrt{0.5|1+m|}\theta'(0), \tag{25}$$

$$\frac{M_w}{\mu u_w(x)^{m-1}} = \frac{1}{2H}(1+m)(1+0.5K)h'(0), \tag{26}$$

where $\mathrm{Re}_x = |(u_w(x+b))/v|$ is the local Reynolds number.

4. Numerical solution

Equations (18)–(20) form a coupled non-linear system which we solve by utilising the quasilinearization technique followed by applying the Chebyshev spectral collocation method. The background theory on these procedures is given in Bellman and Kalaba (1965), Canuto *et al.* (2012) and Trefethen (2000).

4.1 Quasilinearization

Consider a system of n non-linear differential equations which we write, without loss of generality, as:

$$\Gamma_1[H_1, H_2, \ldots, H_n] = 0, \tag{27}$$

$$\Gamma_2[H_1, H_2, \ldots, H_n] = 0, \tag{28}$$

$$\Gamma_n[H_1, H_2, \ldots, H_n] = 0, \tag{29}$$

where:

$$H_1 = \left\{f_1(\eta), f_1'(\eta), f_1''(\eta), \ldots, f_1^{(p)}(\eta)\right\}, \tag{30}$$

$$H_2 = \left\{f_2(\eta), f_2'(\eta), f_2''(\eta), \ldots, f_2^{(p)}(\eta)\right\}, \tag{31}$$

$$H_n = \left\{f_n(\eta), f_n'(\eta), f_n''(\eta), \ldots, f_n^{(p)}(\eta)\right\}, \tag{32}$$

here p denotes the order of differentiation while $f_k(\eta)$ and Γ_k denote the solutions of the system and the non-linear operators containing all the spatial derivatives of $f_k(\eta)$ for $k = 1, 2, \ldots, n$, respectively.

It is assumed that the solution can be approximated using the Lagrange interpolation polynomial of the form:

$$f_k(\eta) = \sum_{j=0}^{N_\eta} f_k(\eta_j)\mathcal{L}(\eta), \tag{33}$$

for $k = 0, 1, \ldots, n$ where:

$$\mathcal{L}(\eta) = \prod_{\substack{j=0 \\ j \neq k}}^{N_\eta} \frac{\eta - \eta_k}{\eta_j - \eta_k}, \tag{34}$$

and:

$$\mathcal{L}(\eta_k) = \begin{cases} 0, & j \neq k \\ 1, & j = k \end{cases}. \tag{35}$$

The grid points η_j for $j = 0, 1, \ldots, n$ which are considered in this study are termed Chebyshev–Gauss–Lobatto grid points and are defined as:

$$\{\eta_j\} = \cos\left(\frac{\pi j}{N_\eta}\right). \tag{36}$$

The system of the n non-linear differential equations under consideration is then linearised by using the quasilinearization technique, which is outlined in great detail by Bellman and Kalaba (1965).

Thus applying the quasilinearization technique leads one to obtain a coupled system n linear of ordinary differential equations given as follows:

$$\sum_{s=0}^{p} a_{1,s,r}^{[1]}(\eta) f_{1,r+1}^{(s)}(\eta) + \sum_{s=0}^{p} a_{2,s,r}^{[1]}(\eta) f_{2,r+1}^{(s)}(\eta) + \cdots + \sum_{s=0}^{p} a_{n,s,r}^{[1]}(\eta) f_{n,r+1}^{(s)}(\eta) = R_1(\eta), \tag{37}$$

$$\sum_{s=0}^{p} a_{1,s,r}^{[2]}(\eta) f_{1,r+1}^{(s)}(\eta) + \sum_{s=0}^{p} a_{2,s,r}^{[2]}(\eta) f_{2,r+1}^{(s)}(\eta) + \cdots + \sum_{s=0}^{p} a_{n,s,r}^{[2]}(\eta) f_{n,r+1}^{(s)}(\eta) = R_2(\eta), \tag{38}$$

$$\sum_{s=0}^{p} a_{1,s,r}^{[n]}(\eta) f_{1,r+1}^{(s)}(\eta) + \sum_{s=0}^{p} a_{2,s,r}^{[n]}(\eta) f_{2,r+1}^{(s)}(\eta) + \cdots + \sum_{s=0}^{p} a_{n,s,r}^{[n]}(\eta) f_{n,r+1}^{(s)}(\eta) = R_n(\eta), \tag{39}$$

where $a_{n,s,r}^{[k]}(\eta) = \partial \Gamma_k / \partial f_{n,r}^{(s)}$ and $s = 0, 1, 2, \ldots, p$ are the variable coefficients of $f_{n,r+1}^{(s)}$ that correspond to the kth equation for $k = 1, 2, \ldots, n$.

The right hand side of the kth equation is given by:

$$R_k(\eta) = \sum_{s=0}^{p} a_{1,s,r}^{[k]}(\eta) f_{1,r}^{(s)}(\eta) + \sum_{s=0}^{p} a_{2,s,r}^{[k]}(\eta) f_{2,r}^{(s)}(\eta) + \cdots + \sum_{s=0}^{p} a_{n,s,r}^{[k]}(\eta) f_{n,r}^{(s)}(\eta) - \Gamma_k\left[H_{1,r},\ H_{2,r},\ \ldots,\ H_{n,r}\right]. \tag{40}$$

By following the above procedures, the linearised system of Equations (18)–(20) becomes:

$$\kappa_4 F''' + F_r F''_{r+1} - 2\kappa_3 F'_r F'_{r+1} + F''_r F_{r+1} = R_1, \tag{41}$$

$$-\kappa_7 \mathrm{Pr}_n \theta_r F'_{r+1} + \mathrm{Pr}_n \theta'_r F_{r+1} + \theta''_{r+1} + \{F_r + \mathrm{Nb}\phi'_r + 2\mathrm{Nt}\theta'_r\} \mathrm{Pr}_n \theta'_{r+1} - \kappa_7 \mathrm{Pr}_n F'_r \theta_{r+1} + \mathrm{Pr}_n \mathrm{Nb} \theta'_r \phi'_{r+1} = R_2, \tag{42}$$

$$\kappa_8 \text{Le}\phi_r F'_{r+1} + \text{Le}\phi'_r F_{r+1} + \frac{\text{Nt}}{\text{Nb}}\theta''_{r+1} + \phi''_{r+1} + \text{Le}F_r\phi'_{r+1} - \kappa_8 \text{Le}F'_r\phi_{r+1} = R_3, \tag{43}$$

where:

$$R_1 = -\kappa_3 \left(F'_r\right)^2 + F''_r F_r, \tag{44}$$

$$R_2 = -\kappa_7 \text{Pr}_n \theta_r F_{r'} + \text{Pr}_n \theta_{r'} F_r + \text{Pr}_n \text{Nt}\left(\theta'_r\right)^2 + \text{Pr}_n \text{Nb}(\theta_r)^2, \tag{45}$$

$$R_3 = \text{Le}F_r\phi'_r - \kappa_8 \text{Le}\phi_r F'_r, \tag{46}$$

and the associated boundary conditions are:

$$F_{r+1}(0) = 0, \;\; \theta_{r+1}(0) = 1, \;\; \phi_{r+1}(0) = 1, \;\; F'_{r+1}(0) = 1, \;\; \theta_{r+1}(\infty) = 0, \;\; \phi_{r+1}(\infty) = 0, \;\; F'_{r+1}(\infty) = 0. \tag{47}$$

4.2 Spectral collocation

The linearised system (41)–(43) is solved by evaluating F, θ and ϕ at the Chebyshev–Gauss–Lobatto grid points η_i, for $i = 0, 1, \ldots, N_\eta$. The derivatives at the grid points are defined by:

$$\frac{df_n}{d\eta}\Big|_{(\eta_i)} = \sum_{\omega=0}^{N_\eta} D_{i\omega} f_n(\eta_\omega), \tag{48}$$

where $D_{i\omega} f_n(\eta_\omega) = d\mathcal{L}(\eta_j)/d\eta$. Higher order derivatives are defined by:

$$\frac{d^p f_n}{d\eta^p}\Big|_{(\eta_i)} = \text{D}^p\text{F}_n, \tag{49}$$

where $\text{D}^p\text{F}_n = \sum_{\omega=0}^{N_\eta} D^p_{i\omega} f_n(\eta_\omega)$ and $F_n = [f_n(\eta_0), f_n(\eta_1), \ldots, f_n(\eta_{N_\eta})]^T$ and T denotes transpose of the matrix.

Initial guesses are selected in such a way that they satisfy the boundary conditions of our system. We chose the initial guesses for our system of equations as $F_0(\eta) = 1 - e^{-\eta}$, $\theta_0 = e^{-\eta}$, $\phi_0 = e^{-\eta}$ and $h_0(\eta) = -(1/2)F''(0)e^{-\eta}$. The system (18)–(20) is solved by the spectral quasilinearization method. The solution for $h(\eta)$ is then deduced from the solution for F. A more detailed treatment on the spectral quasilinearization method can be found in Motsa *et al.* (2011), RamReddy *et al.* (2015) and Sithole *et al.* (2018).

5. Results and discussion

We investigate the effect of increasing or decreasing certain parameters on the flow in order to gain better understanding of the flow dynamics. The results of the dual solutions are depicted graphically in tables and figures. The results are then discussed and conclusions are drawn from them.

Table I illustrates that the error norm $\|y_{r+1} - y_r\| \to 0$ as $r \to \infty$ and this confirms the accuracy and effectiveness of the SQLM scheme in solving the micropolar nanofluid flow problem under consideration. Table II shows numerical results for $\text{Nu}/\text{Re}_x^{1/2}$ and comparison is made with results obtained in Ali (1995) and Zheng *et al.* (2012) and they are found to be in good agreement.

As shown in Figure 1, an increase in viscosity ratio K is associated with the appreciation of $f'(\eta)$. The viscosity ratio is defined as the ratio of the turbulent velocity to the dynamic viscosity. An increase in the viscosity ratio thus leads to the thickening of the momentum boundary layer as expected.

The downward variation of nanoparticle concentration against the increase of Lewis number is shown in Figure 2. Such behaviour is physically possible because the Lewis number is defined by the ratio of the Schmidt number to the Prandtl number (De *et al.*, 2016). Thus increasing the Schmidt number would result in an increase the Lewis number, that would in turn be accompanied by an increase of the concentration. Hence, an inverse relationship exists between Le and ϕ. This trend is in agreement with the results of De *et al.* (2015) and Sithole *et al.* (2018). It is also evident from Figure 3 that an increase in Lewis number is accompanied by a rise in temperature.

The behaviour of the angular velocity variable $h(\eta)$ as the viscosity ratio increases is illustrated in Figure 4. As the viscosity ratio increases, the dual angular velocity decreases for lower values of η but the opposite is true for higher values of η. This trend is consistent with that one observed in Zheng *et al.* (2012).

K	m	Pr_n	λ	Ali (1995)	Zheng *et al.* (2012)	Present results
0	−0.2	0.72	1	0.8342828	0.846583	0.840482
0	−0.2	1	1	1.0063930	1.018910	1.013521
0	−0.2	3	1	1.8221270	1.856360	1.834747
0	−0.2	0.72	0	0.3349597	0.382401	0.336920

Table I. Comparison of values of $\mathrm{Nu}/\mathrm{Re}_x^{1/2}$

Iteration, r	$\|\|F_{r+1}-F_r\|\|_\infty$	$\|\|\theta_{r+1}-\theta_r\|\|_\infty$
1	5.04×10^{-2}	6.58×10^{-1}
2	1.71×10^{-3}	2.72×10^{-5}
3	3.57×10^{-5}	4.60×10^{-5}
4	3.07×10^{-10}	1.18×10^{-9}
5	4.11×10^{-11}	8.11×10^{-11}

Table II. Convergence of the solutions: $\mathrm{Pr} = 1$, $\lambda = 1$, $m = 3$, $K = 0$

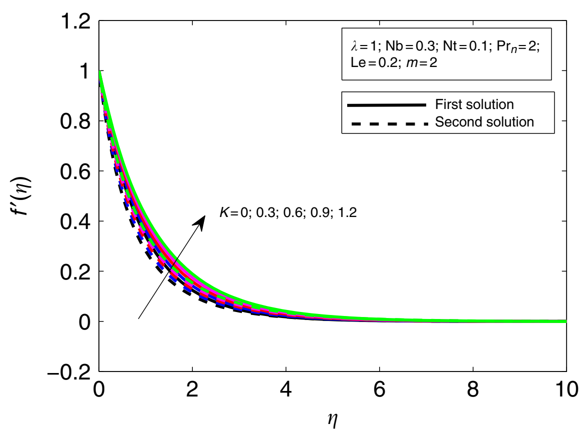

Figure 1. Velocity profiles for changing K

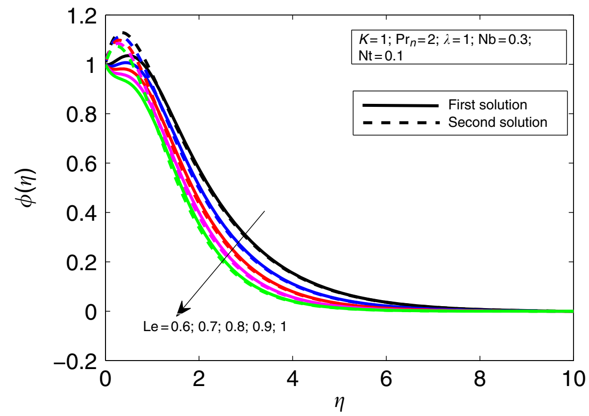

Figure 2.
Concentration profiles for changing Le

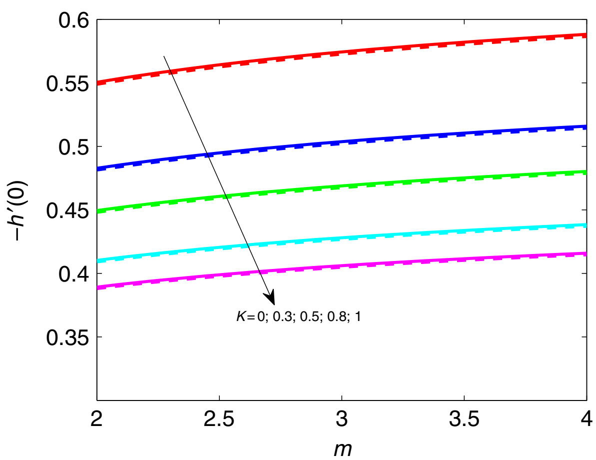

Figure 3.
Couple stress coefficient $-h'(0)$

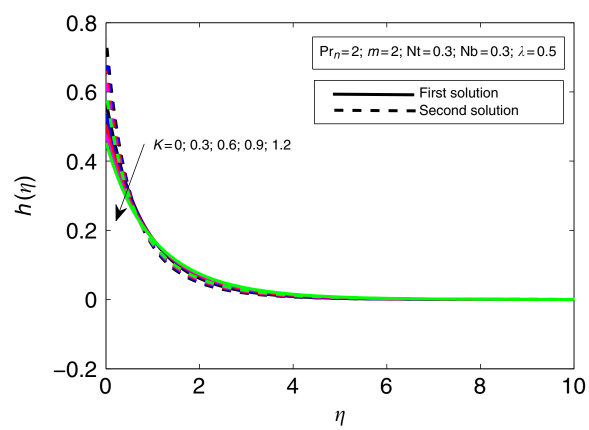

Figure 4.
Effect of K on angular velocity profiles

Figure 5 shows how the thermophoresis parameter Nt affects the temperature of the boundary layer. An upward change in Nt leads to the enhancement of both temperature and concentration profiles. An increase in nanoparticle concentration may be attributed to the improved volume fraction which is the result of an increase of the thermophoresis parameter. The same fluid behaviour is also reported in De *et al.* (2016).

The influence of the thermophoresis parameter Nt on the nanoparticle concentration is shown in Figure 6. It is observed that an increase in Nt enhances the concentration boundary layer as expected, due to the increased volume fraction of the nanoparticles. This was also witnessed in Sithole *et al.* (2018).

The effect of the Prandtl number Pr_n on the temperature and concentration profiles is shown in Figures 7 and 8. The Prandtl number is a dimensionless quantity that correlates the viscosity of a fluid with the thermal conductivity. It is apparent from the plots that a rise in the Prandtl number results in the depletion of the temperature and an increase in the concentration profile. This also agrees with observations reported in Sithole *et al.* (2018). That heat diffuses very quickly in liquid metals ($Pr \ll 1$)) and very slowly in oils ($Pr \gg 1$) has widely been reported in the literature (Agbage *et al.*, 2016). When $Pr \ll 1$, thermal

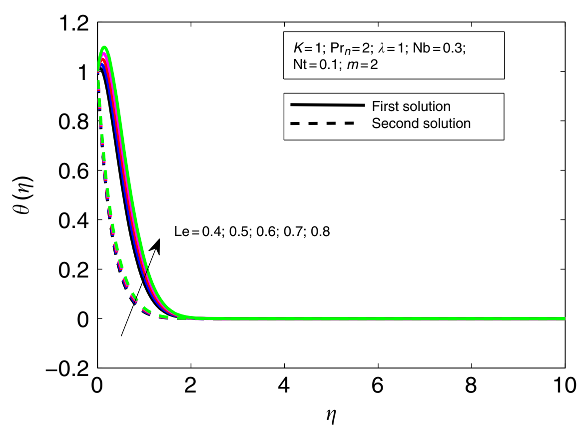

Figure 5. Effects of Le on temperature profiles

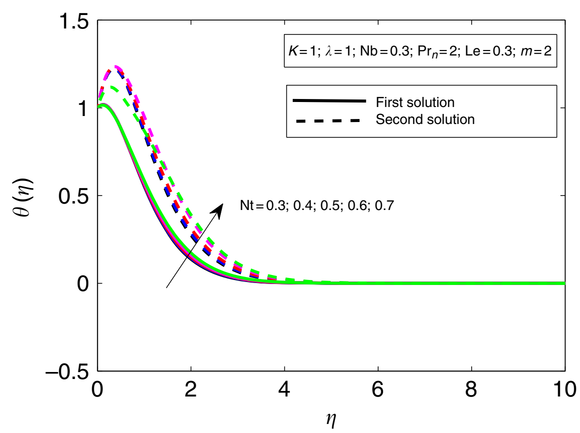

Figure 6. Effects of Nt on temperature profiles

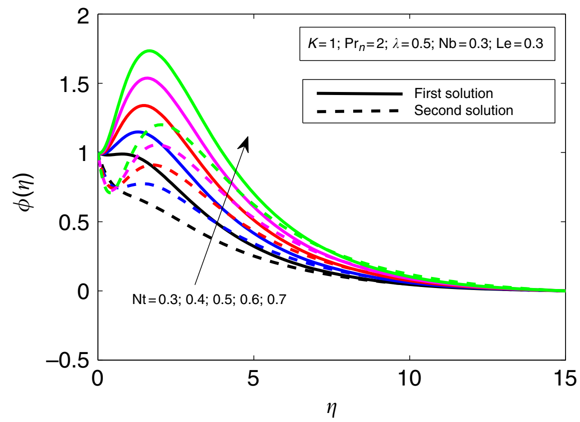

Figure 7.
Effects of Nt on concentration profiles

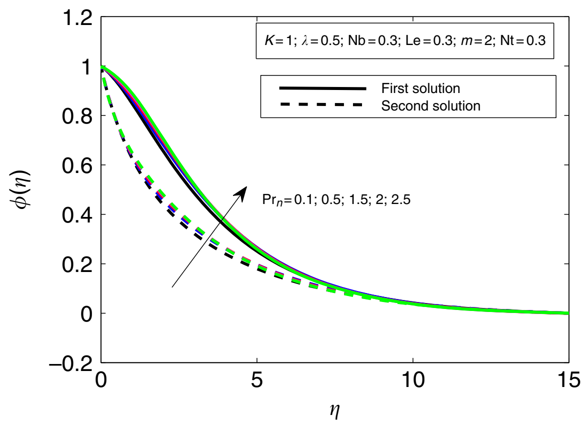

Figure 8.
Effects of $\Pr_n$ on concentration profiles

diffusivity dominates over the momentum diffusivity, while the reverse is true when $\Pr \ll 1$. In our study, the high conductivity of the nanofluid due to the presence of the nanoparticles means that rapid heat and mass diffuse rapidly from the sheet surface resulting in the depletion of the temperature and concentration profiles. In this study, we chose the value $\Pr_n = 2$ to represent the Prandtl number to investigate the flow dynamics of a micropolar fluid over a shrinking or stretching sheet.

Figures 9–11 illustrate the influence of the material parameter m and the viscosity ratio K on the skin friction, heat transfer rate and couple stress. It is observed that an increase in m appreciates the skin friction and couple stress while it depreciates the rate of heat transfer. However, as the viscosity ratio K is increased, the skin friction and couple stress decrease while the heat transfer increases. These findings are consistent with what was reported in Zheng *et al.* (2012).

6. Conclusions

The paper considers the steady and incompressible flow phenomena of a micropolar fluid in which a shrinking or stretching sheet is considered. The spectral quasilinearization method was used to numerically solve the coupled system of partial differential equations and results were presented graphically and analysed.

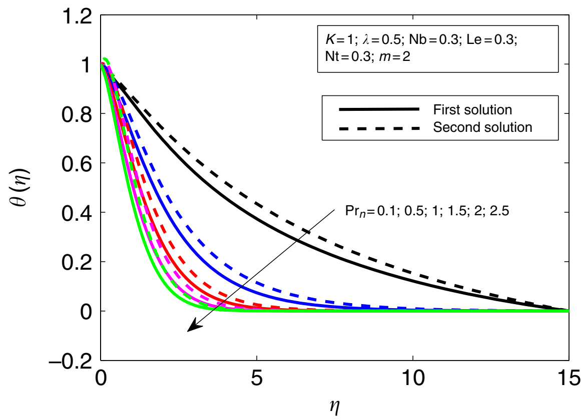

Figure 9.
Effects of Pr_n on temperature profiles

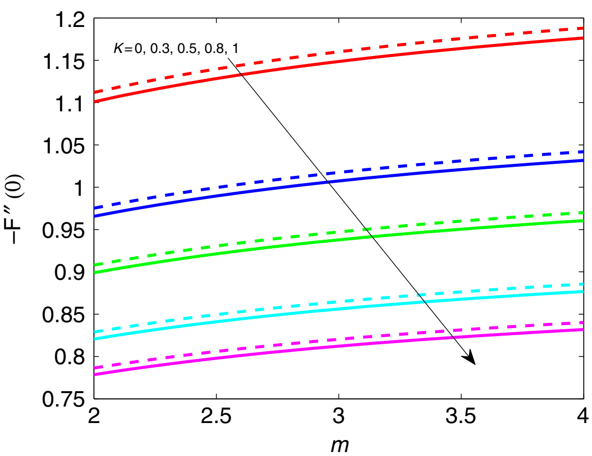

Figure 10.
Skin friction coefficient $-F''(0)$

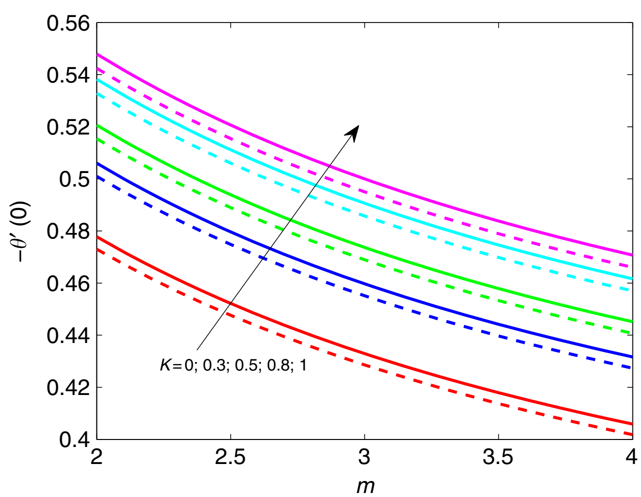

Figure 11.
Heat transfer coefficient $-\theta'(0)$

The study is an extension on the work by Zheng *et al.* (2012). The novelty of this study is that we take into account nanoparticles, Brownian motion and thermophoresis in the flow of a micropolar fluid. The aim of this study was to gain better insight on the phenomenon of boundary layer flow of micropolar nanofluid. The effects of various parameters such as K, Le, Nt, Pr_n on the flow in the presence of thermal radiation were investigated and the following conclusions were drawn from the results:

(1) an increase in the viscosity rate results in the enhancement of momentum boundary layer;

(2) as the viscosity ratio increases, the dual angular velocity decreases for lower values of η but the opposite is true for higher values of η;

(3) an increase in the Lewis number is accompanied by an appreciation of the thermal boundary layer and the depletion of the concentration boundary layer;

(4) an increase in the thermophoresis parameter leads to an increase of both the concentration and temperature boundary layers;

(5) an increase in the Prandtl number results in the depletion of the thermal boundary layer but leads to the thickening of the concentration boundary layer;

(6) an increase in m appreciates the skin friction and couple stress while it depreciates the rate of heat transfer; and

(7) as the viscosity ratio K is increased, the skin friction and couple stress decrease while the heat transfer increases.

7. Implications for research, practice and society

This study considered the flow of micropolar nanofluid by using the spectral quasilinearization method. The study of dual solutions for micropolar nanofluids by applying the quasilinearization method, to the best of our knowledge, has not been considered before. This study therefore aims to enhance a better insight into the dynamics of micropolar nanofluids, as they find wide applications in engineering, technology and industry. In practice, it has been observed that adding nanofluids to a micropolar fluid has the advantage of enhancing the effective heat transfer properties by significantly improving the thermal conductive and convective properties of fluids. This observation has been confirmed by our research and this helps bridge the gap between theory and practice. The spectral quasilinearization technique, which is a recent method, has not been widely used before to study flow regimes involving micropolar nanofluids. Our study therefore plays a role in building up knowledge on the use of the spectral quasilinearization method. This method, which has been found to converge after a few iterations, has several advantages, for example, it is computationally efficient and less time-consuming.

The results of this study, in which we applied spectral quasilinearization method, would create opportunities for collaboration among researchers, some of whom have been using different methods in their own research work. The findings of the study also add knowledge to the discipline of mathematical modelling which can be beneficial to students, especially those focusing on the numerical study of fluid flow. The results of the study would bring to the fore better insight on the dynamics involved in micropolar nanofluid flow and this ensures that more efficient products such as paints, lubricants, coolants, to name just but a few, are manufactured to the benefit of society. The production of improved and more efficient products and new technologies will lead to higher demand for the products and this ensures superior productivity in the industrial, engineering and technology sector. Superior profitability may lead to industrial expansion, increased employment for the society, a better quality of life for the society and this contributes to social, economic and political stability.

References

Agbage, T.M., Mondal, S., Motsa, S.S. and Sibanda, P. (2016), "A numerical study of unsteady non-Newtownian Powell-Eyring nanofluid flow over a shrinking sheet with heat generation and thermal reaction", *Alexandra Engineering Journal*, Vol. 56 No. 1, pp. 81-91.

Ali, M.E. (1995), "On thermal boundary layer on a power-law stretched surface with suction or injection", *International Journal of Heat and Fluid Flow*, Vol. 16 No. 4, pp. 280-290.

Ames, W.F. (2014), *Numerical Methods for Partial Differential Equations*, Academic Press, San Diego, CA.

Bellman, R.E. and Kalaba, R.E. (1965), *Quasilinearization and Nolinear Boundary-Value Problems*, RAND Corporation, Santa Monica, CA.

Bidin, B. and Nazar, R. (2009), "Numerical solution of the boundary layer flow over an exponentially stretching sheet with thermal radiation", *European Journal of Scientific Research*, Vol. 33 No. 4, pp. 710-717.

Canuto, C., Hussaini, M.Y., Quarteroni, A. and Thomas, A. Jr (2012), *Spectral Methods in Fluid Dynamics*, Springer Science & Business Media, Berlin.

Chen, J., Liang, C. and Lee, J.D. (2010), "Theory and simulation of micropolar fluid dynamics", *Proceedings of the Institution of Mechanical Engineers, Part N: Journal of Nanoengineering and Nanosystems*, Vol. 224 Nos 1–2, pp. 31-39.

De, P., Mondal, H. and Bera, U.K. (2015), "Heat and mass transfer in a hydromagnetic nanofluid past a non-linear stretching surface with thermal radiation", *Journal of Nanofluids*, Vol. 4 No. 2, pp. 230-238.

De, P., Mondal, H. and Bera, U.K. (2016), "Dual solutions of heat and mass transfer of nanofluid over a stretching/shrinking sheet with thermal radiation", *Meccanica*, Vol. 51 No. 1, pp. 117-124.

Dhanai, R., Rana, P. and Kumar, L. (2015), "Multiple solutions of MHD boundary layer flow and heat transfer behavior of nanofluids induced by a power-law stretching/shrinking permeable sheet with viscous dissipation", *Powder Technology*, Vol. 273, pp. 62-70, available at: https://doi.org/10.1016/j.powtec.2014.12.035

Eringen, A.C. (1964), "Simple microfluids", *International Journal of Engineering Science*, Vol. 2 No. 2, pp. 205-217.

Eringen, A.C. (1966), "Theory of micropolar fluids", *Journal of Mathematics and Mechanics*, Vol. 16 No. 1, pp. 1-18.

Goqo, S.P., Mondal, S., Sibanda, P. and Motsa, S.S. (2016), "An Unsteady magnetohydrodynamic Jeffery nanofluid flow over a shrinking sheet with thermal radiation and convective boundary condition using spectral quasilinearisation method", *Journal of Computational and Theoretical Nanoscience*, Vol. 13 No. 10, pp. 7483-7492.

Hamid, A., Khan, M. and Khan, U. (2018), "Thermal radiation effects on Williamson fluid flow due to an expanding/contracting cylinder with nanomaterials: dual solutions", *Physics Letters A*, Vol. 382 No. 30, pp. 1982-1991.

Hsiao, K.L. (2017), "Micropolar nanofluid flow with MHD and viscous dissipation effects towards a stretching sheet with multimedia feature", *International Journal of Heat and Mass Transfer*, Vol. 112, pp. 983-990, available at: https://doi.org/10.1016/j.ijheatmasstransfer.2017.05.042

Hussain, S.T., Nadeem, S. and Haq, R.U. (2014), "Model-based analysis of micropolar nanofluid flow over a stretching surface", *The European Physical Journal Plus*, Vol. 129 No. 8, pp. 161-170.

Ishak, A., Nazar, R. and Pop, I. (2009), "Dual solutions in mixed convection boundary layer flow of micropolar fluids", *Communications in Nonlinear Science and Numerical Simulation*, Vol. 14 No. 4, pp. 1324-1333.

Kameswaran, P.K., Shaw, S. and Sibanda, P. (2014), "Dual solutions of Casson fluid flow over a stretching or shrinking sheet", *Sadhana*, Vol. 39 No. 6, pp. 1573-1583.

Liao, S. (2005), "A new branch of solutions of boundary-layer flows over an impermeable stretched plate", *International Journal of Heat and Mass Transfer*, Vol. 48 No. 12, pp. 2529-2539.

Liao, S.J. (2007), “A new branch of solutions of boundary-layer flows over a permeable stretching plate”, *International Journal of Non-Linear Mechanics*, Vol. 42 No. 6, pp. 819-830.

Maripala, S. and Naikoti, K. (2016), “MHD effects on micropolar nanofluid flow over a radiative stretching surface with thermal conductivity”, *Advances in Applied Science Research*, Vol. 7 No. 3, pp. 73-82.

Mishra, S.R., Baag, S. and Mohapatra, D.K. (2016), “Chemical reaction and Soret effects on hydromagnetic micropolar fluid along a stretching sheet”, *Engineering Science and Technology, an International Journal*, Vol. 19 No. 4, pp. 1919-1928.

Mondal, H., Almakki, M. and Sibanda, P. (2019), “Dual solutions for three-dimensional magnetohydrodynamic nanofluid flow with entropy generation”, *Journal of Computational Design and Engineering*, available at: https://doi.org/10.1016/j.jcde.2019.01.003

Motsa, S.S., Dlamini, P.G. and Khumalo, M. (2014), “Spectral relaxation method and spectral quasilinearization method for solving unsteady boundary layer flow problems”, *Advances in Mathematical Physics*, Vol. 2014, 12pp., available at: https://doi.org/10.1155/2014/341964

Motsa, S.S., Sibanda, P. and Shateyi, S. (2011), “On a new quasilinearization method for systems of nonlinear boundary value problems”, *Mathematical Methods in the Applied Sciences*, Vol. 34 No. 11, pp. 1406-1413.

Nadeem, S., Rehman, A., Lee, C. and Lee, J. (2012), “Boundary layer flow of second grade fluid in a cylinder with heat transfer”, *Mathematical Problems in Engineering*, Vol. 2012, 13pp., available at: https://doi.org/10.1155/2012/640289

Nadeem, S., Rehman, A., Vajravelu, K., Lee, J. and Lee, C. (2012), “Axisymmetric stagnation flow of a micropolar nanofluid in a moving cylinder”, *Mathematical Problems in Engineering*, Vol. 2012, 18pp., available at: http://dx.doi.org/10.1155/2012/378259

Noor, N.F.M., Haq, R.U., Nadeem, S. and Hashim, I. (2015), “Mixed convection stagnation flow of a micropolar nanofluid along a vertically stretching surface with slip effects”, *Meccanica*, Vol. 50 No. 8, pp. 2007-2022.

Pal, D. and Mondal, H. (2011), “Effects of Soret Dufour, chemical reaction and thermal radiation on MHD non-Darcy unsteady mixed convective heat and mass transfer over a stretching sheet”, *Communications in Nonlinear Science and Numerical Simulation*, Vol. 16 No. 4, pp. 1942-1958.

Prasad, V.R., Gaffar, S.A. and Bg, O.A. (2014), “Heat and mass transfer of nanofluid from horizontal cylinder to micropolar fluid”, *Journal of Thermophysics and Heat Transfer*, Vol. 29 No. 1, pp. 127-139.

RamReddy, C., Pradeepa, T. and Srinivasacharya, D. (2015), “Numerical study of mixed convection flow of a micropolar fluid towards permeable vertical plate with convective boundary condition”, *Journal of Applied Analysis and Computation*, Vol. 6 No. 2, pp. 254-270.

Raptis, A. (1998), “Flow of a micropolar fluid past a continuously moving plate by the presence of radiation”, *International Journal of Heat and Mass Transfer*, Vol. 18 No. 41, pp. 2865-2866.

Rehman, A. and Nadeem, S. (2012), “Mixed convection heat transfer in micropolar nanofluid over a vertical slender cylinder”, *Chinese Physics Letters*, Vol. 29 No. 12, available at: https://doi.org/10.1088/0256-307X/29/12/124701

Sakiadis, B.C. (1961), “Boundary layer behavior on continuous solid surfaces: I. boundary-layer equations for two-dimensional and axisymmetric flow”, *AIChE Journal*, Vol. 7 No. 1, pp. 26-28.

Schlichting, H. and Gersten, K. (2016), *Boundary-Layer Theory*, Springer, Berlin.

Siddheshwar, P.G., Sekhar, G.N. and Chethan, A.S. (2014), “MHD flow and heat transfer of an exponential stretching sheet in a Boussinesq-Stokes suspension”, *Journal of Applied Fluid Mechanics*, Vol. 7 No. 1, pp. 169-176.

Sithole, H., Mondal, H., Goqo, S., Sibanda, P. and Motsa, S. (2018), “Numerical simulation of couple stress nanofluid flow in magneto-porous medium with thermal radiation and a chemical reaction”, *Applied Mathematics and Computation*, Vol. 339, pp. 820-836, available at: https://doi.org/10.1016/j.amc.2018.07.042

Subhashini, S.V., Sumathi, R. and Pop, I. (2013), "Dual solutions in a thermal diffusive flow over a stretching sheet with variable thickness", *International Communications in Heat and Mass Transfer*, Vol. 48, pp. 61-66, available at: https://doi.org/10.1016/j.icheatmasstransfer.2013.09.007

Sulochana, C., Ashwinkumar, G.P. and Sandeep, N. (2016), "Transpiration effect on stagnation-point flow of a Carreau nanofluid in the presence of thermophoresis and Brownian motion", *Alexandria Engineering Journal*, Vol. 55 No. 2, pp. 1151-1157.

Tan, Y., You, X.C., Xu, H. and Liao, S.J. (2008), "A new branch of the temperature distribution of boundary-layer flows over an impermeable stretching plate", *Heat and Mass Transfer*, Vol. 44 No. 5, pp. 501-504.

Trefethen, L.N. (2000), *Spectral Methods in MATLAB*, Vol. 10, Siam, Philadelphia, PA.

Uddin, M.S., Bhattacharyya, K. and Shafie, S. (2016), "Micropolar fluid flow and heat transfer over an exponentially permeable shrinking sheet", *Propulsion and Power Research*, Vol. 5 No. 4, pp. 310-317.

Zheng, L., Niu, J. and Zhang, X. (2012), "Dual solutions for flow and radiative heat transfer of a micropolar fluid over stretching/shrinking sheet dual solutions for flow and radiative heat transfer of a micropolar fluid over stretching/shrinking sheet", *International Journal of Heat and Mass Transfer*, Vol. 55 Nos 25–26, pp. 7577-7586.

Further reading

Ishak, A. (2011), "MHD boundary layer flow due to an exponentially stretching sheet with radiation effect", *Sains Malaysiana*, Vol. 40 No. 4, pp. 391-395.

Morrison, F.A. (2001), *Understanding Rheology*, Oxford University Press, New York, NY.

Corresponding author
Hiranmoy Mondal can be contacted at: hiranmoymondal@yahoo.co.in

Summary

In this chapter, a study of the dual solutions for a micropolar nanofluid flow past a stretching or shrinking surface was carried out. The model equations were solved numerically by using the spectral quasilinearization method. Important properties of flow were analyzed and presented. The impact of heat radiation, Brownian motion and thermophoresis on the thermal, momentum and concentration profiles was investigated and discussed.

Chapter 3

Effect of Cattaneo-Christov heat flux on the flow of nanofluid between parallel plates

In this chapter, we investigate the impact of Cattaneo-Christov heat flux on the squeezed nanofluid flow between parallel plates. The pioneering study on parallel plates was initiated by Stefan [44]. Squeezing flow between parallel plates finds application in the food processing industry, polymer manufacturing and lubrication technology among numerous others [126]. This study explores the effects of magnetic field, homogeneous chemical reaction, radiation and heat source on the nanofluid flow between squeezing parallel plates. The model equations are solved using the spectral quasilinearization technique that has been shown in the literature to be accurate, robust and to converge rapidly to the correct solution [28]. Detailed discussions on squeezing nanofluid flows between parallel plates can be found in the studies [127–133] among others.

J. Appl. Comput. Mech., xx(x) (2021) 1-11
DOI: 10.22055/JACM.2020.33298.2195

ISSN: 2383-4536
jacm.scu.ac.ir

Shahid Chamran University of Ahvaz

Journal of Applied and Computational Mechanics

Research Paper

Effect of Cattaneo-Christov Heat Flux on Radiative Hydromagnetic Nanofluid Flow between Parallel Plates using Spectral Quasilinearization Method

Mangwiro Magodora[1,2], Hiranmoy Mondal[3], Precious Sibanda[1]

[1] School of Mathematics, Statistics and Computer Science, University of KwaZulu-Natal, Private Bag X01, Scottsvile, Pietermaritzburg-3209, South Africa

[2] DST-NRF Centre of Excellence in Mathematical and Statistical Sciences (CoE-MaSS), University of Zimbabwe, Zimbabwe

[3] Department of Mathematics, Brainware University, Barasat, Kolkata-700125, India

Received April 17 2020; Revised June 20 2020; Accepted for publication June 20 2020.
Corresponding author: H. Mondal (hiranmoymondal@yahoo.co.in)

Abstract. In this paper, we numerically solve the equations for hydromagnetic nanofluid flow past semi-infinite parallel plates where thermal radiation and a chemical reaction are assumed to be present and significant. The objective is to give insights on the important mechanisms that influence the flow of an electrically conducting nanofluid between parallel plates, subject to a homogeneous chemical reaction and thermal radiation. These flows have great significance in industrial and engineering applications. The reduced nonlinear model equations are solved using a Newton based spectral quasilinearization method. The accuracy and convergence of the method is established using error analysis. The changes in the fluid properties with various parameters of interest is demonstrated and discussed. The spectral quasilinearization method was found to be rapidly convergent and accuracy is shown through the computation of solution errors.

Keywords: Cattaneo-Christov; Hydromagnetic flow; Quasilinearization; Chebyshev spectral collocation; Gauss Lobatto grid points.

1. Introduction

A nanofluid consists of a base fluid such as water, kerosene, oil or ethylene glycol and suspensions of nanometer sized particles of average size less than $100nm$ [45]. The nanoparticles are usually metals or metal oxides with higher thermal conductivities than base fluids. The minute size of nanoparticles has the desirable effect of increasing the surface area, which results in increased thermal conductivity of the fluid. Nanoparticles also play the valuable role of improving the viscosity and diffusivity of the base fluid. Nanofluids have important applications in the cooling of heat engines and microsystems, space vehicles, nanomedicine, materials processing, etc. [16]. For this reason, research studies on the rheology of nanofluids has increased on a massive scale in the last few years.

Recently, Muhammad et al. [32] presented a study of bioconvection in the flow of a Carreau nanofluid containing micro-organisms over a wedge. A study using spherical gold (Au) nanoparticles was given by Quresh et al. [38]. Muhammad et al. [35] presented a Darcy-Forcheimer revised model for a nanofluid flow with convective boundary conditions. Sithole et al. [43] discussed the flow of a couple stress nanofluid in a magneto-porous medium while accounting for a chemical reaction and thermal radiation while Pal and Mondal [17] studied the unsteady natural convective MHD boundary-layer flow with a chemical reaction. Sandeep and Sulochana [32] studied the flow of Jeffrey, Maxwell and Oldroyd-B nanofluids with a non-uniform heat source or sink.

Magnetohydrodynamics (MHD) is concerned with the study of electrically conducting fluids. This category of flows finds applications in, *inter alia*, MHD generators, micro MHD pumps, drug delivery, etc. The effects of a magnetic field on different characteristics of electrically conducting fluids have been discussed by, among others, Pal and Mondal [27] and Takhar et al. [47]. Chamkha et al. [4] studied MHD mixed convection flow in a vertical channel. Other studies on MHD flow can be found in Chamkha [4, 6], Patil et al. [18], Pal and Mondal [37], Mondal et al. [26-28] and many others. Research has shown that in wire drawing, subjecting an electrically conducting fluid to a transverse magnetic field may be used to control the rate of stretching and cooling to achieve desirable properties of the finished product [17].

Published online: March 06 2020

Gorla and Chamkha [16] investigated convection in flow past a vertical plate in a porous medium saturated with a nanofluid. Reddy et al. [40] investigated nanofluid flow past a flat plate in a porous medium. They reported that the shape of nanoparticles has a marked effect on the rate of heat transfer. Mondal and Sibanda [29] studied entropy generation in Sakiadis nanofluid flow. Their study revealed that entropy generation rises in tandem with increased Reynolds numbers.

MHD viscous nanofluid flow between parallel plates has of late received considerable attention from researchers due to their wide application in science and industry. Such flows occur in food processing industries, polymer manufacturing industries, lubricating machines, hydro-dynamical equipment among many other areas. The pioneering study on such flows was done by Stefan [46].

A study of unsteady squeezing flow and heat transfer in flow between parallel plates was presented by Mustafa et al. [35]. They observed that the Nusselt number diminishes with the radiation parameter and the Hartmann number but appreciates with increases in the squeeze number and the Eckert number. A squeezing flow of a third grade fluid was investigated by Shafiq et al. [42] while Das and Mohammed [8] investigated unsteady squeezing flow subjected to a magnetic field. Dib et al. [10] obtained analytical solutions of the equations that model unsteady squeezing nanofluid flow using the Duan-Rach Approach. Sobamowo and Akinshilo [44] investigated double diffusive magnetohydrodynamic squeezing nanofluid flow passing two parallel disks with temperature jump and slip boundary conditions using the homotopy perturbation method.

Lately, many researchers have used the Cattaneo-Christov model in place of some classical models in the study of heat transport problems. In these models heat transfer between two objects is due to a temperature gradient existing between the objects. However, it has been noted that Fourier's law has some inadequacies in fully accounting for the characteristics of heat transfer.

Hayat et al. [20] and Farooq et al. [15] analyzed models based on Christov heat and mass fluxes in a porous media. Hayat et al. [19] interrogated stretching surface in Christov heat flux. Additional literature on the Cattaneo-Christov model can be found in Hayat [20-21], Mondal and Sibanda [29], Oyelakin [36] and Dogonchi and Ganji [13].

The objective of this work is to determine the characteristics of nanofluid flow and heat transfer using the Christov heat flux law and to solve the transport equations the spectral quasilinearization method (SQLM). The SQLM is an iterative Newton-based method in which nonlinear terms in a differential equation are linearized using a Taylor series expansion. In the last decade, many studies have been published where the SQLM was used to solve boundary value problems in fluid dynamics. This trend is attributed to the fact that the SQLM has been found to be robust and efficient. Indeed, it leads to faster convergence in comparison with many other numerical methods such as the finite difference method, Runge-Kutta method and so on [[30, 43]. Other recent studies that used the SQLM include papers by Alharbey et al. [1], Magodora et al. [24], Motsa et al. [31], and Pal et al. [37].

In Section 2, we describe the configuration and give the equations that model the flow and the associated boundary conditions for the squeezing flow. In section 3 the steps followed in applying the SQLM to solve model equations are given. The results are discussed in section 4 with comparisons to previously published literature. The convergence analysis of the SQLM is given to justify its use and give confidence to the findings in the study. Methods that give a fast rate of convergence are important in saving computer memory, time and precision. The choices of parameter values used is informed by literature and a consideration of engineering and industrial applications.

2. Mathematical formulation

The two-dimensional incompressible Cattaneo-Christov heat flux model between infinite parallel plates saturated with a nanofluid is considered. The parallel plates are placed at $\pm H(t) = \pm l(1-\alpha t)^{0.5}$ where l is the position at $t = 0$ and α is the squeezing parameter with dimensions of 1/[time]. For the values of $\alpha > 0$, the parallel plates are squeezed with velocity $v(t) = dH/dt$ at $t = 1/\alpha$, while for $t < 0$, the plates are pulled apart $K_1(t) = k_0/(1-\alpha t),$. The nanofluid is assumed to be Newtonian. A homogeneous reaction and the base fluid, having the time-dependent reaction rate, is assumed while a time-dependent magnetic field $B(t) = B_0(1-\alpha t)^{-0.5}$ is applied across the two parallel plates [13, 35]. The slip velocity is assumed to be negligible. Copper nanoparticles are suspended in water which is the base fluid. The thermal and physical properties of these nanofluids are shown in Table 1. The orientations of the x-axis and the y-axis appear in Fig. 1. The velocity components u and v are oriented in x and y directions, respectively. A heat source is placed between plates as depicted on Fig. 1. In tandem with the above assumptions the model equations for mass conservation, linear momentum conservation, energy conservation and mass diffusion are given as:

$$\frac{\partial u}{\partial x} + \frac{\partial v}{\partial y} = 0 \tag{1}$$

$$\rho_{nf}\left(\frac{\partial u}{\partial t} + u\frac{\partial u}{\partial x} + v\frac{\partial u}{\partial y}\right) = -\frac{\partial P}{\partial x} + \mu_{nf}\left(\frac{\partial^2 u}{\partial x^2} + \frac{\partial^2 u}{\partial y^2}\right) - \sigma_f B^2(t)u, \tag{2}$$

$$\rho_{nf}\left(\frac{\partial v}{\partial t} + u\frac{\partial v}{\partial x} + v\frac{\partial v}{\partial y}\right) = -\frac{\partial P}{\partial y} + \mu_{nf}\left(\frac{\partial^2 v}{\partial x^2} + \frac{\partial^2 v}{\partial y^2}\right), \tag{3}$$

$$\left(\rho C_p\right)_{nf}\left(\frac{\partial T}{\partial t} + u\frac{\partial T}{\partial x} + v\frac{\partial T}{\partial y} + \varepsilon\Delta\right) = k_{nf}\left(\frac{\partial^2 T}{\partial x^2} + \frac{\partial^2 T}{\partial y^2}\right) - \frac{\partial q_r}{\partial y} + Q_0 T, \tag{4}$$

$$\frac{\partial C}{\partial t} + u\frac{\partial C}{\partial x} + v\frac{\partial C}{\partial y} = D_B\frac{\partial^2 C}{\partial y^2} + \frac{D_T}{T_\infty}\left(\frac{\partial^2 T}{\partial y^2}\right) + K_1(t)C, \tag{5}$$

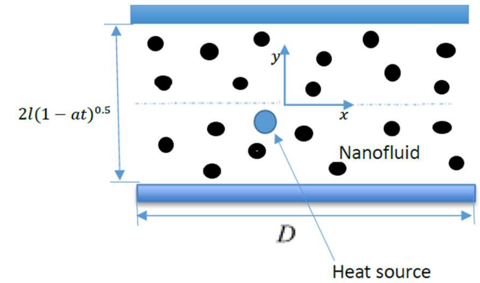

Fig. 1. Flow configuration

where D_T is the thermophoretic diffusion, D_B is the Brownian diffusion, p is the pressure of nanofluid, k_0 is the uniform reaction rate, B_0 is the uniform magnetic field, q_r is the radiative heat flux and:

$$\Delta=\frac{\partial^2 T}{\partial y^2}+\frac{\partial u}{\partial t}\cdot\frac{\partial T}{\partial x}+2u\frac{\partial^2 T}{\partial t\partial x}+2v\frac{\partial^2 T}{\partial t\partial y}+\frac{\partial v}{\partial t}\frac{\partial T}{\partial y}+u\frac{\partial u}{\partial x}\frac{\partial T}{\partial x}+v\frac{\partial v}{\partial y}\frac{\partial T}{\partial y}+u\frac{\partial v}{\partial x}\frac{\partial T}{\partial y}+v\frac{\partial u}{\partial y}\frac{\partial T}{\partial x}+2uv\frac{\partial^2 T}{\partial x\partial y}+u^2\frac{\partial^2 T}{\partial x^2}+v^2\frac{\partial^2 T}{\partial y^2}. \tag{6}$$

The dynamic viscosity is calculated from the Brinkman model [14] as:

$$\mu_{nf}=\frac{\mu_f}{(1-\varphi)^{2.5}} \tag{7}$$

The other properties of nanofluid are defined as in Rashidi et al. [39]:

$$\rho_{nf}=(1-\varphi)\rho_f+\varphi\rho_s \tag{8}$$

$$\left(\rho C_p\right)_{nf}=(1-\varphi)\left(\rho C_p\right)_f+\varphi\left(\rho C_p\right)_s \tag{9}$$

$$\frac{k_{nf}}{k_f}=\frac{k_s+2k_f-2\varphi(k_f-k_s)}{k_s+2k_f+2\varphi(k_f-k_s)}. \tag{10}$$

The boundary conditions for the model are (refer to Dogonchi and Ganji [13] and Mustafa et al. [35]):

$$\begin{aligned}&u=0, v=v_w=\frac{dH}{dt}, T=T_H, C=C_H, \text{ at } \ y=H(t),\\ &\frac{\partial u}{\partial y}=v=\frac{\partial C}{\partial y}=\frac{\partial T}{\partial y}=0 \ \text{ at } y=0,\end{aligned} \tag{11}$$

where v_w denotes velocity at the plate surface. By the Roseland approximation, the radiative index q_r is taken as $q_r=-4\sigma^* / 3k_{nf}^*(\partial T^4/\partial y)$ and $T^4=4T_\infty^3 T-3T_\infty^4$. This implies that $\partial q_r/\partial y=-(16/3)(\sigma^* T_\infty^3/k_{nf}^*)\partial T/\partial y$, hence (4) becomes:

$$\frac{\partial T}{\partial t}+u\frac{\partial T}{\partial x}+v\frac{\partial T}{\partial y}+\varepsilon\Delta=\frac{k_{nf}}{(\rho C_p)_{nf}}\left(\frac{\partial^2 T}{\partial x^2}+\frac{\partial^2 T}{\partial y^2}\right)+\frac{16\sigma^* T_\infty^3}{3(\rho C_p)_{nf}k_{nf}^*}\frac{\partial^2 T}{\partial y^2}+\frac{Q_0}{(\rho C_p)_{nf}}T, \tag{12}$$

Let ψ denote the stream function such that $u=\partial\psi/\partial y$ and $v=-\partial\psi/\partial x$, we introduce the following dimensionless variables:

$$\eta=\frac{y}{l\sqrt{1-\alpha t}}, \theta(\eta)=\frac{T}{T_H}, u=\frac{\alpha x}{2(1-\alpha t)}f'(\eta), v=-\frac{\alpha l}{2\sqrt{1-\alpha t}}f(\eta), g(\eta)=\frac{C}{C_H}, \tag{13}$$

Upon effecting the above similarity variables, the model equations and their associated boundary conditions transform to:

$$f^{iv}-\alpha_1 S(3f''+f'f''+\eta f'''-ff''')-\alpha_2 M f''=0, \tag{14}$$

$$\theta''+\beta_1[f\theta'-\eta\theta'-\gamma(\eta^2\theta''-\eta f'\theta'-2\eta f\theta''+ff'\theta'+f^2\theta'')]+\beta_2\theta=0, \tag{15}$$

$$g''+ScS(fg'-\eta g')-Sc\zeta g=0, \tag{16}$$

The boundary conditions are:

$$\begin{aligned}&f(0)=0, f''(0)=0, \theta'(0)=0, g'(0)=0,\\ &f(1)=1, f'(1)=0, \theta(1)=1, g(1)=1,\end{aligned} \tag{17}$$

Table 1. Material properties of base fluid and nanoparticles.

Property	Water (base fluid)	Copper (nanoparticles)
Density, ρ (kgm^{-3})	997.1	893.3
Specific heat capacity, C_p $\left(Jkg^{-1}K^{-1}\right)$	4179	385
Thermal conductivity, $\kappa\left(Wm^{-1}K^{-1}\right)$	0.613	401

where $\alpha_1 = A_1 / A_2$, $\alpha_2 = 1/A_2$, $\beta_1 = \Pr S A_3 / A_4(3N/(3N+4))$, $\beta_2 = (H_s / A_4)(3N/(3N+4))$. The dimensionless constants A_i for i = 1, 2, 3, 4 are defined as $A_1 = \rho_{nf} / \rho_f$, $A_2 = \mu_{nf} / \mu_f$, $A_3 = (\rho C_p)_{nf} / (\rho C_p)_f$ and $A_4 = k_{nf} / k_f$. Here Pr is the Prandtl number, Sc the Schmidt number, S the squeeze number, ζ is the chemical reaction parameter, H_s the heat source parameter, M the magnetic parameter, N the radiation parameter, γ the reaction parameter are defined as:

$$\Pr = \frac{\upsilon_f(\rho C_p)_f}{k_f},\ Sc = \frac{\upsilon_f}{D_B},\ \zeta = \frac{k_0 l^2}{\upsilon_f},\ S = \frac{\alpha l^2}{2\upsilon_f},\ H_S = \frac{Q_0 l^2(1-\alpha t)}{k_f},\ N = \frac{k^*_{nf} k_{nf}}{4\sigma^* T^3_\infty},\ \gamma = \frac{\alpha\varepsilon}{2(1-\alpha t)},\ M = \frac{\sigma_{nf}(1-\alpha t) l^2 B_0^2}{\mu_f}. \tag{18}$$

Physical properties of scientific and engineering interest are the skin friction C_f, the Nusselt number Nu_f and the Sherwood number Sh_f are defined by:

$$C_f \upsilon_w^2 = \frac{\mu_{nf}}{\rho_f}\frac{\partial u}{\partial y}\bigg|_{y=h(t)},\ k_f T_H Nu_f = \left(k_{nf} + \frac{16\sigma^* T^*_\infty}{3k^*_{nf}}\right)\frac{\partial T}{\partial y}\bigg|_{y=h(t)},\ Sh_f = -\frac{1}{C_H}\frac{\partial C}{\partial y}\bigg|_{y=h(t)} \tag{19}$$

They are deduced from eq. (13) and eq. (19) as:

$$C_f = \left|A_2 f''(1),\right|,\quad Nu = \left|A_4\left(\frac{3N+4}{3N}\right)\right|,\ \sqrt{1-\alpha t} = -g'(1). \tag{20}$$

3. Method of Solution

The method of quasilinearization is used to linearize the nonlinear ordinary differential eq. (14)-(16). Details of this method can be found in Bellman and Kalaba [2]. The iterative scheme that is obtained from applying quasilinearization is:

$$f^{iv}_{r+1} + a_{13r} f'''_{r+1} + a_{12r} f''_{r+1} - a_{11r} f'_{r+1} + a_{10r} f_{r+1} = R_1 \tag{21}$$

$$a_{21r} f'_{r+1} + a_{20r} f_{r+1} + b_{22r}\theta''_{r+1} + b_{21r}\theta'_{r+1} + b_{20r}\theta_{r+1} = R_2 \tag{22}$$

$$a_{30r} f_{r+1} + g'''_{r+1} + c_{31r} g'_{r+1} - c_{30r} g_{r+1} = R_3, \tag{23}$$

where

$$a_{13r} = \alpha_1 S(f_r - \eta), a_{12r} = \alpha_1 S(3 + f'_r) + \alpha_2 M, \tag{24}$$

$$a_{11r} = \alpha_1 S f'_r, a_{10r} = \alpha_1 f''_r, \tag{25}$$

$$a_{21r} = \beta_1\gamma\theta'_r - \beta_1\gamma f_r\theta'_r,\ a_{20r} = \beta_1\theta'_r + 2\beta_1\gamma\eta\theta''_r - \beta_1\gamma f'_r\theta'_r - 2\beta_1\gamma f_r\theta''_r, \tag{26}$$

$$b_{22r} = 1 - 1\beta_1\gamma\eta^2 + 2\beta_1\gamma\eta f_r - \beta_1\gamma f_r^2, b_{21r} = \beta_1 f_r - \beta_1\eta + \beta_1\gamma\eta f'_r - \beta_1\gamma f_r f'_r, \tag{27}$$

$$b_{20r} = \beta_2, a_{30r} = Sc S g'_r, c_{31r} = Sc S f_r - Sc S\eta, c_{30r} = Sc\zeta, \tag{28}$$

with the boundary conditions are

$$\begin{aligned} &f_{r+1}(0) = 0, f'_{r+1}(0) = 0, \theta'_{r+1}(0) = 0, g'_{r+1}(0) = 0, \\ &f_{r+1}(1) = 1, f'_{r+1}(1) = 0,\ \theta_{r+1}(1) = 1,\ g_{r+1}(1) = 1, \end{aligned} \tag{29}$$

where the subscript r denote the previous approximation while the r+1 denotes the current iteration. Further discussion of the quasilinearization method can be found in Magodora et al. [24], Motsa et al. [30], Mondal and Bharti [28] and Mondal and Sibanda [29].

The next step in using the SQLM is to apply the spectral method to the linearized system eq. (23) - (25). Details of the spectral method can be found in Canuto et al. [3], Sithole et al. [43], Pal et al. [37] and Trefethen [48]. The domain of the problem is $\eta \in [0,1]$.

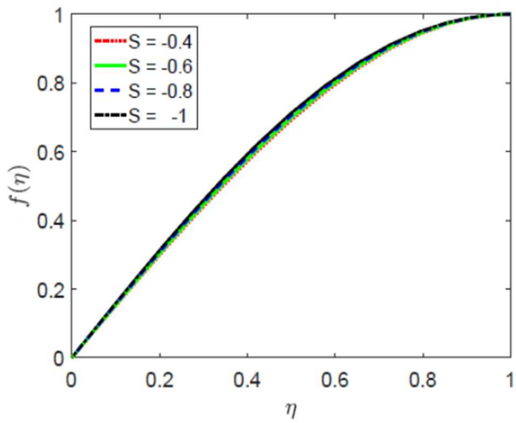

Fig. 2. The impact of squeeze parameter S on nanofluid velocity.

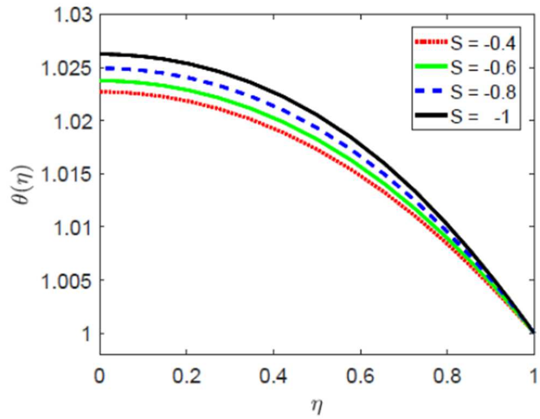

Fig. 3. The impact of squeeze parameter S on temperature.

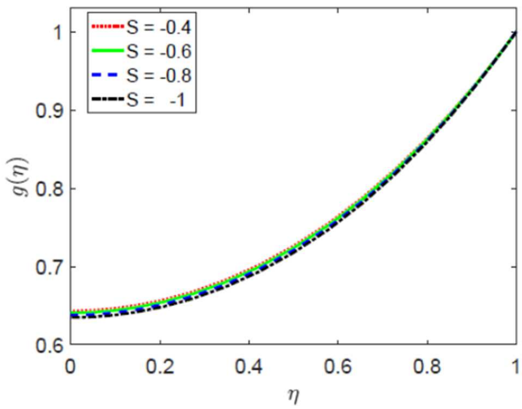

Fig. 4. The impact of squeeze parameter S on concentration of diffusing species.

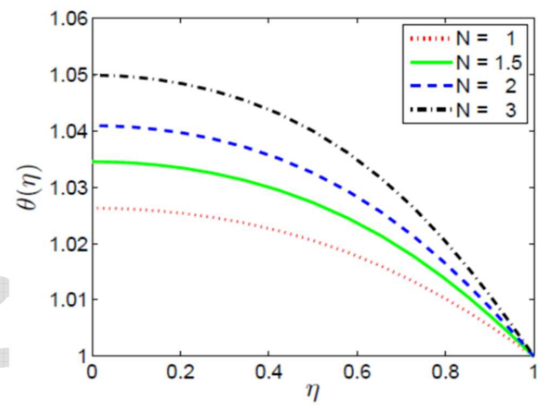

Fig. 5. The impact of the radiation parameter N on temperature.

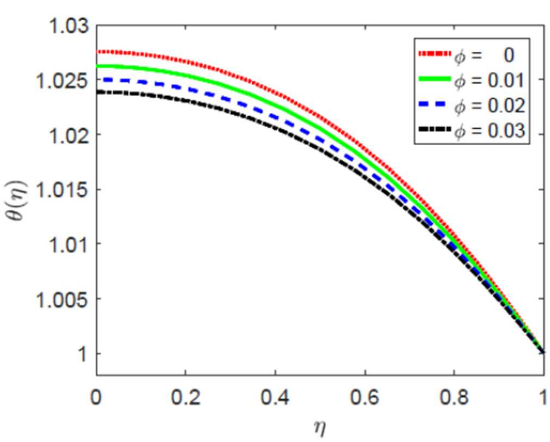

Fig. 6. The impact of solid volume fraction φ on temperature.

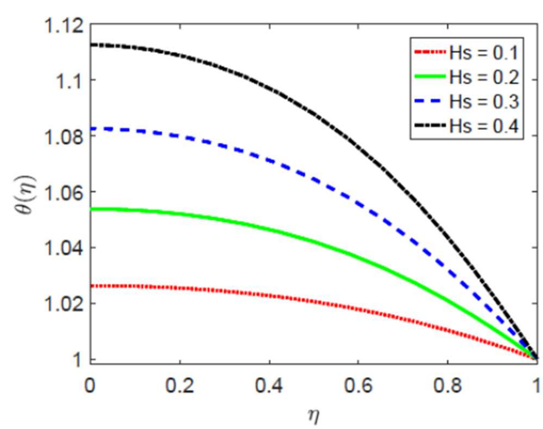

Fig. 7. The impact of heat source parameter H_S on temperature of diffusing species.

To solve the system (22)-(24) with the spectral method, we convert the domain $\eta \in [0,1]$ to $z \in [-1,1]$ by letting $\eta = (z+1)/2$. For discretization, we use the Gauss-Lobatto grid points $\eta_i = \cos(\pi i / N)$ for $i = 0, 1, 2, \ldots, N$. The derivatives at the Gauss-Lobatto nodes are calculated as $df_n / d\eta|_{\eta_i} = \sum_{w=0}^{N} D_{iw} f_n(\eta_w)$, where D is the Chebyshev differential matrix and $D_{iw} f_n(\eta_w) = d\tau_w(\eta_i)/d\eta$. Higher order derivatives are defined as $d^p f_n / d\eta^p{}_{\eta_i} = D^p F_n$ where $D^p F_n = \sum_{w=0}^{N_\eta} D^p_{iw} f_n(\eta_w)$ and $F_n = [f_n(\eta_0), f_n(\eta_1), \ldots, f_n(\eta_N)]^T$ and T denotes transpose of the matrix.

The following initial guesses are chosen in such a way that they satisfy the boundary conditions

$$r = -\frac{1}{2}\eta^3 + \frac{3}{2}\eta,\ \theta = \eta^2,\ and\ g = \eta^2.$$

Applying spectral method to system (21)-(23) yields

$$A_{11} f_{r+1} + A_{12}\theta_{r+1} + A_{13} g_{r+1} = R_1 \tag{30}$$

$$A_{21} f_{r+1} + A_{22}\theta_{r+1} + A_{23} g_{r+1} = R_2 \tag{31}$$

$$A_{31} f_{r+1} + A_{32}\theta_{r+1} + A_{33} g_{r+1} = R_3 \tag{32}$$

The boundary conditions for f, θ, g and their derivatives are imposed on the first row, second row, second last row or last row of the square matrices A_{11}, A_{22} and A_{33} as illustrated by Sithole et al. [43]. The linear system AY=R is then solved using MATLAB code where

$$A = \begin{pmatrix} A_{11} & A_{12} & A_{13} \\ A_{21} & A_{22} & A_{23} \\ A_{31} & A_{32} & A_{33} \end{pmatrix},\ \ Y = [f_{r+1}\theta_{r+1}g_{r+1}]^T,\ R = [R_1 R_2 R_3]^T \tag{33}$$

4. Results and discussion

The study used the spectral quasilinearization method to investigate the momentum, thermal and concentration properties of a hydromagnetic flow of copper nanofluid between parallel plates in the presence of a homogeneous chemical reaction and thermal radiation. The validity of our methodology and accuracy of results is demonstrated in Table 2 by comparison with previously published results. Excellent agreement is observed.

To show the convergence of the numerical scheme, we computed the solution errors in f, θ, g respectively. The solution errors give the differences between successive iterations, as defined by the norms above. The solution errors are shown in Figs. 13-15 and it is observed that they all reduce, to the order of 10^{-12} after a few iterations, thereby demonstrating fast convergence of the numerical scheme.

The different profiles when the parameters $S, M, \varphi, \gamma, N, H_S$, Sc and ζ are varied are shown in Figs. 2-11. For the purpose of our numerical simulation we have used the values of $S=1$, $M=1$, $\varphi=0.01$, $\Pr=1$, $Sc=1$, $\gamma=0.1$, $N=1$, $H_S=0.1$ and $\zeta=1$ unless otherwise stated. When a particular parameter is varied, all other parameters are taken to be constant.

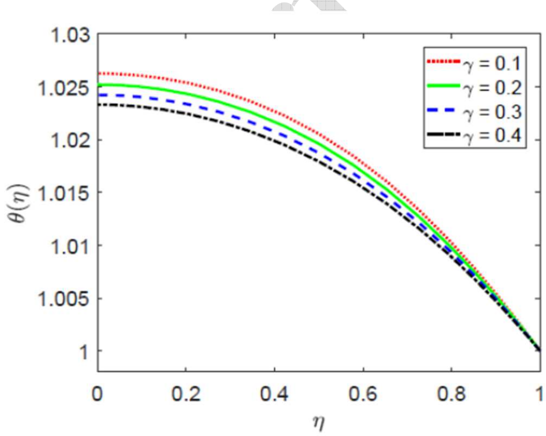

Fig. 8. The impact of the relaxation parameter γ on temperature.

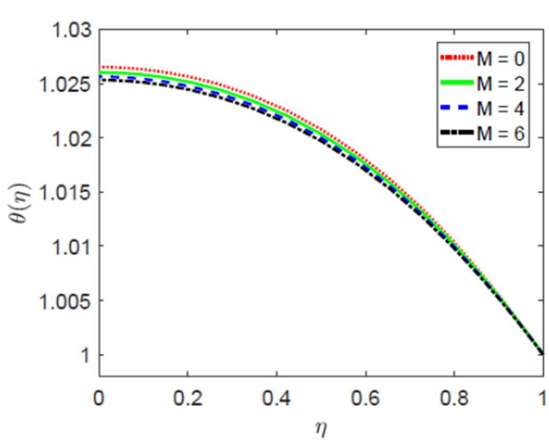

Fig. 9. The impact of magnetic parameter M on temperature.

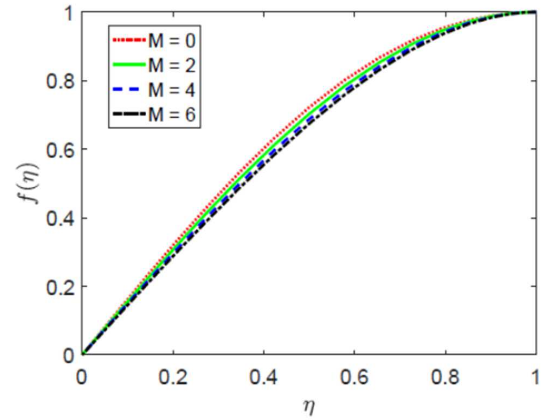

Fig. 10. The impact magnetic parameter M on velocity.

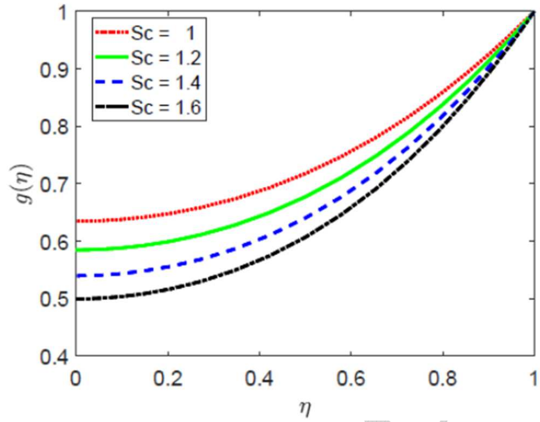

Fig. 11. The impact of the Schmidt number Sc on concentration.

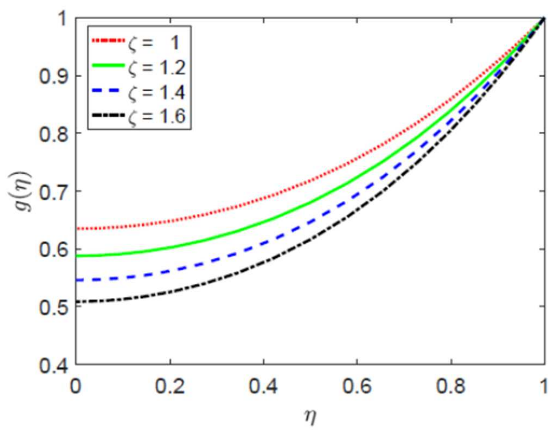

Fig. 12. The impact of chemical reaction parameter ζ on concentration.

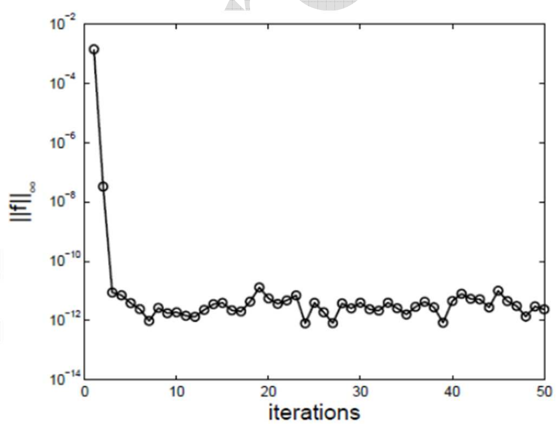

Fig. 13. Solution error for f when $S = -0.3, \varphi = 0.01$, $M = 0.1$, $Sc = 1$ and $\zeta = 1$.

Figs. 2-4 indicate the influence of the squeezing parameter S, on the various profiles. A downward variation of the squeezing parameter is associated with increased momentum and thermal boundary layers, while the opposite is true for the concentration boundary layer. We considered only negative values of S which correspond to squeezing flow where the plates move towards each other. This action squeezes out the nanofluid and enhances the fluid velocity. Coupled with a greater surface area of the nanoparticles, increased velocity implies enhanced kinetic energy of the nanofluid. This in turn leads to higher thermal conductivity in the nanofluid, hence the increased temperature profiles. It is also apparent that the increased reaction rate causes the species diffusion to reduce significantly due to enhanced velocity and temperature of nanofluid.

The influence of the radiation parameter *N* on the temperature profiles is shown in Fig. 5 where an increase in radiation leads to an increase in the temperature. As expected, this rise in the temperature increases the Nusselt number as shown in Table 3. It is assumed there is no velocity slip, and as a consequence, Fig. 6 shows that an increase in the volume fraction φ, reduces the fluid temperature profiles. The volume fraction is the volumetric concentration of the nanoparticles in the base fluid. Such a relationship between the volume fraction and the temperature were also obtained by Dongonchi et al. [8].

The temperature profiles when heat source parameter *Hs* is varied, is illustrated in Fig. 7. It is observed, as would be expected, that the temperature increases with the heat source parameter. The physical interpretation of this scenario is that an increased heat source parameter implies increased heat energy being released into the flow, thereby enhancing the thermal boundary layer thickness.

Figure 8 shows the impact of different values of the relaxation parameter γ, where an increase in γ is accompanied by a diminished thermal boundary layer hence a reduced temperature profile. Figures 9 and 10 show the impact of the magnetic parameter on the thermal and momentum profiles respectively. An increased magnetic field reduces the thermal and momentum boundary layers. Strengthening the magnetic field normal to the flow causes the rise of a Lorenz force, which opposes the flow of the electrically conducting nanofluid.

Table 2. Comparison of skin friction coefficient and local Sherwood number values as squeeze parameter S varies at x=1 and when $\mathrm{Sc}=1$, $\mathrm{Pr}=1$, $\varphi=0.01$, $H_S=0$, .

S	$-f''(1)$			$g'(1)$	
	Mustafa et al. [35]	Dogonchi and Ganji [11]	Present Result	Mustafa et al.[35]	Present Results
2	4.1673389	4.167041	4.1673892	0.7018132	0.7018132
0.5	3.336449	3.336449	3.3364495	0.7442243	0.7442243
0.01	3.007134	3.007133	3.0071338	0.7612252	0.7612252
-0.5	2.614038	2.617403	2.6174038	0.7814023	0.7814023
-1	2.170090	2.170090	2.1700909	0.8045580	0.8045588

Table 3. Effects of certain parameters on skin friction coefficient, local Nusselt and Sherwood numbers.

Parameter	Value	$-f''(1)$	$-\theta'(1)$	$g'(1)$
φ	0	2.4244886	0.0595669	0.8030504
	0.01	2.3706990	0.0565725	0.8033708
S	-0.4	2.8912768	0.0465793	0.7768018
	-0.6	2.7288755	0.0494688	0.7850880
γ	0.1	2.3706990	0.0565725	0.8033708
	0.2	2.3706990	0.0540696	0.8033708
M	0	2.1179478	0.0572280	0.8048802
	2	2.6048013	0.0559913	0.8048802
H_S	0.1	2.3706990	0.0565725	0.8033708
	0.2	2.3706990	0.1153963	0.8033708
ζ	1	2.3706990	0.0565725	0.9205214
	1.2	2.3706990	0.0565725	1.1287782

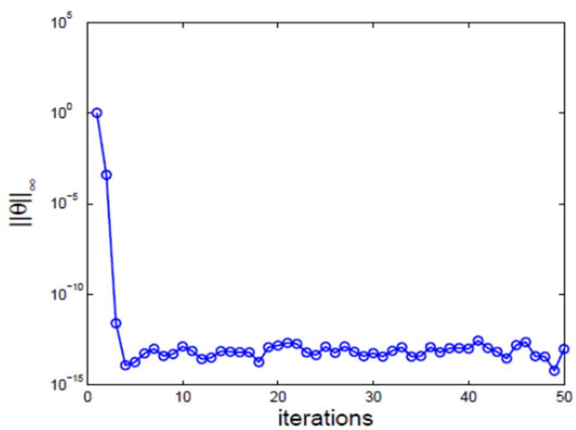

Fig. 14. Solution error for θ when $S=-0.3, \varphi=0.01$, $M=0.1$, $Sc=1$ and $\zeta=1$.

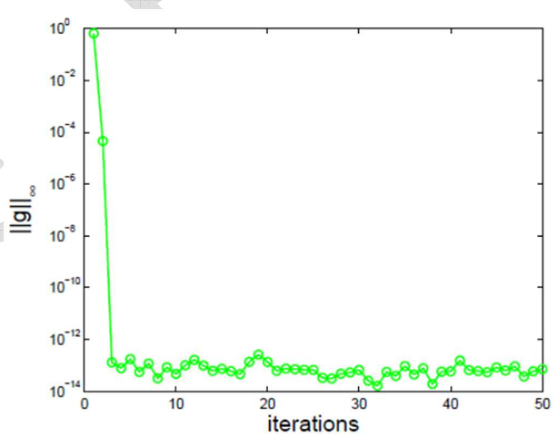

Fig. 15. Solution error for g when $S=-0.3, \varphi=0.01$, $M=0.1$, $Sc=1$, and $\zeta=1$.

The effect of different values of Schmidt number on the species concentration profiles is shown in Fig. 11. The Schmidt number is a ratio of mass diffusion to momentum diffusion. It is noted that reduced molecular activity occurs due to increased Schmidt number. The influence of the chemical reaction parameter ζ on the species concentration is portrayed in Fig. 12. It is noticeable that an increased chemical reaction parameter leads to increased chemical reaction, which consequently leads to decreased concentration of the diffusing species, as expected. Table 3 shows the effects of varying the parameter S, M, φ, γ, H_S and ζ on $-f''(1)$, $\theta'(1)$ and $g'(1)$. It is apparent that an increase in the magnetic parameter M is associated with a decrease in $\theta'(1)$ *and* $g'(1)$ but is accompanied by an increase in $-f''(1)$.

5. Conclusion

The study considered heat and mass transfer in an electrically conducting nanofluid between parallel plates with radiation, homogeneous chemical reaction and a magnetic field that is transverse to the flow. The model equations were solved numerically using the spectral quasilinearization method. The accuracy of the method was shown through convergence analysis and by comparing current results with published results in the literature, excellent agreement was established. This study illustrates the efficiency and precision of the spectral quasilinearization method in solving nonlinear flow problems. The impact of the Schmidt number Sc, the relaxation parameter γ , the squeeze parameter S, the solid volume fraction φ , the radiation parameter N, the heat source parameter H_S, the magnetic parameter M and the chemical reaction parameter ζ on the skin friction coefficient, Nusselt number, Sherwood number, velocity, temperature and concentration profiles was examined and the results discussed in detail. Highlights of the results from the study are that:

1. An increase in the magnetic parameter leads to a decrease in the local Nusselt and Sherwood numbers but is accompanied by an increase in the skin friction coefficient.
2. An increase in the volume fraction acts to reduce the Sherwood numbers.
3. The temperature decreased with the relaxation parameter and increased with the heat source parameter.

Author Contributions

The manuscript was written through the contribution of all authors. All authors discussed the results, reviewed and approved the final version of the manuscript.

Acknowledgement

The authors are grateful for the financial support rendered by the University of KwaZulu-Natal and the DST-NRF Centre of Excellence in Mathematical and Statistical Sciences (CoE-MaSS).

Conflict of Interest

The authors declared no potential conflicts of interest with respect to the research, authorship and publication of this article.

Nomenclature

A_i	dimensionless constants, where i =1, 2, 3, 4	Sc	Schmidt number
$B(t)$	variable magnetic field	$SQLM$	spectral quasilinearization method
B_0	uniform magnetic field	T	temperature (K)
C	concentration (mol/m^3)	T_H	temperature of plate (K)
C_H	concentration at plate surface (mol/m^3)	T_∞	free stream temperature (K)
C_∞	free stream concentration (mol/m^3)	*Greek letters*	
C_p	specific heat capacity ($Jkg^{-1}K^{-1}$)	α	squeeze rate (s^{-1})
D_B	Brownian diffusion	η	dimensionless variable
D_T	thermophoretic diffusion	ρ	density (kgm^{-3})
f	dimensionless velocity	φ	volume fraction of nanoparticles
g	dimensionless concentration	Θ	dimensionless temperature
Hs	heat source parameter	σ	electrical conductivity (Ωm)
k	thermal conductivity ($Wm^{-1}K^{-1}$)	σ^*	Stefan-Boltzmann constant
k_0	uniform reaction rate	μ	dynamic viscosity (Nsm^{-2})
k^*	mean absorption coefficient	υ	kinematic viscosity (m^2s^{-1})
$K_1(t)$	time - dependent reaction rate	γ	reaction parameter
M	magnetic parameter	ζ	chemical reaction parameter
N	radiation parameter	*Subscripts*	
Pr	Prandtl number	f	base fluid
q_r	radiative heat flux	nf	nanofluid
S	squeeze parameter		

References

[1] Alharbey, R.A., Mondal, H., Behl, R., Spectral Quasilinearization Method for Non-Darcy Porous Medium with Convective Boundary Condition, *Entropy*, 21(9), 2019, 838-850.
[2] Bellman, R.E., Kalaba, R.E., *Quasilinearization and nonlinear boundary-value problems,* American Elsevier Pub. Co., New York, 1965.
[3] Canuto, C., Hussaini, M.Y., Quarteroni, A., Thomas Jr, A., *Spectral methods in fluid dynamics,* Springer-Verlag, Heidelberg, 1988.
[4] Chamkha, A.J., On laminar hydromagnetic mixed convection flow in a vertical channel with symmetric and asymmetric wall heating conditions, *International Journal of Heat and Mass Transfer*, 45(12), 2002, 2509-2525.
[5] Chamkha, A.J., Takhar, H.S., Soundalgekar, V.M., Radiation effects on free convection flow past a semi-infinite vertical plate with mass transfer, *Chemical Engineering Journal*, 84(3), 2001, 335-342.
[6] Chamkha, A.J., Nath, G., MHD flow over a moving plate in a rotating fluid with magnetic field, Hall currents and free stream velocity, *International Journal of Engineering Science*, 40(13), 2002, 1511-1527
[7] Daniel, Y.S., Aziz, Z.A., Ismail, Z., Salah, F., Entropy analysis in electrical magnetohydrodynamic (MHD) flow of nanofluid with effects of thermal radiation, viscous dissipation, and chemical reaction, *Theoretical and Applied Mechanics Letters*, 7(4), 2017, 235-242.
[8] Das, K., Mohammed, U., Radiation effects on an unsteady squeezing flow in the presence of a magnetic field, *Moldavian Journal of the Physical Sciences*, 15(1-2), 2002, 101-110.
[9] De, P., Mondal, H., Bera, U.K., Heat and Mass Transfer in a Hydromagnetic Nanofluid Past a Non-Linear Stretching Surface with Thermal Radiation, *Journal of Nanofluids*, 4(2), 2015, 230-238.
[10] Dib, A., Haiahem, A., Bou-Said, B., Approximate analytical solution of squeezing unsteady nanofluid flow, *Powder Technology*, 269, 2015, 193-199.
[11] Dogonchi, A.S., Divsalar, K., Ganji, D.D., Flow and heat transfer of MHD nanofluid between parallel plates in the presence of thermal radiation, *Computer Methods in Applied Mechanics and Engineering*, 310, 2016, 58-76.
[12] Dogonchi A.S., Ganji D.D., Investigation of MHD nanofluid flow and heat transfer in a stretching/shrinking convergent/divergent channel considering thermal radiation, *Journal of Molecular Liquids*, 220, 2016, 592-603.
[13] Dogonchi, A.S., Ganji, D.D., Impact of Cattaneo-Christov heat flux on MHD nanofluid flow and heat transfer between parallel plates considering thermal radiation effect, *Journal of the Taiwan Institute of Engineers*, 80, 2017, 52-63
[14] Fadhilah, S.A., Hidayah, I., Hilwa, M.Z., Faizah, H.N., Marhamah, R.S., Thermophysical properties of Copper/Water nanofluid for automotive cooling system, *Journal of Mechanical Engineering and Technology*, 5(2), 2013, 1-10.
[15] Farooq, M., Ahmad, S., Javed, M., Anjum, A., Analysis of Cattaneo-Christov heat and mass fluxes in the squeezed flow embedded in porous medium with variable mass diffusivity, *Results in Physics*, 7, 2017, 3788-3796.

[16] Gorla, R.S.R., Chamkha, A., Natural Convective Boundary Layer Flow Over a Nonisothermal Vertical Plate Embedded in a Porous Medium Saturated With a Nanofluid, *Nanoscale and Microscale Thermophysical Engineering*, 15(2), 2011, 81-94.
[17] Haroun, N.A., Mondal, S., Sibanda, P., Unsteady natural convective boundary-layer flow of MHD nanofluid over a stretching surfaces with chemical reaction using the spectral relaxation method: A revised model, *Procedia Engineering*, 127, 2015, 18-24.
[18] Haroun, N.A., Sibanda, P., Mondal, S., Motsa, S.S., On unsteady MHD mixed convection in a nanofluid due to a stretching/shrinking surface with suction/injection using the spectral relaxation method, *Boundary value problems*, 2015, 2015, 24.
[19] Hayat, T., Farooq, M., Alsaedi, A., Al-Solamy, F., Impact of Cattaneo-Christov heat flux in the flow over a stretching sheet with variable thickness, *AIP Advances*, 5(8), 2015, 087159.
[20] Hayat, T., Muhammad, K., Farooq, M., Alsaedi, A., Squeezed flow subject to Cattaneo-Christov heat flux and rotating frame, *Journal of Molecular Liquids*, 220, 2016, 216-222.
[21] Hayat, T., Khan, M.W.A., Alsaedi, A., Ayub, M., Khan, M.I., Stretched flow of Oldroyd-B fluid with Cattaneo-Christov heat flux, *Results in Physics*, 7, 2017, 2470-2476.
[22] Khan, N.A., Aziz, S., Ullah, S., Entropy generation on MHD flow of Powell-Eyring fluid between radially stretching rotating disk with diffusion-thermo and thermo-diffusion effects, *Acta Mechanica et Automatica*, 11(1), 2017, 20-32.
[23] Hussain, S.A., Muhammad, S., Ali1, G., Shah, S.I.A., Ishaq, M., Shah, Z., Khan, H., Tahir, M., Naeem, M., A Bioconvection Model for Squeezing Flow between Parallel Plates Containing Gyrotactic Microorganisms with Impact of Thermal Radiation and Heat Generation/Absorption, *Journal of Advances in Mathematics and Computer Science*, 27(4), 2018, 1-22
[24] Magodora, M., Mondal, H., Sibanda, P., Dual solutions of a micropolar nanofluid flow with radiative heat mass transfer over stretching/shrinking sheet using spectral quasilinearization method, *Multidiscipline Modeling in Materials and Structures*, 16(2), 2019, 238-255.
[25] Mahian, O., Kianifar, A., Kleinstreuer, C., Moh'd, A.A.N., Pop, I., Sahin, A.Z., Wongwises, S., A review of entropy generation in nanofluid flow, *International Journal of Heat and Mass Transfer*, 65, 2013, 514-532.
[26] Mondal, H., Mishra, S., Kundu, P.K., Sibanda, P., Entropy generation of variable viscosity and thermal radiation on magneto nanofluid flow with dusty fluid, *Journal of Applied and Computational Mechanics*, 6(1), 2020, 171-182.
[27] Mondal, H., Almakki, M., Sibanda, P., Dual solution for three-dimensional MHD nanofluid flow with entropy generation, *Journal of Computational Design and Engineering*, 6, 2019, 657–665
[28] Mondal, H., Bharti, S., Spectral quasilinearization for MHD nanofluid stagnation boundary layer flow due to a stretching/shrinking surface, *Journal of Applied and Computational Mechanics*, 2019, doi: 10.22055/JACM.2019.30677.1766
[29] Mondal, H., Sibanda, P., Spectral Quasi-Linearization Method for Entropy Generation Using the Cattaneo–Christov Heat Flux Model, *International Journal of Computational Methods*, 17(05), 2020, 1940002.
[30] Motsa, S.S., Dlamini, P.G., Khumalo, M., Spectral relaxation method and spectral quasilinearization method for solving unsteady boundary layer flow problems, *Advances in Mathematical Physics*, 2014, Article ID 341964.
[31] Motsa, S.S., Sibanda, P., Shateyi, S., On a new quasilinearization method for systems of nonlinear boundary value problems, *Mathematical Methods in the Applied Sciences*, 34(11), 2011, 1406-1413.
[32] Muhammad, T., Alamri, S.Z., Waqas, H., Habib, D., Ellahi, R., Bioconvection flow of magnetized Carreau nanofluid under the influence of slip over a wedge with motile microorganisms, *Journal of Thermal Analysis and Calorimetry*, 143, 2021, 945–957.
[33] Muhammad, T., Alsaedi, A., Shehzad, S.A., Hayat, T., A revised model for Darcy-Forchheimer flow of Maxwell nanofluid subject to convective boundary condition, *Chinese Journal of Physics*, 55(3), 2017, 963-976.
[34] Muhammad, T., Alsaedi, A., Hayat, T., AliShehzad, S., A revised model for Darcy-Forchheimer three-dimensional flow of nanofluid subject to convective boundary condition, *Results in Physics*, 7, 2017, 2791-2797.
[35] Mustafa, M., Hayat, T., Obaidat, S., On heat and mass transfer in the unsteady squeezing flow between parallel plates, *Meccanica*, 47(7), 2012, 1581-1589.
[36] Oyelakin, I.S., Mondal, S., Sibanda, P., Cattaneo-Christov Nanofluid Flow and Heat Transfer with Variable Properties Over a Vertical Cone in a Porous Medium, *International Journal of Applied and Computational Mathematics*, 3(1), 2017, 1019-1034.
[37 Pal, D., Mondal, S., Mondal, H., Entropy generation on MHD Jeffrey nanofluid over a stretching sheet with nonlinear thermal radiation using spectral quasilinearisation method, *International Journal of Ambient Energy*, 2019, https://doi.org/10.1080/01430750.2019.1614984.
[38] Qureshi, M.Z.A., Rubbab, Q., Irshad, S., Ahmad, S., Aqeel, M., Heat and mass transfer analysis of MHD nanofluid flow with radiative heat effects in the presence of spherical Au-metallic nanoparticles, *Nanoscale Research Letters*, 11(1), 2016, 472.
[39] Rashidi, M.M., Ganesh, N.V., Hakeem, A.A., Ganga, B., Buoyancy effect on MHD flow of nanofluid over a stretching sheet in the presence of thermal radiation, *Journal of Molecular Liquids*, 198, 2014, 234-238.
[40] Reddy, J.V.R., Sugunamma, V., Sandeep, N., Sulochan, C., Influence of chemical reaction, radiation and rotation on MHD nanofluid flow past a permeable flat plate in porous medium, *Journal of the Nigerian Mathematical Society,* 35, 2016, 48-65.
[41] Sakiadis, B.C., Boundary layer behavior on continuous solid surfaces: Boundary-layer equations for two-dimensional and axisymmetric flow, *AIChE Journal*, 7(1), 1961, 26-28.
[42] Shafiq, A., Jabeen, S., Hayat, T., Alsaedi, A., Cattaneo-Christov Heat Flux Model For Squeezed Flow Of Third Grade Fluidm, *Surface Review and Letters*, 24(07), 2017, 1750098.
[43] Sithole, H., Mondal, H., Goqo, S., Sibanda, P., Motsa, S., Numerical simulation of couple stress nanofluid flow in magneto-porous medium with thermal radiation and a chemical reaction, *Applied Mathematics and Computation*, 339, 2018, 820-836.
[44] Sobamowo, G.M., Akinshilo, A.T., Double diffusive magnetohydrodynamic squeezing flow of nanofluid between two parallel disks with slip and temperature jump boundary conditions, *Applied and Computational Mechanics*, 11(2), 2017, 167-182.
[45] Sridhara, V., Satapathy, L.N., Al_2O_3-based nanofluids: A Review, *Nanoscale Research Letters*, 6(1), 2011, 456.
[46] Stefan M.J., Versuch Über die scheinbare adhesion, Akademie *der Wissenschaften. Math Naturwissenschaftliche*, 69, 1874, 713-721.
[47] Takhar, H.S., Chamkha, A.J., Nath, G., Unsteady three-dimensional MHD-boundary-layer flow due to the impulsive motion of a stretching surface, *Acta Mechanica*, 146, 2001, 59-71.
[48] Trefethen, L.N., *Spectral methods in MATLAB,* Volume 10, SIAM, 2000.

ORCID iD

Mangwiro Magodora https://orcid.org/0000-0002-0449-2474
Hiranmoy Mondal https://orcid.org/0000-0002-9153-300X
Precious Sibanda https://orcid.org/0000-0003-2115-4642

How to cite this article: Magodora M., Mondal, H., Sibanda P. Effect of Cattaneo-Christov Heat Flux on Radiative Hydromagnetic Nanofluid Flow between Parallel Plates using Spectral Quasilinearization Method, *J. Appl. Comput. Mech.*, xx(x), 2021, 1–11. https://doi.org/10.22055/JACM.2020.33298.2195

Summary

The study interrogated the effects of Cattaneo-Christov heat flux on the flow of nanofluid between parallel plates. The squeezing flow between parallel plates is key in many industrial processes. The findings of the study showed that the rates of heat and mass transfer decrease with increased magnetic field strength while the reverse trend was witnessed for the skin friction. The temperature was found to decline with increasing relaxation parameter. The contrary trend was observed for the heat source parameter.

Chapter 4

Numerical studies on gold-water chemical reacting nanofluid with activation energy past a rotating disk

In Chapter 3, the effect of the Cattaneo-Christov heat flux on nanofluid flow between squeezing parallel plates was studied. In the current chapter, attention is shifted to nanofluid flow past a rotating disk where the effects of binary chemical reaction and activation energy are taken into consideration. The pioneering study of fluid flow over an infinite rotating disk was done by Von-Kármán in 1921 [56]. Activation energy is the minimum amount of energy that is required to start a chemical reaction [134] while a binary chemical reaction occurs in two stages [135]. Problems involving rotating disks, binary chemical reaction and activation energy occur frequently in industrial processes [136]. Varying the parameters of interest and observing their effects on the flow properties such as velocity, concentration, thermal, skin friction rates of heat and mass transfer has implications on controlling the chemical reaction processes in order to improve efficiency and production. More discussions on nanofluid flows with activation energy and binary chemical reaction can be viewed in the references [137–141], etc.

[1]

[1] Accepted

Numerical studies on gold-water nanofluid flow with activation energy past a rotating disk

Mangwiro Magodora[a]

Hiranmoy Mondal[b*]

Sandile Motsa[c]

Precious Sibanda[a]

[a] *School of Mathematics, Statistics and Computer Science, University of KwaZulu-Natal, Private Bag X01, Scottsvile, Pietermaritzburg-3209, South Africa*

[b] *Department of Applied Science, Maulana Abul Kalam Azad University of Technology, West Bengal, Kolkata-700064, India*

[c] *University of Eswatini, Department of Mathematics, Private Bag 4, Kwaluseni, M201, Eswatini*

Abstract

The present study examines the steady incompressible gold-water chemically reacting nanofluid flow near a rotating disk in the presence of activation energy and Brownian diffusion. The model equations are treated with the Newton-based spectral quasilinearization method to ascertain the effects of different parameters of interest such as volume fraction and the Prandtl number on the velocity, temperature, concentration and heat and mass transfer rates. This method has been shown in the literature to be robust and rapidly convergent. The validity of the results is checked by comparing numerical results, in the limiting case, with published results in the literature. The study showed that the rate of flow, heat and mass transfer appreciate with increased volume fraction of the nanoparticles. Increasing the Prandtl number was found to decrease temperature but increase concentration. A rise in the Schmidt number resulted in decreased temperature but did not have any appreciable effect on the concentration. Additionally, a lower temperature was predicted from a rise in activation energy while concentration was predicted to appreciate as a result of increased activation energy. The study has applications in the removal of contaminants in the beverages and waste water recovery industries.

Key words: Nanofluid, Binary chemical reaction, Activation energy, Quasilinearization, Rotating disk, Brownian motion, Chebyshev spectral collocation.

*Corresponding author.
Email address : hiranmoymondal@yahoo.co.in (H. Mondal)

Nomenclature

a_0, a_u	constants
C	concentration
C_0	concentration at disk surface
C_f	skin-friction coefficient
C_p	specific heat capacity at constant pressure
D_B	Brownian diffusion coefficient
D_m	mass diffusivity
E_a	activation energy
k_f	thermal conductivity of base fluid
k_{nf}	thermal conductivity of nanofluid
k_{r^2}	reaction rate constant
L	non-dimensional length scale
m	non-dimensional length scale
n	fitted rate constant
Nu	Nusselt number
P	pressure
$P(\xi)$	non-dimensional pressure
Pr	Prandtl number
q_m	surface mass flux
q_w	surface heat flux
r	radial coordinate
Re	local Reynolds number
Sc	Schmidt number
T	temperature
T_0	temperature on the disk surfce
T_∞	temperature of the fluid far away from the disk surface
(u, v, w)	radial, azimuthal and axial velocity components
(U, V, W)	radial, azimuthal and axial non-dimensional velocity components
U_0	characteristic velocity
z	axial coordinate

Greek Symbols

ξ	non-dimensional axial coordinate
θ	azimuthal coordinate
ρ_{nf}	density of nanofluid
ρ_f	density of base fluid
ρ_s	density of nanoparticles
μ_{nf}	dynamic viscosity of nanofluid
ν_f	kinematic viscosity of base fluid
λ	chemical reaction constant
ϕ	nanofluid volume fraction
τ	local shear stress
τ_{zr}	radial component of shear stress
$\tau_{z\theta}$	azimuthal component of shear stress

1. Introduction

Fluid flow over rotating surfaces has attracted immense attention by researchers thanks to its wide industrial, technological and engineering applications. Pioneering studies on Newtonian fluid flow over rotating infinite disks were mooted by Von Karman in 1921 [1, 2]. Such flows are prevalent in air cleaning devices, cooling of electronic components, turbine systems, aerodynamics, food processing, and so on [3]. The focus on fluid flow over rotating disks has grown in leaps and bounds to also include non-Newtonian fluids like Sisko fluid, paints, colloids, micropolar fluids, among many others.

A nanofluid consists of a base fluid like water, kerosene, oil or glycol and suspensions of very minute solid particles whose average diameters lie between $1 - 100\ nm$ [4]. Nanoparticles are often made from metals or metal oxides and they possess more desirable properties than the base fluids. For example, nanofluids have higher viscosity and diffusivity as a consequence of their increased area [5, 6]. Nanoparticles find widespread application within the sugar industry, food processing industry, footwear industry, textile industry, gas industry, wastewater industry etc [7]. Additionally, nanoparticles are exploited within the biomedical field, for instance, in drug therapy, cancer therapy and diabetes therapy. Nanoparticles also feature prominently in microchips cooling, water treatment, wire rolling and drawing, radiators, paints, polymer production, wastewater treatment, materials processing, etc [8, 9]. The phenomenon of non-linear thermal radiation and gyrotactic microorganisms on the Magneto-Burgers nanofluid was tackled by Khan et al. [10]. Khan et al [11] also investigated effects of non-linear thermal radiation on 3D Carreau fluid flow. Other recent studies on different types of nanofluids include the works of [12, 13].

The immense industrial, engineering and technological applications of rotating nanofluid flows have led to numerous research outputs in the recent past. Turkyilmazoglu [14] investigated nanofluid flow past a rotating disk. In his work, he considered five different nanoparticles immersed in water as the base fluid. Yin et al. [15] researched on flow of rotating disk with uniform stretching rate in velocity components with enhanced nanoparticle volume fraction on the flow. They also observed that the axial velocity increased with increases in volume fraction far away from the disk surface. Rehman et al. [6] interrogated entropy analysis of radioactive rotating nanofluid with thermal slip. As part of their findings, they reported the Bejan number as a decreasing function of nanoparticle volume fraction. Their study also revealed that more entropy is generated due to the presence of nanoparticles as compared to regular fluid flow. Oloniiju et al. [16] investigated the unsteady flow of a second-grade fluid with viscous dissipation effects in a rotating coordinate system. Their findings show that slow rotation results in a rapid depreciation within the thickness of the thermal, momentum and concentration boundary layers.

Recently, several researches that specialize on the influence of Arrhenius energy of activation on nanofluid flow are reported in literature. Dhlamini et al. [17] reported on the consequences of energy of activation and binary reaction effects in double-diffusive flow of nanofluid with convective boundary conditions. The researchers acknowledged that the thermophoresis and activation parameters were positively correlated with the concentration of the chemical species while the reaction rate constant and therefore the Brownian parameter reduced the chemical species concentration. Abbas et al.[18] analyzed the consequences of binary reaction and energy of activation on unsteady physical phenomenon flow of a Casson fluid near a stagnation point over a shrinking/stretching sheet. They determined that a rise the in energy of activation enhances the concentration.

Maleque et al. [19] reported on the influence of the energy of activation and binary reaction on the hydromagnetic flow of a viscous fluid with heat generation/absorption and viscous dissipation. They found that increasing activation leads to increased temperature, concentration and velocity distributions. More recently, Ijaz et al.[3] explored the entropy generation optimization, energy of activation and binary reaction for convective flow of Sisko model on a rotating disk that's radially stretchable within the presence of a consistent vertical magnetic flux . They observed that concentration reduces with increasing Schmidt number but appreciates with increasing energy of activation. Subbarayudu et al. [20] investigated binary reaction and activation energy and CNTs and Maxwell nanofluid considering the Cattaneo-Christov heat diffusion model. Meanwhile the impact of activation energy on Eyring-Powell nanofluid above a stretching cylinder was studied by Reddy et al. [21]. The same investigators also reported on the impact of the binary chemical reaction on magnetohydrodynamic flow of Casson nanofluid by considering Cattaneo-Christov heat flux model [22]. Quite recently Mabood et al. [23] tackled second law analysis on hydromagnetic flow of nanofluid over a rotating disk.

The main aim of our current work is to research the consequences of binary chemical reaction and energy of activation on the steady incompressible flow of gold-water nanofluid past an impermeable rotating disk.

We consider water as the base fluid and gold nanoparticles as the nanomaterial. Gold is nonreactive at the macroscopic level but becomes very reactive at the nanoscale level. Gold nanoparticles have also been found to possess superior optoelectronic and catalytic properties [9, 24]. Aside from being used as a store and symbol of wealth, research has in recent years shown that gold (Au) nanoparticles can find effective application in water treatment. The high absorption capacity of gold nanoparticles has been utilized in removing mercury from contaminated water [24]. In our current study, the governing equations are presented as a system of coupled non-linear partial differential equations which are then solved numerically using the spectral quasilinearization method. This study seeks to offer more insight into the effects of various parameters on the steady flow of gold-water nanofluid past a rotating disk. It is hoped this study will motivate future research on how gold could be used to, among other things, improve removal of contaminants from beverages and drinking water. This will result in improved health and better quality of life for humanity.

2. Problem formulation

We consider nanofluid flow over a horizontal infinite disk that is rotating about the z-axis in the presence of Arrhenius activation energy and binary chemical reaction. The cylindrical polar coordinate system (r, θ, z) is chosen so that u, v and w are the velocity components in the radial, azimuthal and axial directions, respectively. The geometry of the problem is depicted in Fig. 1 below.

The concentration of the diffusing species is represented by C while T represents the temperature of the nanofluid. The concentration and temperature far away from the disk surface are denoted as C_∞ and T_∞ while at the disk surface they are C_0 and T_0, respectively. It is assumed that:

1. the flow is steady and incompressible,
2. the disk is impermeable,
3. the disk rotates at a uniform angular velocity Ω.

The basic equations of motion, heat and mass transportation are represented by [14, 25]:

$$\frac{\partial u}{\partial r} + \frac{u}{r} + \frac{\partial w}{\partial z} = 0, \tag{1}$$

$$u\frac{\partial u}{\partial r} - \frac{v^2}{r} + w\frac{\partial u}{\partial z} = -\frac{1}{\rho_{nf}}\frac{\partial p}{\partial r} + \frac{\mu_{nf}}{\rho_{nf}}\left(\frac{\partial^2 u}{\partial r^2} + \frac{1}{r}\frac{\partial u}{\partial r} - \frac{u}{r^2} + \frac{\partial^2 u}{\partial z^2}\right), \tag{2}$$

$$u\frac{\partial v}{\partial r} + \frac{uv}{r} + w\frac{\partial v}{\partial z} = \frac{\mu_{nf}}{\rho_{nf}}\left(\frac{\partial^2 v}{\partial r^2} + \frac{1}{r}\frac{\partial v}{\partial r} - \frac{v}{r^2} + \frac{\partial^2 v}{\partial z^2}\right), \tag{3}$$

$$u\frac{\partial w}{\partial r} + w\frac{\partial w}{\partial z} = -\frac{1}{\rho_{nf}}\frac{\partial p}{\partial z} + \frac{\mu_{nf}}{\rho_{nf}}\left(\frac{\partial^2 w}{\partial r^2} + \frac{1}{r}\frac{\partial w}{\partial r} + \frac{\partial^2 w}{\partial z^2}\right), \tag{4}$$

$$u\frac{\partial T}{\partial r} + w\frac{\partial T}{\partial z} = \frac{k_{nf}}{(\rho C_p)_{nf}}\left(\frac{\partial^2 T}{\partial r^2} + \frac{1}{r}\frac{\partial T}{\partial r} + \frac{\partial^2 T}{\partial z^2}\right) \tag{5}$$

$$u\frac{\partial C}{\partial r} + w\frac{\partial C}{\partial z} = D_B\left(\frac{\partial^2 C}{\partial r^2} + \frac{1}{r}\frac{\partial C}{\partial r} + \frac{\partial^2 C}{\partial z^2}\right) - k_r^2 e^{-E_a/\kappa T}(C - C_\infty)\,(T/T_\infty)^n \tag{6}$$

where p is the pressure, μ_{nf} and ρ_{nf} are the dynamic viscosity and density of the nanofluid respectively, C and T are the concentration and temperature of the nanofluid respectively, $(\rho C_p)_s$ is the specific heat capacity of the nanoparticles, $(\rho C_p)_{nf}$ is the specific heat capacity of the nanofluid, μ_{nf} is the dynamic viscosity of the nanofluid, D_B is the Brownian diffusion coefficient, k_{nf} is the thermal conductivity of the nanofluid, $e^{E_a/kT}(C - C_\infty)\,(T/T_\infty)^n$ is the Arrhenius function, $\kappa = 8.61\ x\ 10^{-5} eV/K$ is the Boltzmann constant, ${k_r}^2$ is the chemical reaction rate constant, E_a is the activation energy and n is a fitted rate constant that lies in the range $-1 < n < 1$ [3, 19].

The boundary conditions are:

$$\begin{aligned} &u = 0,\ v = \Omega r,\ w = 0\ , T = T_0,\ C = C_0 \ \text{ at } z = 0, \\ &u = 0,\ v = 0,\ T \to T_\infty,\ C \to C_\infty,\ p \to p_\infty \ \text{ as } z \to \infty. \end{aligned} \tag{7}$$

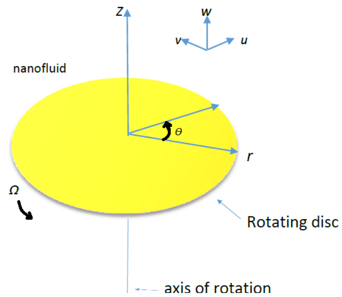

Figure 1: Geometry of the problem.

We make use of the Brinkman model to define as the nanofluid [26]:

$$\mu_{nf} = \frac{\mu_f}{(1-\phi)^{2.5}}, \tag{8}$$

where μ_f is the viscosity of the base fluid and ϕ the volume fraction of the nanopartiles.

The other properties of the nanofluid are given as [14, 15, 27]:

$$\rho_{nf} = (1-\phi)\rho_f + \phi\rho_s \tag{9}$$

$$(\rho C_p)_{nf} = (1-\phi)(\rho C_p)_f + \phi(\rho C_p)_s \tag{10}$$

$$\frac{k_{nf}}{k_f} = \frac{k_s + 2k_f - 2\phi(k_f - k_s)}{k_s + 2k_f + 2\phi(k_f - k_s)}, \tag{11}$$

where ρ_f is the density of the base fluid, ρ_s the density of the nanoparticles, ϕ the nanoparticle volume fraction.

The thermo-physical properties of the nanomaterial are given in Table 1 below as [28]:

Table 1: Thermo-physical properties of base fluid and nanoparticles.

Property	Water (base fluid)	Gold (nanoparticles)
Density, ρ (kgm^{-3})	997.1	19300
Specific heat capacity, C_p $(Jkg^{-1}K^{-1})$	4179	1290
Thermal conductivity, k $(Wm^{-1}K^{-1})$	0.613	318

We make use of the Von-Kármán similarity transformations [15, 29, 30] shown in (12) to convert the system of partial differential equations(1)-(6) to a sytem of ordinary differential equations:

$$\begin{gathered} u = r\Omega U(\xi),\ v = r\Omega V(\xi),\ w = L\Omega W(\xi),\ p = p_\infty + 2\rho_{nf}\nu_{nf}\Omega P(\xi), \\ T = \theta(\xi)(T_0 - T_\infty) + T_\infty,\ C = \varphi(\xi)(C_0 - C_\infty) + C_\infty,\ \xi = (1/L)\,z \end{gathered} \tag{12}$$

where $U(\xi),\ V(\xi), W(\xi)$ are the non-dimensional forms of radial, azimuthal and axial velocities respectively, $P(\xi)$ the non-dimensional pressure, $L = \sqrt{(\nu_f/\Omega)}$ the non-dimensional length scale, ν_f the kinematic viscosity for the flow and ξ the non-dimensional axial coordinate.

Applying the transformations (12) to the model equations (1)-(6), gives the non-dimensional form of the equations as:

$$
\begin{aligned}
&2U + W' = 0, && (13)\\
&a_u U'' - U^2 + V^2 - WU' = 0, && (14)\\
&a_u V'' - 2UV - WV' = 0, && (15)\\
&\frac{1}{Pr} a_\theta \theta'' - W\theta' = 0, && (16)\\
&\frac{1}{Sc}\varphi'' - W\varphi' - \lambda^2 e^{-E/(1+m\theta)}(1+mn\theta)\varphi = 0, && (17)\\
&a_u(W'' - 2P') - WW' = 0, && (18)
\end{aligned}
$$

in which prime ($'$) signifies the derivative with respect to ξ, $m = (T_0 - T_\infty)/T_\infty$ is the relative temperature constant, λ the dimensionless chemical reaction rate constant where $\lambda^2 = k_r^2/\Omega$, $Sc = \nu_f/D_B$ the Schmidt number, $Pr = (\mu_f C_{pf})/k_f$ is the Prandtl number, a_u and a_θ are constants that are defined by:

$$
a_u = \frac{1}{\left((1-\phi)^{2.5}(1-\phi+\phi\frac{\rho_s}{\rho_f}\right)},\ a_\theta = \frac{(k_{nf}/k_f)}{\left(1-\phi+\phi\frac{(\rho C_p)_s}{(\rho C_p)_f}\right)}. \tag{19}
$$

The associated boundary conditions are:

$$
\begin{aligned}
&U = 0,\ V = 1,\ W = 0\ , T = T_0,\ C = C_0, \quad \text{at } \xi = 0,\\
&U = 0,\ V = 0,\ \theta = 0,\ \varphi = 0, P = 0, \quad \text{as } \xi \to \infty.
\end{aligned} \tag{20}
$$

The skin friction, Nusselt Number and Sherwood number are the physical quantities of interest and are defined as:

$$
C_f = \frac{\tau}{\rho_{nf} U_0^2},\ Nu = \frac{r q_w}{k_f(T_0 - T_\infty)},\quad Sh = \frac{r q_m}{D_m(C_0 - C_\infty)}, \tag{21}
$$

where U_0 is a characteristic velocity, $\tau = \left({\tau_{zr}}^2 + {\tau_{z\theta}}^2\right)^{0.5}$ the local shear stress, τ_{zr} the radial component of shear stress, $\tau_{z\theta}$ the azimuthal component of shear stress, q_w the surface heat flux, q_m the surface mass flux, D_m the mass diffusivity. We define $\tau_{zr},\ \tau_{z\theta},\ q_w,\ q_m,\ D_m$ as:

$$
\tau_{zr} = \mu_{nf}\left(\frac{\partial u}{\partial z} + \frac{\partial w}{\partial r}\right)\bigg|_{\hat{z}=0},\ \tau_{z\theta} = \mu_{nf}\left(\frac{\partial v}{\partial z} + \frac{1}{r}\frac{\partial w}{\partial \theta}\right)\bigg|_{\hat{z}=0},\ q_w = -k_{nf}\left.\frac{\partial T}{\partial z}\right|_{\hat{z}=0},\ q_m = -D_m\left.\frac{\partial C}{\partial z}\right|_{\hat{z}=0}. \tag{22}
$$

It follows that the skin friction coefficient, Nusselt number and Sherwood number, are given by:

$$
Re^{\frac{1}{2}} C_f = [U'(0)^2 + V'(0)^2]^{0.5}/(1-\phi)^{2.5},\ Re^{-\frac{1}{2}} Nu = -(k_{nf}/k_f)\theta'(0),\ Re^{-\frac{1}{2}} Sh = \phi'(0), \tag{23}
$$

where $Re = \Omega r^2/\nu_f$ is the local Reynolds number.

The non-linear sytem of ordinary differential equations (13)-(18) is solved by utilizing the spectral quasililinearization method. We begin by solving the equations (13)-(17 for $U,\ V\ W, \theta$ and φ first, while equation (18) can be manipulated at a later stage to determine the pressure distribution if required [29, 31].

3. Numerical solution

The non-linear ordinary differential equations (13)-(17) subject to the boundary conditions (20) are solved by applying the spectral quasilinearization method, which has been shown in literature to be highly robust and rapidly convergent [17, 32, 33] As an initial step of this method, we implement the quasilinearization procedure, to obtain the following system of linear algebraic equations:

$$a_{10r}U_{r+1} + c_{11r}W'_{r+1} = R_1, \tag{24}$$
$$a_{22r}U''_{r+1} + a_{21r}U'_{r+1} + a_{20r}U_{r+1} + b_{20r}V_{r+1} + c_{20r}W_{r+1} = R_2 \tag{25}$$
$$a_{30r}U_{r+1} + b_{32r}V''_{r+1} + b_{31r}V'_{r+1} + b_{30r}V_{r+1} + c_{30r}W_{r+1} = R_3 \tag{26}$$
$$c_{40r}W_{r+1} + d_{42r}\theta''_{r+1} + d_{41r}\theta'_{r+1} = R_4, \tag{27}$$
$$c_{50r}W_{r+1} + d_{50r}\theta_{r+1} + e_{52r}\varphi''_{r+1} + e_{51r}\varphi'_{r+1} + e_{50r}\varphi_{r+1} = R_5, \tag{28}$$

where,

$$a_{10r} = 2, \quad c_{11r} = 1, \quad R_1 = 0, \tag{29}$$
$$a_{22r} = a_u, \quad a_{21r} = -W_r, \quad a_{20r} = -2U_r, \quad b_{20r} = 2V_r, \quad c_{20r} = -U'_r, \quad R_2 = -U_r^2 - U'_rW_r + V_r^2, \tag{30}$$
$$a_{30r} = -2V_r, \quad b_{32r} = a_u, \quad b_{31r} = -W_r, \quad b_{30r} = -2U_r, \quad c_{30r} = -V'_r, \quad R_3 = -2V_rU_r - V'_rW_r, \quad c_{40r} = -\theta'_r, \tag{31}$$
$$d_{42r} = a_\theta/Pr, \quad d_{41r} = -W_r, \quad R_4 = -W_r\theta'_r, \tag{32}$$
$$d_{50r} = -\frac{1}{(1+m\theta_r)^2}mE\lambda^2\varphi_r e^{-\frac{E}{1+m\theta_r}} - mn\lambda^2\varphi_r e^{-\frac{E}{1+m\theta_r}} - \frac{1}{(1+m\theta_r)^2}Enm^2\lambda^2\theta_r\varphi_r e^{-\frac{E}{1+m\theta_r}}, \tag{33}$$
$$c_{50r} = -\varphi'_r, \quad e_{52r} = 1/Sc, \quad e_{51r} = -W_r, \quad e_{50r} = -\lambda^2 e^{-\frac{E}{1+m\theta_r}} - mn\lambda^2\theta_r e^{-\frac{E}{1+m\theta_r}}, \tag{34}$$
$$R_5 = c_{50r}W_r + d_{50r}\theta_r + e_{52r}\varphi''_r + e_{51r}\varphi'_r + e_{50r}\varphi - \Gamma_5, \tag{35}$$

where $\Gamma_5 = \frac{1}{Sc}\varphi''_r - W_r\varphi'_r - \lambda^2 e^{-\frac{E}{1+m\theta_r}}(1+mn\theta_r)\varphi_r$.
The transformed boundary conditions are now

$$\begin{aligned} &U_{r+1}(0) = 0,\ V_{r+1}(0) = 1,\ W_{r+1}(0) = 0,\ \theta_{r+1}(0) = 1,\ \varphi_{r+1}(0) = 1, \\ &U_{r+1}(\infty) = 0,\ V_{r+1}(\infty) = 0,\ \theta(\infty)_{r+1} = 0,\ \varphi_{r+1}(\infty) = 0. \end{aligned} \tag{36}$$

The domain of the flow problem is $\xi \in [0,\infty)$. To solve the system of equations (24)-(28) with the spectral method, we need to transform the domain from $\xi = [0,\infty)$ to $x = [-1,1]$. We use the truncation method [29] to approximate $[0,\infty)$ with the computational domain $[0, L_x]$, where L_x is a fixed length that is larger than the boundary layer thickness. The domain $[0, L_x]$ is transformed from $[0, L_x]$ to $x = [-1,1]$ by letting $\xi = L_x(x+1)/2$ [17, 29].

The scaled differentiation matrices are now $\mathbf{D} = 2\mathrm{D}/L_x$, $\mathbf{D}^2 = 4\mathrm{D}^2/L_x^2$, where D is the Chebyshev spectral differentiation matrix. For a general function $f(\xi)$ on a given interval, using Gauss-Lobatto grid points
$\eta_i = \cos\left(\frac{\pi i}{N}\right)$, for $i = 0,1,...,N$ are defined as

$$\left.\frac{df_n}{d\xi}\right|_{(\xi_i)} = \sum_{\omega=0}^{N} D_{i\omega}f_n(\xi_\omega) \tag{37}$$

where $D_{i\omega}f_n(\xi_\omega) = \dfrac{d}{d\xi}\left(L_\omega(\xi_i)\right)$ and L is the Lagrange polynomial [34]

Higher order derivatives are defined as:

$$\left.\frac{d^pf_n}{d\xi^p}\right|_{(\xi_i)} = D^p\mathbf{F}_n, \tag{38}$$

where $D^p\mathbf{F}_n = \sum_{\omega=0}^{N_\eta} D^p_{i\omega}f_n(\xi_\omega)$ and $\mathbf{F}_n = [f_n(\xi_0), f_n(\xi_1), ..., f_n(\xi_N)]^T$

The initial guesses satisfy the boundary conditions:
$U = \xi^3 e^{-\xi}, V = e^{-\xi},\ W = \xi^3,\ \theta = e^{-\xi}$ and $\varphi = e^{-\xi}$.

Applying the Chebyshev spectral collocation procedure to system (24)-(28) yields [34]:

$$A_{11}\mathbf{U}_{r+1} + A_{12}\mathbf{V}_{r+1} + A_{13}\mathbf{W}_{r+1} + A_{14}\boldsymbol{\theta}_{r+1} + A_{15}\boldsymbol{\varphi}_{r+1} = \mathbf{R}_1 \tag{39}$$
$$A_{21}\mathbf{U}_{r+1} + A_{22}\mathbf{V}_{r+1} + A_{23}\mathbf{W}_{r+1} + A_{24}\boldsymbol{\theta}_{r+1} + A_{25}\boldsymbol{\varphi}_{r+1} = \mathbf{R}_2 \tag{40}$$
$$A_{31}\mathbf{U}_{r+1} + A_{32}\mathbf{V}_{r+1} + A_{33}\mathbf{W}_{r+1} + A_{34}\boldsymbol{\theta}_{r+1} + A_{35}\boldsymbol{\varphi}_{r+1} = \mathbf{R}_3 \tag{41}$$
$$A_{41}\mathbf{U}_{r+1} + A_{42}\mathbf{V}_{r+1} + A_{43}\mathbf{W}_{r+1} + A_{44}\boldsymbol{\theta}_{r+1} + A_{45}\boldsymbol{\varphi}_{r+1} = \mathbf{R}_4 \tag{42}$$
$$A_{51}\mathbf{U}_{r+1} + A_{52}\mathbf{V}_{r+1} + A_{53}\mathbf{W}_{r+1} + A_{54}\boldsymbol{\theta}_{r+1} + A_{55}\boldsymbol{\varphi}_{r+1} = \mathbf{R}_5 \tag{43}$$

where

$$A_{11} = diag(a_{10r})\mathbf{I},\ A_{12} = 0,\ A_{13} = diag(c_{11r})\mathbf{D},\ A_{14} = A_{15} = \mathbf{0} \tag{44}$$
$$A_{21} = diag(a_{22r})\mathbf{D}^2 + diag(a_{21r})\mathbf{D} + diag(a_{20r})\mathbf{I},\ A_{22} = diag(b_{20r})\mathbf{I},\ A_{23} = diag(c_{20r})\mathbf{I},\ A_{24} = A_{25} = \mathbf{0}, \tag{45}$$
$$A_{31} = diag(a_{30r})\mathbf{I},\ A_{32} = diag(b_{32r})\mathbf{D}^2 + diag(b_{31r})\mathbf{D} + diag(b_{30r})\mathbf{I},\ A_{33} = diag(c_{30r})\mathbf{I},\ A_{34} = A_{35} = \mathbf{0}, \tag{46}$$
$$A_{41} = A_{42} = A_{45} = \mathbf{0},\ A_{43} = diag(c_{40r})\mathbf{D},\ A_{44} = diag(d_{42r})\mathbf{D}^2 + diag(d_{41r})\mathbf{D}, \tag{47}$$
$$A_{51} = A_{52} = \mathbf{0},\ A_{53} = diag(c_{50r})\mathbf{I},\ A_{54} = diag(d_{52r})\mathbf{D}^2 + diag(d_{50r})\mathbf{I}, \tag{48}$$
$$A_{55} = diag(e_{52r})\mathbf{D}^2 + diag(e_{51r})\mathbf{D} + diag(e_{50r})\mathbf{I}, \tag{49}$$
$$\mathbf{U}_{r+1} = [U_{1,r+1},\ U_{2,r+1}, ..., U_{N+1,r+1}]^T,\ \mathbf{V}_{r+1} = [V_{1,r+1},\ V_{2,r+1}, ..., V_{N+1,r+1}]^T, \tag{50}$$
$$\mathbf{W}_{r+1} = [W_{1,r+1},\ W_{2,r+1}, ..., W_{N+1,r+1}]^T, \boldsymbol{\theta}_{r+1} = [\boldsymbol{\theta}_{1,r+1},\ \boldsymbol{\theta}_{2,r+1}, ..., \boldsymbol{\theta}_{N+1,r+1}]^T, \tag{51}$$
$$\boldsymbol{\varphi}_{r+1} = [\boldsymbol{\varphi}_{1,r+1},\ \boldsymbol{\varphi}_{2,r+1}, ..., \boldsymbol{\varphi}_{N+1,r+1}]^T, \tag{52}$$
$$\mathbf{0} \text{ is the } (N+1)\ \times\ (N+1) \text{ null matrix.} \tag{53}$$

The boundary conditions (36) are imposed on the first row, second row, second to last row or last row of the square matrices $A_{11},\ A_{22}, ..., A_{33}$ accordingly and the linear system $A\mathbf{Y} = \mathbf{R}$ is then solved to get $\mathbf{Y} = A^{-1}\mathbf{R}$ where

$$A = \begin{bmatrix} A_{11} & A_{12} & A_{13} & A_{14} & A_{15} \\ A_{21} & A_{22} & A_{23} & A_{24} & A_{25} \\ A_{31} & A_{32} & A_{33} & A_{34} & A_{35} \\ A_{41} & A_{42} & A_{43} & A_{44} & A_{45} \\ A_{51} & A_{52} & A_{53} & A_{54} & A_{55} \end{bmatrix}, \mathbf{Y} = \begin{bmatrix} \mathbf{U}_{r+1} \\ \mathbf{V}_{r+1} \\ \mathbf{W}_{r+1} \\ \boldsymbol{\theta}_{r+1} \\ \boldsymbol{\varphi}_{r+1} \end{bmatrix}, \mathbf{R} = \begin{bmatrix} \mathbf{R}_1 \\ \mathbf{R}_2 \\ \mathbf{R}_3 \\ \mathbf{R}_4 \\ \mathbf{R}_5 \end{bmatrix},$$

4. Results & Discussion

The study investigated the momentum, thermal and concentration properties of a gold-water chemical reacting nanofluid past a rotating disc with activation energy and Brownian diffusion. The validity of our results were checked by making a comparison of present results for $U'(0),\ -V'(0), -W(\infty)$ and $-\theta'(0)$ with those presented by Rashidi et al. [35], Turkyilmazoglu [14] and Yin et al. [15]. Excellent agreement was observed as displayed in Table 2.

We analyze the effects of varying the parameters of interest one at a time, while keeping the others constant. The solutions are evaluated at $\phi = 0.1$, $Sc = 1$, $Pr = 6.2$, $\lambda = 1$, $m = 1$, $n = 0.1$ and $E = 1$, unless stated otherwise. The numerical results are displayed graphically in Figs. 2-16.

Pr_n	Ref. [35]	Ref. [14]	Ref. [15]	Present results
$U'(0)$	0.510186	0.51023262	0.51022941	0.510229411
$-V'(0)$	0.61589	0.61592201	0.61591990	0.615919910
$-W(\infty)$	- - - - - -	0.88447411	0.88446912	0.884014124
$-\theta'(0)$	- - - - - -	0.93387794	0.93387285	0.933872852

Table 2: Comparison of numerical solutions for $U'(0)$, $-V'(0)$, $-W(\infty)$ and $-\theta'(0)$ when $Pr = 6.2$, $\phi = 0$ and $\varphi = 0$

Figs. 2-5 exhibit the influence of the volume fraction of nanoparticles on the velocity components and temperature distribution. The upward variation of the nanofluid volume fraction on the cylindrical velocity components has insignificant effects very close to the rotating disk surface. However further away from the disk surface, the velocity components are shown to depreciate, while the opposite trend is observed for the axial component, where increased volume fraction implies higher axial velocity.

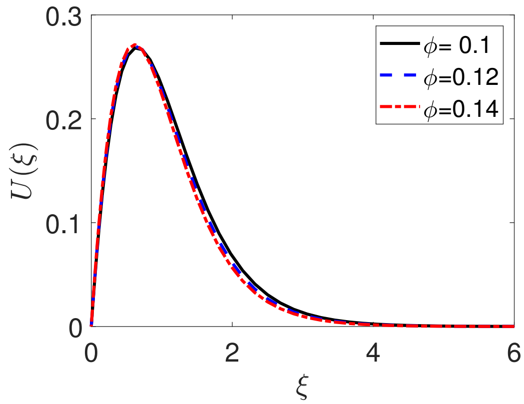

Figure 2: The impact of nanofluid volume fraction ϕ on radial velocity $U(\xi)$.

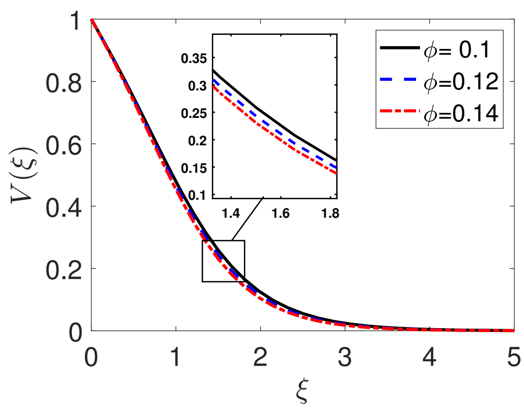

Figure 3: The impact of nanofluid volume fraction ϕ on azimuthal velocity $V(\xi)$.

The influence of the chemical reaction constant (λ), the relative temperature constant (m) and the fitted rate constant index (n) are shown in Figs. 6-11. The profiles demonstrate the depletion of both temperature and concentration as λ, m and n increase. Such an occurrence has important applications, for example, in the cooling of devices.

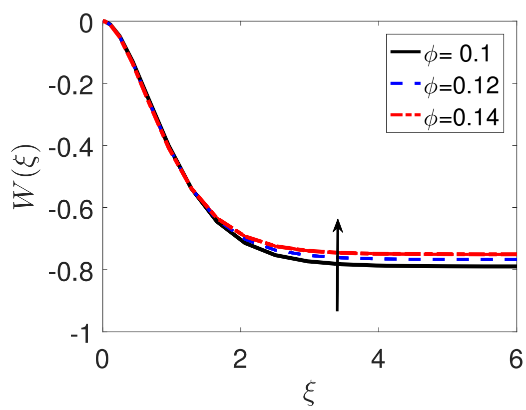

Figure 4: The impact of nanofluid volume fraction ϕ on axial velocity $W(\xi)$.

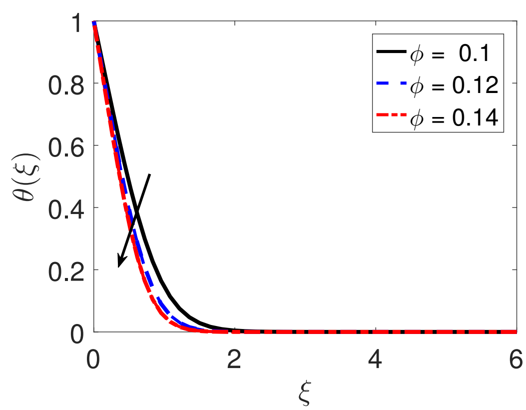

Figure 5: The impact of nanofluid volume fraction ϕ on temperature $\theta(\xi)$.

Figs. 12-16 depict the variation of temperature and concentration with Prandtl number (Pr), Schmidt number (Sc) and dimensionless activation energy (E). Fig. 12 shows that an increased Prandtl number leads to decrease temperature while Fig. 13 indicates that an increased Prandtl number results in a rise in concentration. A value of Prandtl number that is greater than unity signifies the dominance of momentum diffusivity over the thermal conductivity. Increasing the Prandtl number would imply that the thermal boundary layer decreases [36]. This trend, as expected, is shown in Fig. 12.

The Schmidt number is defined as the ratio of momentum diffusivity (kinematic viscosity) to mass diffusivity. As illustrated in Fig. 14, an increase in the Schmidt number implies a reduction in mass diffusivity, which leads to reduced concentration. Fig. 15 shows that an increase in activation energy results in a lower temperature, while the reverse is depicted in Fig. 16. This agrees with Awad et al. [37] who also obtained the same result.

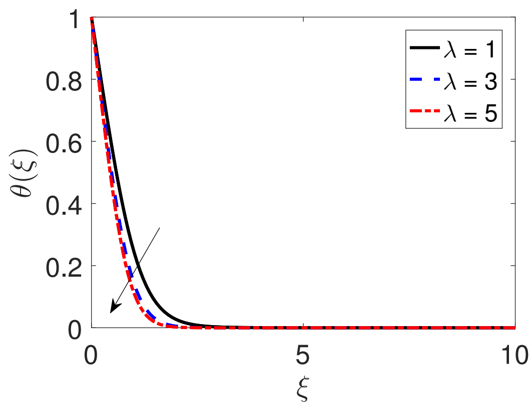

Figure 6: Effect of λ on temperature.

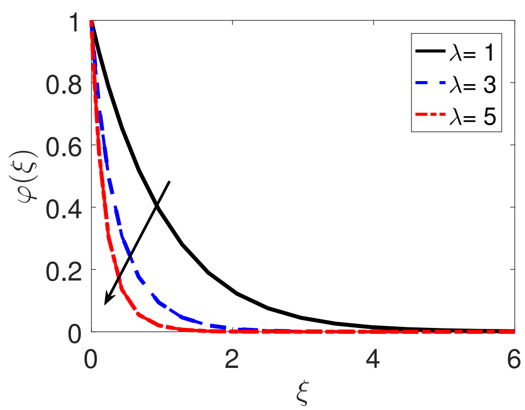

Figure 7: Effect of λ on concentration.

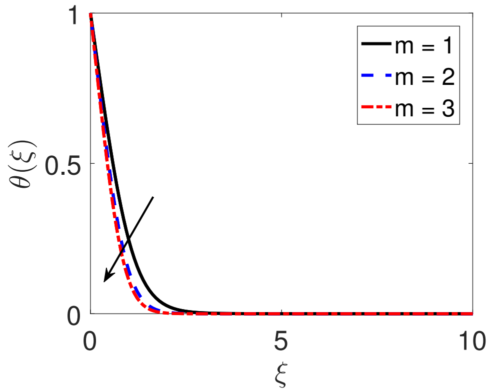

Figure 8: Effect of m on temperature.

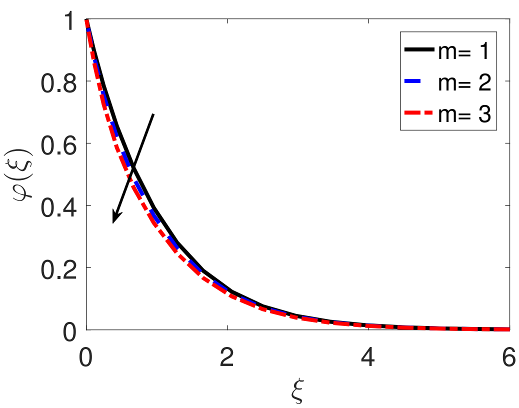

Figure 9: Effect of m on concentration.

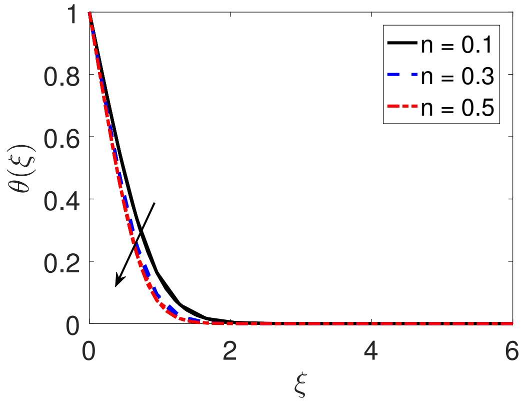

Figure 10: Effect of n on temperature.

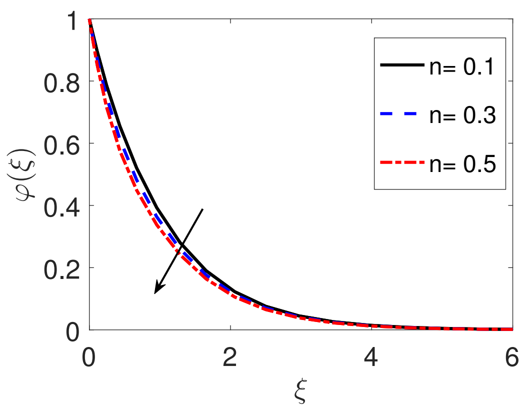

Figure 11: Effect of n on concentration.

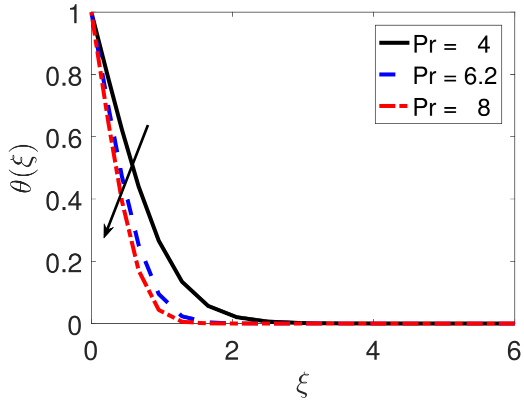

Figure 12: Effect of Pr on temperature.

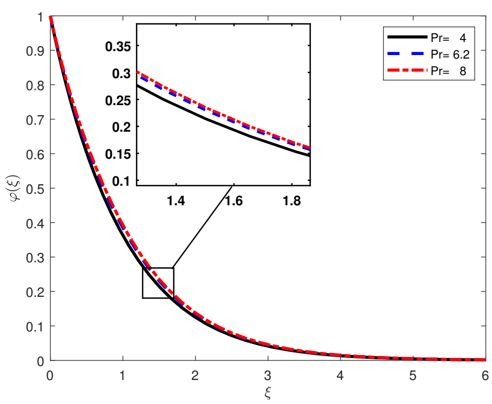

Figure 13: Effect of Pr on concentration.

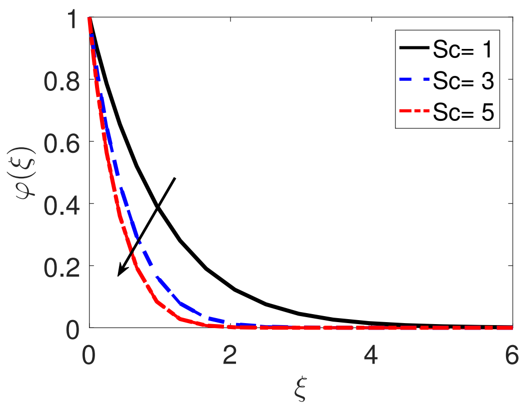

Figure 14: Effect of Sc on concentration.

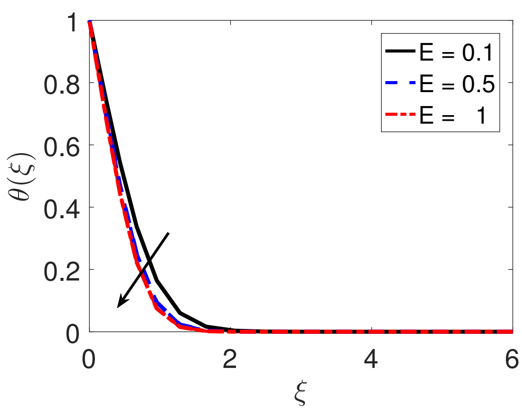

Figure 15: Effect of activation energy on temperature.

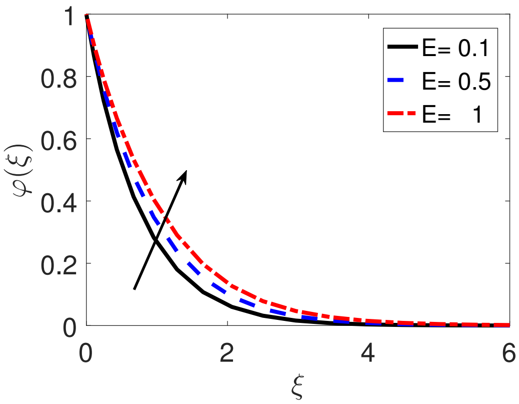

Figure 16: Effect of activation energy on concentration.

Parameter	Symbol	Value	$Re^{0.5}C_f$	$Re^{-0.5}Nu$	$Re^{-0.5}Sh$
Volume fraction	ϕ	0.1	1.4135	1.6203	1.0062
		0.12	1.5461	1.7255	1.0095
		0.14	1.6810	1.8313	1.0134
Prandtl number	Pr	6.2		1.6203	1.0062
		7		1.7080	0.9991
		8		1.8081	0.9914
Schmidt number	Sc	1			1.0062
		3			1.8395
		5			2.4076
Activation energy	E	0.1			1.3076
		0.5			1.1625
		1			1.0062
Reaction rate constant	λ	1			1.0062
		3			3.0930
		5			5.2927

Table 3: Effects of ϕ, Pr, Sc, E and λ on the skin friction coefficient, Nusselt number, and Sherwood number for $\phi = 0.1,\ Sc = 1,\ Pr = 6.2,\ \lambda = 1, m = 1,\ n = 1$ and $E = 1$.

Table 3 shows the effects of ϕ, Pr, Sc, E and λ on the skin friction, Sherwood number and Nusselt number. The volume fraction of the nanoparticles is positively correlated with C_f, NU_x and the Sh_x. Increased volume fraction implies increased thermal conductivity, which in turn leads to increased thermal and mass diffusivities. It is also apparent from Table 3 that the Prandtl number increases the Nusselt number but reduces the Sherwood number. An increased Prandtl number signifies the dominance of momentum diffusivity. Hence the velocity boundary layer diminishes more than the thermal boundary layer which in turn implies a higher rate of heat transfer. The Sherwood number appreciates with increased Schmidt number and the same trend is observed with the reaction rate. However, it is observed that activation energy has the effect of reducing the mass flow rate.

5. Conclusion

In this study, we investigated the momentum, thermal and concentration properties of a gold-water chemical reacting nanofluid past a rotating disc with activation energy and Brownian diffusion. We solved the problem by employing the spectral quasilinearization method. We verified the accuracy and validity of the results by comparing numerical solutions with published results in the literature. We also validated the convergence of the method by analyzing the residual errors. We found that the parameters ϕ, λ, m, n, Pr, Sc and E had varying effects on the radial velocity, azimuthal velocity, axial velocity, temperature and concentration distributions. The impact of these parameters were graphically presented and analyzed. Among other findings, we found that

1. increasing the volume fraction of the gold nanoparticles leads to a depletion of the radial and tangential velocities, while it increases the axial velocity,
2. a rise in nanoparticle volume fraction results in decreased temperature,

3. an increase in activation energy leads to elevated concentration but depressed temperature,
4. a rise in nanofluid volume fraction leads to increased skin friction and heat and mass transfer rates.

Acknowledgements

The authors are grateful for the financial support provided by the University of KwaZulu-Natal, South Africa.

Declaration

No data are available in this manuscript.

References

[1] Jasmine, H. A., & Gajjar, J. S. (2005). Absolute instability of the von Kármán, Bödewadt and Ekman flows between a rotating disc and a stationary lid. Philosophical Transactions of the Royal Society A: Mathematical, Physical and Engineering Sciences, 363(1830), 1131-1144.

[2] Lingwood, R. J. (1997). Absolute instability of the Ekman layer and related rotating flows. Journal of Fluid Mechanics, 331, 405-428.

[3] Ijaz, M., Ayub, M., & Khan, H. (2019). Entropy generation and activation energy mechanism in nonlinear radiative flow of Sisko nanofluid: rotating disk. Heliyon, 5(6), e01863.

[4] Mabood, F., Khan, W. A.,& Makinde, O. D. (2017). Hydromagnetic flow of a variable viscosity nanofluid in a rotating permeable channel with hall effects. Journal of Engineering Thermophysics, 26(4), 553-566.

[5] Mondal, H., De, P., Chatterjee, S., Sibanda, P., Roy, P. K. (2017). MHD three-dimensional nanofluid flow on a vertical stretching surface with heat generation/absorption and thermal radiation. Journal of Nanofluids, 6(1), 189-195.

[6] Rehman, A. U., Mehmood, R., Nadeem, S. (2017). Entropy analysis of radioactive rotating nanofluid with thermal slip. Applied Thermal Engineering, 112, 832-840.

[7] Gamasaee, N. A., Muhammad, H. A., Tadayon, E., Ale-Ebrahim, M., Mirpour, M., Sharifi, M., Salihi, A., Shekha, M.S., Alasady, A.A.B., Aziz, F.M., Akhtari, K., Hasan, A., & Falahati, M. (2019). The Effects of Nickel Oxide Nanoparticles on Structural Changes, Heme Degradation, Aggregation of Hemoglobin and Expression of Apoptotic Genes in Lymphocyte Cells. Journal of Biomolecular Structure and Dynamics, DOI: 10.1080/07391102.2019.1662850.

[8] Esakkimuthu, T., Sivakumar, D., & Akila, S. (2014). Application of nanoparticles in waste water treatment. Pollution Research, 33(03), 567-571.

[9] Pantapasis, K., Grumezescu, A. M. (2017). Gold nanoparticles: advances in water purification approaches. In Water Purification, 447-477, Academic Press, London.

[10] Khan, M., Irfan, M., & Khan, W. A. (2017). Impact of nonlinear thermal radiation and gyrotactic microorganisms on the Magneto-Burgers nanofluid. International Journal of Mechanical Sciences, 130, 375-382.

[11] Khan, M., Irfan, M., Khan, W. A., & Alshomrani, A. S. (2017). A new modeling for 3D Carreau fluid flow considering nonlinear thermal radiation. Results in physics, 7, 2692-2704.

[12] Irfan, M., Khan, M., Khan, W. A., & Rafiq, K. (2020). Physical aspects of shear thinning/thickening behavior in radiative flow of magnetite Carreau nanofluid with nanoparticle mass flux conditions. Applied Nanoscience, 1-13.

[13] Irfan, M., Anwar, M. S., Rashid, M., Waqas, M., & Khan, W. A. (2020). Arrhenius activation energy aspects in mixed convection Carreau nanofluid with nonlinear thermal radiation. Applied Nanoscience, 10(12), 4403-4413.

[14] Turkyilmazoglu, M. (2014). Nanofluid flow and heat transfer due to a rotating disk. Computers Fluids, 94, 139-146.

[15] Yin, C., Zheng, L., Zhang, C., Zhang, X. (2017). Flow and heat transfer of nanofluids over a rotating disk with uniform stretching rate in the radial direction. Propulsion and Power Research, 6(1), 25-30.

[16] Oloniiju, S. D., Goqo, S. P., Sibanda, P. (2019). Heat and mass transfer of an unsteady second grade nanofluid with viscous heating dissipation. International Journal of Computational Methods, 1940005.

[17] Dhlamini, M., Kameswaran, P. K., Sibanda, P., Motsa, S., & Mondal, H. (2019). Activation energy and binary chemical reaction effects in mixed convective nanofluid flow with convective boundary conditions. Journal of Computational Design and Engineering, 6(2), 149-158.

[18] Abbas, Z., Sheikh, M., & Motsa, S. S. (2016). Numerical solution of binary chemical reaction on stagnation point flow of Casson fluid over a stretching/shrinking sheet with thermal radiation. Energy, 95, 12-20.

[19] Maleque, K. (2013). Effects of binary chemical reaction and activation energy on MHD boundary layer heat and mass transfer flow with viscous dissipation and heat generation/absorption. ISRN Thermodynamics, 2013.

[20] Subbarayudu, K., Suneetha, S., Reddy, P. B. A., Rashad, A. M. (2019). Framing the activation energy and binary chemical reaction on CNT's with Cattaneo–Christov heat diffusion on Maxwell nanofluid in the presence of nonlinear thermal radiation. Arabian Journal for Science and Engineering, 44(12), 10313-10325.

[21] Reddy, S. R. R., Reddy, P. B. A., Rashad, A. M. (2020). Activation energy impact on chemically reacting Eyring–Powell Nanofluid flow over a stretching cylinder. Arabian Journal for Science and Engineering, 1-16.

[22] Reddy, S. R. R., Reddy, P. B. A., Rashad, A. M. (2020). Effectiveness of binary chemical reaction on magneto-fluid flow with Cattaneo–Christov heat flux model. Proceedings of the Institution of Mechanical Engineers, Part C: Journal of Mechanical Engineering Science, 0954406220950347.

[23] Mabood, F., Yusuf, T. A., Rashad, A. M., Khan, W. A., Nabwey, H. A. (2021). Effects of Combined Heat and Mass Transfer on Entropy Generation due to MHD Nanofluid Flow over a Rotating Frame. CMC-COMPUTERS MATERIALS CONTINUA, 66(1), 575-587.

[24] Qian, H., Pretzer, L. A., Velazquez, J. C., Zhao, Z., Wong, M. S. (2013). Gold nanoparticles for cleaning contaminated water. Journal of Chemical Technology & Biotechnology, 88(5), 735-741.

[25] Lingwood, R. J. (1995). Absolute instability of the boundary layer on a rotating disk. Journal of Fluid Mechanics, 299, 17-33.

[26] Fadhilah, S. A., Hidayah, I., Hilwa, M. Z., Faizah, H. N., & Marhamah, R. S. (2013). Thermophysical properties of Copper/Water nanofluid for automotive cooling system. Journal of Mechanical Engineering and Technology (JMET), 5(2).

[27] Andrews, J., & Devi, S. A. (2012). Nanofluid Flow over a Rotating Disk with Prescribed Heat Flux. Mapana-Journal of Sciences, 11(3), 77-92.

[28] Qureshi, M. Z. A., Rubbab, Q., Irshad, S., Ahmad, S., Aqeel, M. (2016). Heat and mass transfer analysis of MHD nanofluid flow with radiative heat effects in the presence of spherical Au-metallic nanoparticles. Nanoscale research letters, 11(1), 472.

[29] Makukula, Z., Sibanda, P., Motsa, S. (2010). A note on the solution of the von Kármán equations using series and Chebyshev spectral methods. Boundary Value Problems, 2010(1), 471793.

[30] Von Kármán, T. (1921). Uber laminare und turbulente Reibung. Z. Angew. Math. Mech., 1, 233-252.

[31] Attia, H. A. (2009). Steady flow over a rotating disk in porous medium with heat transfer. Nonlinear Analysis: Modeling and Control, 14(1), 21-26.

[32] Bellman, R. E., & Kalaba, R. E. (1965). Quasilinearization and nonlinear boundary-value problems.

[33] Motsa, S. S., Sibanda, P., Shateyi, S. (2011). On a new quasilinearization method for systems of nonlinear boundary value problems. Mathematical Methods in the Applied Sciences, 34(11), 1406-1413.

[34] Trefethen, L. N. (2000). Spectral methods in MATLAB (Vol. 10). Siam, Philadelphia.

[35] Rashidi, M. M., Abelman, S., Mehr, N. F. (2013). Entropy generation in steady MHD flow due to a rotating porous disk in a nanofluid. International Journal of Heat and Mass Transfer, 62, 515-525.

[36] Abolbashari, M. H., Freidoonimehr, N., Nazari, F., & Rashidi, M. M. (2015). Analytical modeling of entropy generation for Casson nano-fluid flow induced by a stretching surface. Advanced Powder Technology, 26(2), 542-552.

[37] Awad, F. G., Motsa, S., & Khumalo, M. (2014). Heat and mass transfer in unsteady rotating fluid flow with binary chemical reaction and activation energy. PloS one, 9(9), e107622.

Summary

In this chapter, the effect of activation energy and a binary chemical reaction on nanofluid flow past a rotating disk was studied. The model equations were solved numerically using the spectral quasilinearization method. Comparison of results for limiting cases with those in the literature were made for some parameters of interest and good agreement was obtained. The residual errors showed that convergence was fast thereby confirming the effectiveness of the method.

Chapter 5

Effect on entropy generation analysis for heat transfer nanofluid near a rotating disk using quasilinearization method

In Chapter 4, the effects of binary chemical reaction and activation energy past a rotating disk were studied. In this chapter, the effects of the magnetic field, suction and prescribed heat flux on nanofluid flow past a permeable rotating disk are investigated. In addition, an analysis of entropy generation is given for the flow. Entropy generation analysis plays an important role in identifying sources of irreversibilities in thermal systems [142]. This aids in reducing energy losses and inefficiencies for the system. Detailed discussions of entropy generation in nanofluid flows past rotating disks are available in the references [143–147], among other studies.

[1]

[1]Accepted

Effect on entropy generation analysis for heat transfer nanofluid near a rotating disk using quasilinearization method

Mangwiro Magodora[a]

Hiranmoy Mondal[b*]*

Sandile Motsa[a]

Precious Sibanda[a]

[a] *School of Mathematics, Statistics and Computer Science,University of KwaZulu-Natal, Private Bag X01, Scottsvile, Pietermaritzburg-3209, South Africa*

[b] *Department of Applied Science, Maulana Abul Kalam Azad University of Technology, West Bengal-741249, India*

Abstract

The study considers gold-water nanofluid flow past a porous rotating disk while accounting for prescribed heat flux and suction at the disk surface. The impact of selected physical parameters such as the nanoparticle volume fraction, magnetic parameter and Prandtl number on the entropy generation are investigated and presented in this paper. The model equations are solved numerically using the spectral quasilinearization method. Results are presented in graphical form and discussed for variations of the flow parameters. The findings indicate that increased nanoparticle volume concentration leads to a fall in velocity but a rise in temperature, while enhancing the magnetic parameter is associated with reduced velocity distribution and increased skin friction. Among other findings, the results also show that increasing the Brinkman number leads to increased entropy generation but reduced Bejan number, while increasing the Reynolds number results in the generation of elevated levels of entropy production. The accuracy and reliability of the method are checked through convergence error analysis. The accuracy is further tested through a comparison of results for limiting cases with those in the literature. The findings of this study have significant applications in engineering, science and technology.

Key words: Nanofluid; Spectral quasilinearization; Rotating disk; Magnetic parameter; Entropy generation.

---

*Corresponding author.
Email address : hiranmoymondal@yahoo.co.in (H. Mondal)

Nomenclature

B_0	constant magnetic flux density
Be	Bejan number
Br	rotational Brinkman number
C_f	coefficient of skin friction
C_p	specific heat capacity at constant pressure (J/kgK)
k	thermal conductivity (W/mK)
L	non-dimensional length scale
M	magnetic parameter
N_G	local entropy generation number
Nu	local Nusselt number
p	nanofluid pressure (N/m^2)
Pr	Prandtl number
q_w	surface heat flux (W/m^2)
$\bar{r}$	dimensionless radial coordinate
Re	rotational Reynolds number
S	suction parameter
S_G	local entropy generation rate
S_0'''	characteristic entropy generation rate
T	nanofluid temperature (K)
T_w	temperature at the disk surface (K)
T_∞	temperature of the ambient nanofluid (K)
u, v, w	velocities in the r, ψ and z directions (m/s)
r, ψ, z	cylindrical coordinates (m)
U	dimensionless radial velocity
V	dimensionless tangential velocity
W	dimensionless axial velocity
w_0	axial velocity at the disk surface (m/s)

Greek Symbols

ξ	dimensionless axial coordinate
θ	dimensionless temperature
σ	electrical conductivity (S/m)
ρ	density (kg/m^3)
κ	dimensionless temperature difference ($[T_w - T_\infty]/T_\infty$)
μ	dynamic viscosity (Ns/m^2)
ν	kinematic viscosity (m^2/s)
ϕ	nanoparticle volume fraction
Ω	uniform angular velocity (s^{-1})
τ	local shear stress (N/m^2)

1. Introduction

High heat transfer dissipation is among the most popular reasons why many scientists have made numerous attempts to build new cooling systems. The term nanofluid refers to the relatively special generation of fluids that fuses a base liquid with metals, metal oxides, carbides or non-metallic nano-sized particles which suspended in it [1]. Such strategies have remarkably improved thermo-physical properties of base liquids such as heat capacity, specific heat and coefficient of thermal expansion. Choi [2] is touted as the first researcher to coin the term nanofluid in his work [3]. Nanofluids have a desirable property of enhancing the thermal conductivity and convective thermal performance of base fluids [4, 5].

Nanofluids find wide applications in aeronautical and space science, motor vehicle industry as coolants, nanomedicine, food processing industry, cooling of nuclear reactors, microsystem cooling, air cleaning devices, cooling of production materials, consumer products, etc [6–8]. Due to their varied and significant applications in engineering and technology, several studies on nanofluid flow have been carried out in recent years. Dogonchi et al. [9] investigated the hydromagnetic nanofluid flow between squeezed parallel plates while accounting for thermal radiation, Joule heating and viscous dissipation. Krishna and Chamkha [10] investigated Hall and ion slip influences on nanofluid flow past a vertical plate embedded in a porous medium. Hazarika et al. [11] explored hydromagnetic nanofluid flow of copper, silver and iron (III) oxide over a stretching sheet while Chamkha et al. [12] examined natural convective nanofluid flow in a cavity with shape factor and thermal radiation. Rao et al. [13] discussed bioconvection in nanofluid containing gyrotactic micro-organisms. More studies dealing with nanofluid flows are found in [14–25] among several others.

In this paper, we focus attention on magnetohydrodynamic (MHD) flow of nanofluids past a rotating infinite disk. Magnetohydrodynamics, also referred to as hydromagnetics, deals with the study of electrically conducting fluids in a magnetic field [26]. Examples of such fluids are electrolytes, plasmas, salt water and liquid metals. The study of MHD flows was pioneered by Hannes Alfven in 1970 [27]. Magnetohydrodynamics find applications in micro MHD pumps, drug delivery and MHD generators among others. Consequently, several studies dedicated to magnetohydrodynamic fluid flows have been done in the recent past. Krishna et al. [28] discussed free convective MHD flow over a vertical porous plate. Hydromagnetic flow of Jefferey nanofluid was reported by Rasool et al. [29]. More studies on MHD fluid flows can be found in [30–32].

The pioneering work on fluid flow over an infinite rotating disk was carried out by von-Karman in 1921 [33], who utilized the famous von-Karman transformations to transform the nonlinear Navier-Stokes equations from partial to ordinary differential equations. Rotating disk flows have significant industrial and engineering applications such as computer storage devices, design of nuclear reactors, rotational air cleaners, gas turbine engineering, centrifugal pumps, among others [34, 35]. In his work, Turkyilmazoglu [36] studied nanofluid flow over a spinning disk while Andrews and Devi [37] investigated nanofluid flow past a rotating disk with prescribed heat flux. Krishna et al. [38] explored ion slip and Hall effects on rotating flow of second grade fluid. More studies on rotating fluid flows are found in [39–51] among others.

Entropy generation analysis can be described as the most appropriate method for identifying the causes of inefficiency in a thermal system and accounts for energy losses [52]. The analysis of entropy generation is based on the second law of thermodynamics that states that the operation of real systems is characterized by a loss of available work. Controlling entropy generation or minimizing irreversibility, has the desirable effect of improving the design and performance of engineering systems [53]. Rashidi et al [54] analyzed entropy generation in MHD nanofluid flow past a rotating porous disk with variable properties. They focused on the nanomaterials of copper (Cu), copper oxide (CuO) and aluminium oxide (Al_2O_3) with water as the base fluid. They applied the fourth-order Runge-Kutta method to explore entropy production on a nanofluid flowing over a rotating disk. Rehman et al. [55] tackled entropy generation analysis on a radioactive rotating disk while Makinde and Aziz [56] presented results for heat generation analysis for Poiseuille flow of fluid possessing variable viscosity. Seyyedi et al. [57] performed entropy analysis on a wavy-hexagonal enclosure filled with nanofluid. Pal et al. [58] investigated entropy generation of Jeffrey nanofluid flow past a stretching sheet. Other studies dealing with entropy generation can be viewed in [59–67].

The motivation for the current investigation is that the domain of nanofluids is a developing area of research with many questions that still need to be answered. In this study we investigate heat transfer and entropy generation analysis for hydromagnetic gold-water nanofluid near a porous rotating disk with suction and prescribed heat flux. Gold nanoparticles find application in water treatment and also act as carriers in gene and drug delivery applications [68–70]. Gold nanoparticles also find application in chemical processing, fuel cells and pollution control [71]. Quresh et al [72] studied gold-water nanofluid flow between porous and coaxial rotating disks. The investigation by Rehman et al. [55] focuses on nanofluids that are composed of gold, copper oxide and silver nanoparticles suspended in water as the base fluid. This study has significant applications in optimization of thermal systems that occur in manufacturing engineering, chemical engineering, biomedical engineering, nuclear engineering and industrial engineering among others [73].

The constitutive equations that describe the flow of nanofluids are highly complex and nonlinear such that solving them analytically has often proved intractable [74]. As a result, several numerical schemes have been proposed to solve the equations to a high degree of accuracy but no method has been found to be adequate in fully accounting for nanofluid flow. Examples of numerical methods that have been used in the past include the Runge-Kutta method, finite difference method, Runge–Kutta–Fehlberg method, finite element method, shooting method and the Keller-box method among others [75–78]. In this study, we apply the spectral quasilinearization method to solve the gold-water nanofluid flow for a porous rotating disk with suction and prescribed heat flux. This method has been chosen because it is relatively recent and has not been adequately used by researchers to solve related problems. Previous studies have shown that this method is very accurate, efficient and robust in solving boundary value problems when compared with other methods such as the finite difference methods, finite element method, etc [79, 80]. The novelty of the current study is that we consider entropy generation analysis for MHD gold-water nanofluid flow past a rotating disk using quasilinearization method, which to the best of our knowledge, has not been considered before. The parameters of interest are presented and discussed by plotting the graphs of velocity, temperature, skin friction, Bejan number and entropy generation number. The accuracy and validity of the results are tested through convergence error analysis and a comparison of results for limiting cases with those in the literature. The results of this study will be complimentary to the existing knowledge on nanofluid flow over a rotating disk. This helps in identifying causes of inefficiency in a thermal system and finding appropriate ways to minimize entropy generation in order to mitigate loss of useful and scarce energy resources which in turn leads to optimum system performance.

The paper is structured as follows: Section 2 looks at the formulation of the problem and the associated boundary conditions. The conversion of the model equations from the nonlinear system of partial differential equations to the system of nonlinear ordinary differential equations is done in this section by means of the famous von-Karman transformations. Section 3 details the solution obtained by utilizing the spectral quasilinearization method. Section 4 presents and discusses the results with the aid of tables and graphs. Conclusions and recommendations for further investigation are presented in Section 5.

2. Formulation

We consider the steady and incompressible flow of gold-water nanofluid over a porous infinite disk that is positioned at $z = 0$ and is rotating at an angular velocity Ω about the z-axis as shown in Figure 1. We assume the nanofluid to be Newtonian and the flow to be laminar. We also consider heat transfer while accounting for suction, prescribed heat flux and uniform magnetic field that acts in the axial direction. The magnetic field strength and the concentration, temperature and prescribed heat flux at the surface of the disk are denoted B_0, C_w, T_w and q_w respectively. The continuity, momentum and energy equations for the flow are given in cylindrical form in a fixed frame of reference as [81, 82]:

$$\frac{\partial u}{\partial r} + \frac{u}{r} + \frac{\partial w}{\partial z} = 0, \tag{1}$$

$$\rho_{nf}\left(u\frac{\partial u}{\partial r} - \frac{v^2}{r} + w\frac{\partial u}{\partial z}\right) + \frac{\partial p}{\partial r} = \mu_{nf}\left(\frac{\partial^2 u}{\partial r^2} + \frac{1}{r}\frac{\partial u}{\partial r} - \frac{u}{r^2} + \frac{\partial^2 u}{\partial z^2}\right) - \sigma_{nf}\beta_0^2 u, \tag{2}$$

$$\rho_{nf}\left(u\frac{\partial v}{\partial r} + \frac{uv}{r} + w\frac{\partial v}{\partial z}\right) = \mu_{nf}\left(\frac{\partial^2 v}{\partial r^2} + \frac{1}{r}\frac{\partial v}{\partial r} - \frac{v}{r^2} + \frac{\partial^2 v}{\partial z^2}\right) - \sigma_{nf}\beta_0^2 v, \tag{3}$$

$$\rho_{nf}\left(u\frac{\partial w}{\partial r} + w\frac{\partial w}{\partial z}\right) + \frac{\partial p}{\partial z} = \mu_{nf}\left(\frac{\partial^2 w}{\partial r^2} + \frac{1}{r}\frac{\partial w}{\partial r} + \frac{\partial^2 w}{\partial z^2}\right), \tag{4}$$

$$(\rho C_p)_{nf}\left(u\frac{\partial T}{\partial r} + w\frac{\partial T}{\partial z}\right) = k_{nf}\left(\frac{\partial^2 T}{\partial r^2} + \frac{1}{r}\frac{\partial T}{\partial r} + \frac{\partial^2 T}{\partial z^2}\right) \tag{5}$$

where ρ_{nf} and μ_{nf} are the density and dynamic viscosity of nanofluid, p and T are the nanofluid pressure and temperature, $(\rho C_p)_s$ and $(\rho C_p)_{nf}$ are the specific heat capacity of nanomaterial and nanofluid, μ_{nf} is the nanofluid dynamic viscosity, B_0 is the magnetic field strength and σ_{nf} is the electrical conductivity.

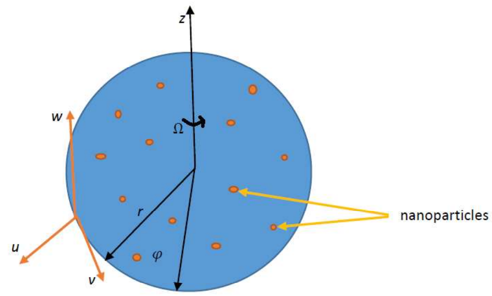

Figure 1: Flow configuration.

The boundary conditions for the system (1)-(5) are [37]:

$$\begin{aligned} &u = 0,\ v = \Omega r,\ w = -\sqrt{\nu_{nf}\Omega} S\ , q_w = -k_{nf}\frac{\partial T}{\partial z}\ \text{ at } z = 0,\\ &u \to 0,\ v \to 0,\ T \to T_\infty\ \text{ as } z \to \infty. \end{aligned} \tag{6}$$

The variable $S = w_0/\sqrt{\nu_{nf}\Omega}$ is the uniform suction parameter, ν_{nf} is the kinematics viscosity of nanofluid, q_w is the constant heat flux imposed at the surface and w_0 is the axial velocity component at the disk surface $z = 0$.

Following the Brinkman model [83], we define the nanofluid dynamic viscosity as ;

$$\mu_{nf} = \frac{\mu_f}{(1-\phi)^{2.5}}, \tag{7}$$

where ϕ the nanosolid volume fraction and μ_f is the viscosity of base fluid.

The other nanofluid properties are defined as [36]:

$$\rho_{nf} = (1-\phi)\rho_f + \phi\rho_s,\ (\rho C_p)_{nf} = (1-\phi)(\rho C_p)_f + \phi(\rho C_p)_s,\ \frac{k_{nf}}{k_f} = \frac{k_s + 2k_f - 2\phi(k_f - k_s)}{k_s + 2k_f + 2\phi(k_f - k_s)}.$$

Here ρ_s is the nanoparticle density, ρ_f base fluid density, k_f thermal conductivity of the fluid fraction and k_s thermal conductivity of solid fraction.

The thermo-physical properties of the nanomaterial and the base fluid are shown in Table 1 below:

Property	Water	Gold
Density, ρ (kgm^{-3})	997.1	19300
Thermal conductivity, k $(Wm^{-1}K^{-1})$	0.613	318
Specific heat capacity, C_p $(Jkg^{-1}K^{-1})$	4179	1290

Table 1: Thermo-physical properties of nanoparticles and base fluid.

We make use of the famous Von-Kármán similarity transformations [84];

$$u = r\Omega U(\xi),\ v = r\Omega V(\xi),\ w = \sqrt{\nu_{nf}\Omega}W(\xi),\ p = -\rho_{nf}\nu_{nf}\Omega P(\xi) \tag{8}$$

and the similarity variables

$$T = (q_w/k_{nf})(\nu_{nf}/\Omega)^{0.5}\theta(\xi) + T_\infty,\ \xi = (1/L)\, z,\ \text{where } L = (\nu_f/\Omega)^{0.5}, \tag{9}$$

to transfigure the system (1)-(5) to ;

$$2U + W' = 0, \tag{10}$$
$$\alpha U'' - U^2 + V^2 - WU' - \beta MU = 0, \tag{11}$$
$$\alpha V'' - 2UV - WV' - \beta MV = 0, \tag{12}$$
$$\delta\theta'' - PrW\theta' = 0, \tag{13}$$
$$\alpha(W'' + P') - WW' = 0, \tag{14}$$

Here prime ($'$) signifies differentiation with respect to the non-dimensional axial coordinate ξ, while $U(\xi),\ V(\xi), W(\xi),\ P(\xi)$ are the non-dimensional forms of radial velocity, azimuthal velocity and and pressure while ν_f is the kinematic viscosity for the flow. The parameter $Pr = (\mu_f C_{pf})/k_f$ is the Prandtl number, $M = \frac{\sigma_{nf}B_0^2}{\Omega\rho_f}$ represents the magnetic parameter, while the parameters $\alpha,\ \beta$ and δ are defined by;

$$\alpha = \frac{1}{(1-\phi)^{2.5}(1-\phi+\phi\frac{\rho_s}{\rho_f})},\ \delta = \frac{(k_{nf}/k_f)}{1-\phi+\phi\frac{(\rho C_p)_s}{(\rho C_p)_f}},\ \beta = \frac{1}{1-\phi+\phi\frac{\rho_s}{\rho_f}}. \tag{15}$$

The associated transfigured boundary conditions are:

$$\begin{aligned} &U = V - 1 = W + S = \theta' + 1 = 0 \ \text{ at } \xi = 0, \\ &U = V = \theta = 0 \ \text{ as } \xi \to \infty. \end{aligned} \tag{16}$$

The physical quantities of interest are the skin friction and the Nusselt Number which are defined as;

$$C_f = \frac{\tau}{\rho_{nf}U_0^2},\ Nu = \frac{rq_w}{k_f(T_0 - T_1)}, \tag{17}$$

where $U_0 = \Omega r$ is the characteristic velocity, $\tau = ({\tau_{zr}}^2 + {\tau_{z\psi}}^2)^{0.5}$ is the local shear stress, τ_{zr} is the radial component of shear stress, $\tau_{z\psi}$ is the azimuthal component of shear stress, q_w is the surface heat flux and $\tau_{zr},\ \tau_{z\psi},\ q_w$ are defined as:

$$\tau_{zr} = \mu_{nf}\left(\frac{\partial u}{\partial z} + \frac{\partial w}{\partial r}\right)\bigg|_{\hat{z}=0},\ \tau_{z\theta} = \mu_{nf}\left(\frac{\partial v}{\partial z} + \frac{1}{r}\frac{\partial w}{\partial \theta}\right)\bigg|_{\hat{z}=0},\ q_w = -k_{nf}\left.\frac{\partial T}{\partial z}\right|_{\hat{z}=0}, \tag{18}$$

It follows that the skin friction coefficient and Nusselt number are given by:

$$Re^{\frac{1}{2}}C_f = [U'(0)^2 + V'(0)^2]^{0.5}/(1-\phi)^{2.5}, \; Re^{-\frac{1}{2}}Nu = -(k_{nf}/k_f)\theta'(0), \tag{19}$$

where $Re = \Omega r^2/\nu_f$ represents the local Reynolds number.

The other quantities of keen interest are the local entropy generation rate, the local entropy generation number and the Bejan number which are denoted as S'''_G, N_G and Be respectively. As shown in [54] and [64], the local entropy generation rate is derived from a combination of thermal irreversibility, fluid friction irreversibility and Joule friction irreversibility and is given as

$$S'''_G = \frac{k_{nf}}{T_\infty^2}\left(\frac{\partial T}{\partial z}\right)^2 \tag{20}$$

$$+\frac{\mu_{nf}}{T_\infty}\left[2\left\{\left(\frac{\partial U}{\partial r}\right)^2 + \frac{U^2}{r} + \left(\frac{\partial W}{\partial z}\right)^2 + \left(\frac{\partial U}{\partial z}\right)^2 + \left(\frac{\partial V}{\partial z}\right)^2 + \left(r\frac{\partial}{\partial r}\left[\frac{V}{r}\right]\right)^2\right\}\right] \tag{21}$$

$$+\frac{B_0\sigma_{nf}}{T_\infty}\left[U^2 + V^2\right] \tag{22}$$

The Von-Karman transformations in equation (8), when applied to the local entropy generation rate, yield the local entropy generation number which is given below as

$$N_G = \kappa(\theta')^2 + Br\left\{\frac{3}{Re}(W')^2 + \overline{r}^2\left(\left[U'^2 + V'^2\right] + M\left[U^2 + V^2\right]\right)\right\} \tag{23}$$

where $\kappa = (T_w - T_\infty)/T_\infty$ and $Br = \mu_{nf}\Omega^2 L^2/k_{nf}(T_w - T_\infty)$ defines the rotational Brinkman number.

The Bejan number is defined as the ratio of entropy generation due to heat transfer to the overall entropy generation rate and is given by

$$Be = \frac{\kappa\theta'^2}{\kappa\theta'^2 + Br\left[\frac{4}{Re}U^2 + \frac{2}{Re}W'^2 + \overline{r}\left(U'^2 + V'^2 + M\left\{U^2 + V^2\right\}\right)\right]}. \tag{24}$$

The Bejan number lies between 0 and 1 inclusive. When $Be = 0$, fluid friction and Joule dissipation dominate the irreversibility whilst $Be = 1$ signifies dominance of irreversibility due to heat transfer. The value $Be = 1/2$ indicates equality between the contribution of heat transfer to entropy generation and the sum of irreversibilities due to Joule dissipation and fluid friction.

3. Numerical solution

The solution to the nonlinear system (10)-(14) is obtained by utilizing the spectral quasililinearization method which has been demonstrated in literature to be highly robust and efficient in solving boundary value problems [85]. We perform the solution procedure by linearizing, discretizing and solving the equations (10)-(13) for U, V W and θ, while equation (14) can be used to determine the pressure distribution if required [86].

Substituting (10) into (11) and (12) yields the reduced system

$$\alpha W''' - WW'' + \frac{1}{2}(W')^2 - \beta M W' - 2V^2 = 0, \tag{25}$$

$$\alpha V'' + W'V - WV' - \beta M V = 0, \tag{26}$$

$$\delta\theta'' - PrW\theta' = 0, \tag{27}$$

subject to the boundary conditions

$$\begin{aligned} &V - 1 = W + S = W' = V - 1 = \theta' + 1 = 0 \ \text{ at } \xi = 0, \\ &V \to 0, \ W' \to 0, \ P \to 0, \ \theta \to 0 \ \text{ as } \xi \to \infty. \end{aligned} \tag{28}$$

The system is subsequently solved by applying the spectral quasilinearization method, which we will omit in this paper. The detailed procedure for implementing the spectral quasilinearization method can be found in the references [87–90].

4. Results & Discussion

The nonlinear differential equations (25)-(27) are solved numerically by using the quasilinearization method for specific values of the nanoparticle volume fraction ϕ, suction parameter S, Prandtl number Pr and magnetic parameter M. For the current study the Prandtl number is taken to be 6.2 (for water), unless otherwise stated.

4.1. Validation

To determine the accuracy of the results, a comparison is made between current results and those of Yin et al. [3] and Turkylmazoglu [36] for limiting cases as shown in Table 2 below. Excellent agreement is observed, thereby confirming the accuracy of our results.

4.2. Skin friction, Prandtl number, magnetic field, nanofluid volume fraction and temperature

Figures 2-5 depict the effects of varying the nanoparticle volume fraction on the velocity components and temperature. It is demonstrated in Figures 2-4 that as the nanofluid volume fraction is increased, all the three velocity components decrease. Increasing the nanofluid volume fraction results in increased temperature as depicted in Figure 5. This phenomena is expected since a surge in the nanoparticle volume fraction leads to enhanced thermal conductivity, hence the appreciation of the thermal boundary layer thickness.

Figures 6-9 portray the effects of the suction parameter on the velocity and temperature distributions. As Figures 6-8 show, increasing the suction parameter signifies the downward axial escape of nanofluid at the disk surface. This process is accompanied by a decrease in the radial and azimuthal directions as fluid is sucked away at a faster rate on the disk surface. Figure 9 demonstrates that as suction increases, temperature decreases. An upward variation of suction results in more heated nanofluid escaping at the surface of the porous disk. The escaping nanofluid is replaced by the cooler nanofluid moving from the ambient nanofluid, and this explains the drop in the temperature.

Figure 10 exhibits the impact of increasing the Prandtl number on the temperature. The Prandtl number is a dimensionless quantity that relates fluid viscosity to thermal conductivity. In other words, the Prandtl number is the ratio of the momentum diffusivity to thermal diffusivity. The graph reveals that an ascension of the Prandtl number is associated with a decrease in the temperature. More details on the Prandtl number can be accessed in the references [89, 91].

Figures 11-14 show the variation of velocity and temperature distributions with the magnetic parameter. Increasing the magnetic parameter leads to depressed velocity components. This behaviour can be explained by the fact that an increased magnetic field strength leads to an enhanced Lorentz force. The Lorentz force has a tendency to oppose the flow of the nanofluid, hence the decreased radial, axial and circumferential velocities. Increased Lorentz force implies increased resistance to nanofluid flow leading to a rise in temperature as illustrated by Figure 14. These results imply that the magnetic field can be used to control the momentum and temperature of the nanofluid to required specifications. The impact of the magnetic parameter M and suction S on the skin friction are shown on Figure 15. The figure demonstrates that increasing the magnetic force and the suction tend to increase the skin friction.

4.3. Entropy generation analysis

Figures 16-18 show the effects of the rotational Brinkman number and the Reynolds number on the entropy generation and Bejan numbers. As depicted in Figure 16, increasing the Reynolds number is accompanied by an increase in the entropy generation number. A rise in the Reynolds number implies an increase in the velocity of the nanofluid and chaotic fluid motions appear. As a result more fluid collisions occur leading to a rise in entropy generation. Figure 17 shows that increasing the rotational Brinkman number has the effect of elevating the production of entropy. It is also apparent that the entropy generation is higher in the vicinity of the disk surface but gradually falls to zero further away from the disk. This behaviour is attributed to the presence of higher temperature and velocity gradients as well as decreased fluid friction in close proximity to the spinning disk. Figure 18 shows that the rotational Brinkman number causes the Bejan number to diminish, indicating the increasing contribution of fluid friction to entropy generation.

4.4. Error and convergence

Figures 19-22 show the rate of convergence analysis for various values of nanofluid volume fraction. The rate of convergence is shown to be fast and convergence is attained after only a few iterations. This validates our results and shows that the spectral quasilinearization method is efficient and robust in accordance with the published literature.

	Ref. [3]	Ref. [36]	Current results
$U'(0)$	0.51023262	0.51022941	0.510232616
$-V'(0)$	0.61591990	0.61592201	0.615922013
$-W(\infty)$	0.88446912	0.88447411	0.884473415
$-\theta'(0)$	0.93387285	0.93387794	0.933877935

Table 2: Values of $U'(0), \ -V'(0), \ -W(\infty)$ and $-\theta'(0)$ for $Pr = 6.2, \ S = 0, M = 0, \ \phi = 0$.

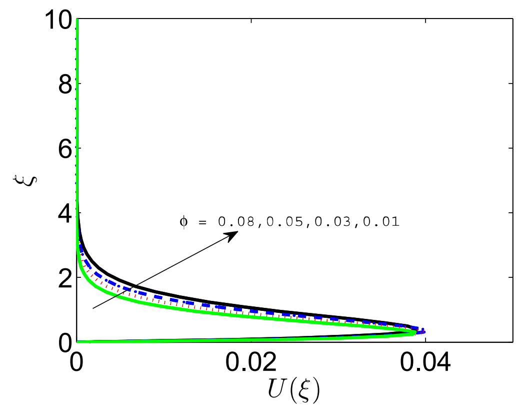

Figure 2: Effect of nanofluid volume fraction ϕ on radial velocity $U(\xi)$ when $M = 1, \ S = 1, \ Pr = 6.2$.

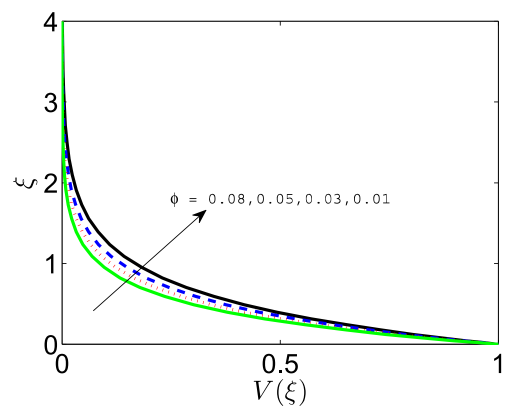

Figure 3: Effect of nanofluid volume fraction ϕ on azimuthal velocity $V(\xi)$ when $M = 1, \ S = 1, \ Pr = 6.2$.

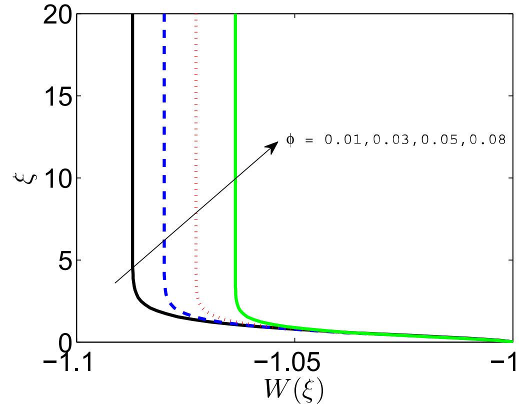

Figure 4: Effect of nanofluid volume fraction ϕ on axial velocity $W(\xi)$ when $M = 1,\ S = 1,\ Pr = 6.2$.

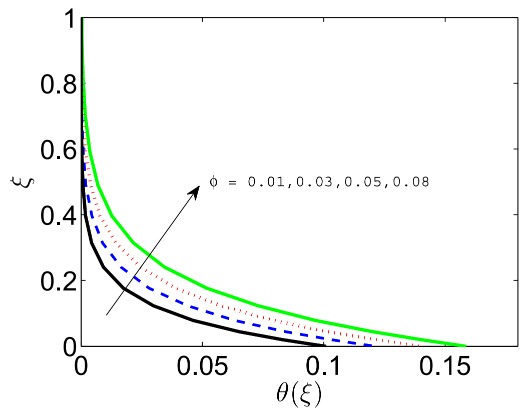

Figure 5: Effect of nanofluid volume fraction ϕ on temperature $\theta(\xi)$ for $M = 1,\ S = 1,\ Pr = 6.2$.

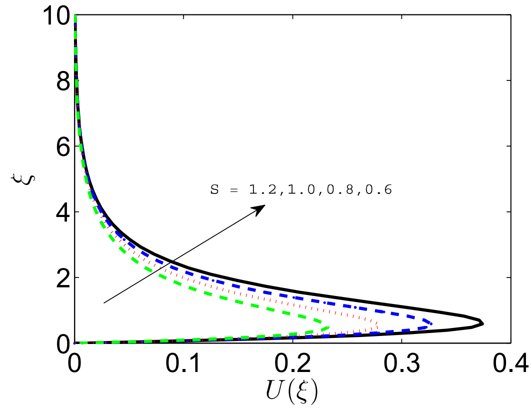

Figure 6: Effect of varying the suction parameter S on the radial velocity $U(\xi)$ for $M = 1,\ \phi = 0.1$.

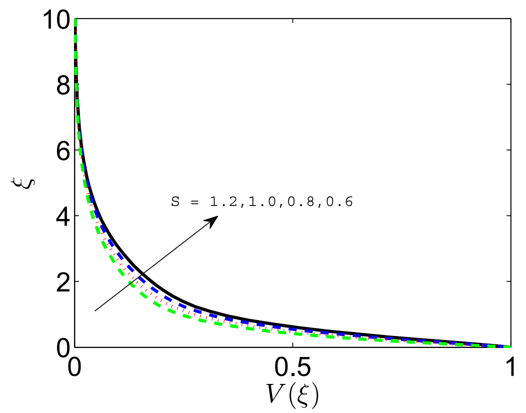

Figure 7: Impact of varying the suction parameter S on the tangential velocity $V(\xi)$ for $M = 1,\ \phi = 0.1$.

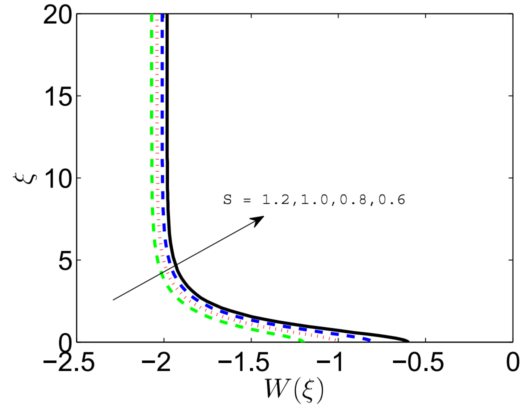

Figure 8: Effect of varying the suction parameter S on the axial velocity $V(\xi)$ for $Pr = 6.2,\ M = 1,\ \phi = 0.1$.

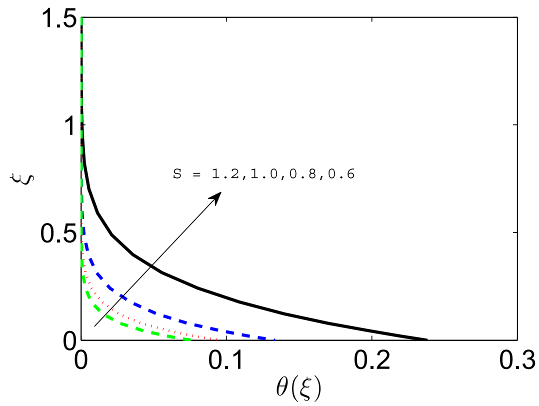

Figure 9: Variation of the temperature $\theta(\xi)$ with the suction parameter S when $Pr = 6.2,\ M = 1,\ \phi = 0.1$.

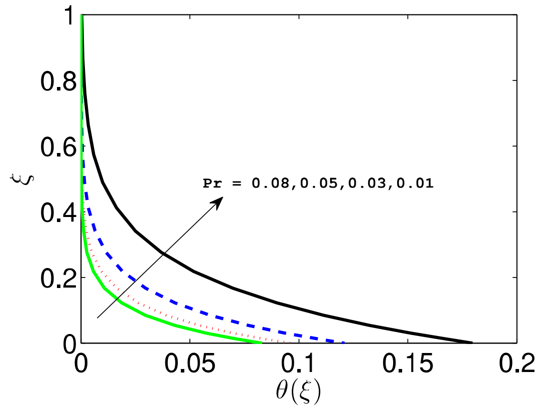

Figure 10: Effect of varying Prandtl number Pr on temperature $\theta(xi)$ for $S = 1,\ M = 1,\ \phi = 0.1$.

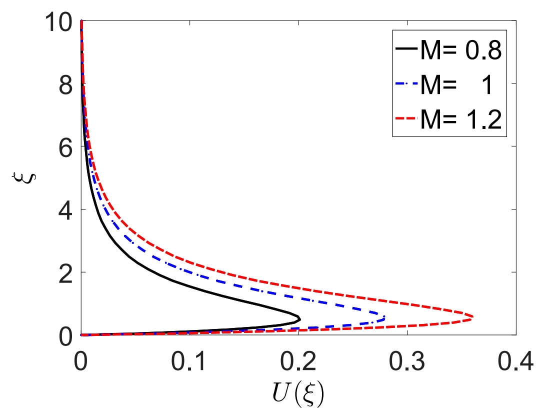

Figure 11: Impact of the magnetic parameter M on the radial velocity when $Pr = 6.2,\ S = 1,\ \phi = 0.1$.

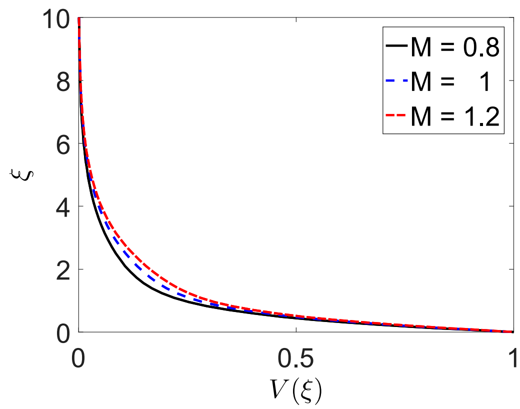

Figure 12: Impact of the magnetic parameter M on the tangential velocity when $Pr = 6.2,\ S = 1,\ \phi = 0.1$.

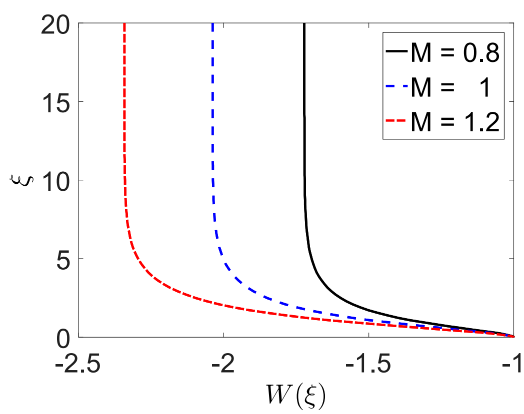

Figure 13: Impact of the magnetic parameter M on the axial velocity when $Pr = 6.2,\ S = 1,\ \phi = 0.1$.

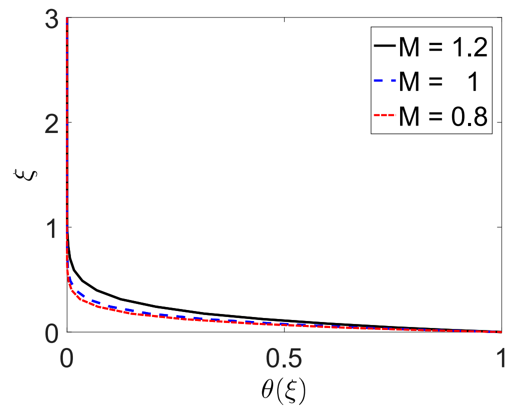

Figure 14: Impact of the magnetic parameter M on the temperature when $Pr = 6.2,\ S = 1,\ \phi = 0.1$.

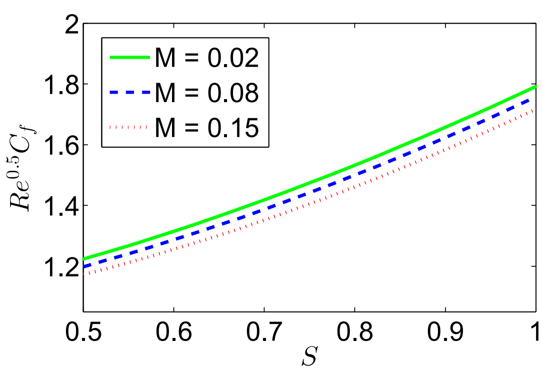

Figure 15: Impact of the suction S and the magnetic parameter M on the skin friction.

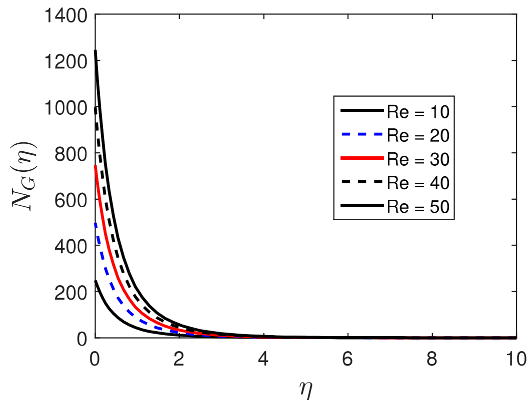

Figure 16: Impact of the Reynolds number on entropy generation.

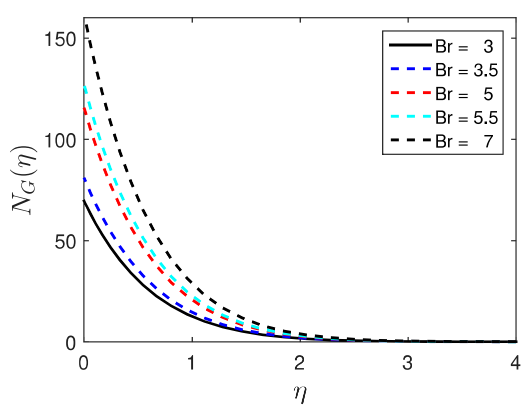

Figure 17: Impact of the rotational Brinkman number on entropy generation.

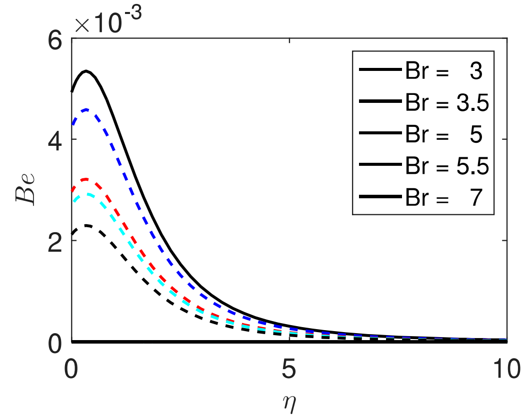

Figure 18: Impact of the rotational Brinkman number on the Bejan number.

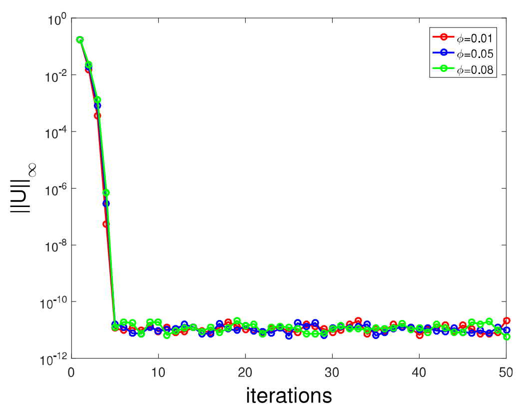

Figure 19: Convergence of $||U||_\infty$ for different values of ϕ when $Pr = 6.2,\ M = 1,\ S = 1$.

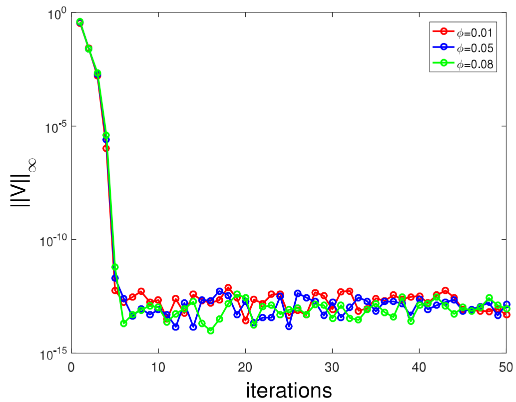

Figure 20: Convergence of $||V||_\infty$ for different values of ϕ when $Pr = 6.2,\ M = 1,\ S = 1.$

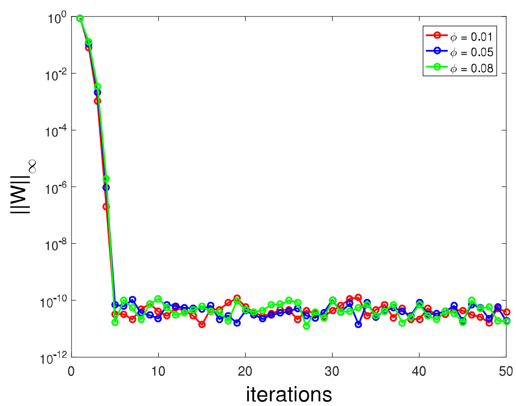

Figure 21: Convergence of $||W||_\infty$ for different values of ϕ when $Pr = 6.2,\ M = 1,\ S = 1.$

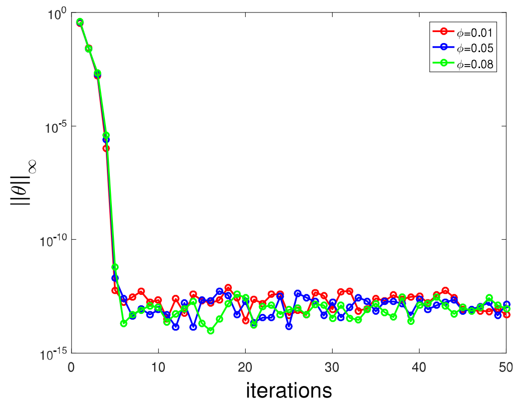

Figure 22: Convergence of $||\theta||_\infty$ for different values of ϕ when $Pr = 6.2,\ M = 1,\ S = 1$.

5. Conclusions

The study has considered a numerical investigation into the steady flow of gold-water nanofluid past a porous rotating disk while accounting for prescribed heat flux and suction at the disk surface. The impact of some physical flow parameters such as the nanoparticle volume fraction, suction, magnetic parameter and Prandtl number on the velocity and temperature distributions and entropy generation. The following conclusions have been drawn from the study;

1. The velocity distribution is depleted while the temperature distribution is enhanced by a rise in the volume fraction of the nanoparticles.
2. Increasing the suction parameter depreciates both the velocity and temperature distributions.
3. The increase in the magnetic parameter leads to decreased radial, axial and circumferential velocities.
4. Increasing the magnetic parameter and the suction parameter improve the skin friction.
5. Enhancing the nanoparticle volume fraction leads to a fall in velocity but a rise in temperature .
6. Increasing the magnetic field is associated with reduced velocity distribution and increased skin friction.
7.Increasing the rotational Brinkman number leads to increased entropy but reduced Bejan number.
8. Increasing the Reynolds number results in the generation of elevated levels of entropy.

It is hoped that the results of this study will be complimentary to existing knowledge on nanofluid flow over rotating disks. This helps in identifying causes of inefficiency in thermal systems and finding appropriate ways to minimize entropy generation in order to mitigate loss of useful and scarce energy resources.

Acknowledgements

The authors are pleased to express their gratitude for the financial support rendered by the University of KwaZulu-Natal and the DSI-NRF Centre of Excellence in Mathematical and Statistical Sciences (CoE-MaSS).

Competing Interests

The authors declare that there are no competing interests regarding the publication of this paper.

References

[1] Hojjat, M., Etemad, S. G., & Bagheri, R. (2010). Laminar heat transfer of non-Newtonian nanofluids in a circular tube. Korean Journal of Chemical Engineering, 27(5), 1391-1396.

[2] Choi, S. U. S., Singer, D. A., & Wang, H. P. (1995). Developments and applications of non-Newtonian flows. Asme Fed, 66, 99-105.

[3] Yin, C., Zheng, L., Zhang, C., & Zhang, X. (2017). Flow and heat transfer of nanofluids over a rotating disk with uniform stretching rate in the radial direction. Propulsion and Power Research, 6(1), 25-30.

[4] Das, K. (2015). Nanofluid flow over a nonlinear permeable stretching sheet with partial slip. Journal of the Egyptian mathematical society, 23(2), 451-456.

[5] Ghalambaz, M., Mehryan, S. A. M., Zahmatkesh, I., & Chamkha, A. (2020). Free convection heat transfer analysis of a suspension of nano–encapsulated phase change materials (NEPCMs) in an inclined porous cavity. International Journal of Thermal Sciences, 157, 106503.

[6] Aldabesh, A., Rout, B. C., Mishra, S. R., Henda, M. B., & Tlili, I. (2020). Impact of magnetohydrodynamic and buoyancy-driven forces on carbon nanotube-water nanofluid. Mathematical Methods in the Applied Sciences.

[7] Ijaz, M., Ayub, M., & Khan, H. (2019). Entropy generation and activation energy mechanism in nonlinear radiative flow of Sisko nanofluid: rotating disk. Heliyon, 5(6), e01863.

[8] Mahian, O., Kianifar, A., Kleinstreuer, C., Moh'd A, A. N., Pop, I., Sahin, A. Z., & Wongwises, S. (2013). A review of entropy generation in nanofluid flow. International Journal of Heat and Mass Transfer, 65, 514-532.

[9] Dogonchi, A. S., Waqas, M., Afshar, S. R., Seyyedi, S. M., Hashemi-Tilehnoee, M., Chamkha, A. J., & Ganji, D. D. (2019). Investigation of magneto-hydrodynamic fluid squeezed between two parallel disks by considering Joule heating, thermal radiation, and adding different nanoparticles. International Journal of Numerical Methods for Heat & Fluid Flow.

[10] Krishna, M. V., & Chamkha, A. J. (2019). Hall and ion slip effects on MHD rotating boundary layer flow of nanofluid past an infinite vertical plate embedded in a porous medium. Results in Physics, 15, 102652.

[11] Hazarika, S., Ahmed, S., & Chamkha, A. J. (2021). Investigation of nanoparticles Cu, Ag and Fe_3O_4 on thermophoresis and viscous dissipation of MHD nanofluid over a stretching sheet in a porous regime: A numerical modeling. Mathematics and Computers in Simulation, 182, 819-837.

[12] Chamkha, A. J., Dogonchi, A. S., & Ganji, D. D. (2018). Magnetohydrodynamic nanofluid natural convection in a cavity under thermal radiation and shape factor of nanoparticles impacts: a numerical study using CVFEM. Applied Sciences, 8(12), 2396.

[13] Rao, M. V. S., Gangadhar, K., Chamkha, A. J., & Surekha, P. (2021). Bioconvection in a convectional nanofluid flow containing gyrotactic microorganisms over an isothermal vertical cone embedded in a porous surface with chemical reactive species. Arabian Journal for Science and Engineering, 46(3), 2493-2503.

[14] Krishna, M. V., & Chamkha, A. J. (2019). Hall effects on MHD squeezing flow of a water-based nanofluid between two parallel disks. Journal of Porous media, 22(2).

[15] Mabood, F., Khan, W. A.,& Makinde, O. D. (2017). Hydromagnetic flow of a variable viscosity nanofluid in a rotating permeable channel with hall effects. Journal of Engineering Thermophysics, 26(4), 553-566.

[16] Tayebi, T., & Chamkha, A. J. (2020). Magnetohydrodynamic natural convection heat transfer of hybrid nanofluid in a square enclosure in the presence of a wavy circular conductive cylinder. Journal of Thermal Science and Engineering Applications, 12(3).

[17] Dogonchi, A. S., Seyyedi, S. M., Hashemi-Tilehnoee, M., Chamkha, A. J., & Ganji, D. D. (2019). Investigation of natural convection of magnetic nanofluid in an enclosure with a porous medium considering Brownian motion. Case Studies in Thermal Engineering, 14, 100502.

[18] Magodora, M., Mondal, H., & Sibanda, P. (2020). Effect of Cattaneo-Christov heat flux on radiative hydromagnetic nanofluid flow between parallel plates using spectral quasilinearization method. Journal of Applied and Computational Mechanics.

[19] Mondal, H., De, P., Chatterjee, S., Sibanda, P., & Roy, P. K. (2017). MHD three-dimensional nanofluid flow on a vertical stretching surface with heat generation/absorption and thermal radiation. Journal of Nanofluids, 6(1), 189-195.

[20] Oloniiju, S. D., Goqo, S. P.,& Sibanda, P. (2020). Heat and mass transfer of an unsteady second grade nanofluid with viscous heating dissipation. International Journal of Computational Methods, 17(5), 1940005.

[21] Oztop, H. F., & Abu-Nada, E. (2008). Numerical study of natural convection in partially heated rectangular enclosures filled with nanofluids. International journal of heat and fluid flow, 29(5), 1326-1336.

[22] Mehryan, S. A. M., Izadpanahi, E., Ghalambaz, M., & Chamkha, A. J. (2019). Mixed convection flow caused by an oscillating cylinder in a square cavity filled with Cu–Al_2O_3/water hybrid nanofluid. Journal of Thermal Analysis and Calorimetry, 137(3), 965-982.

[23] Ghalambaz, M., Groşan, T., & Pop, I. (2019). Mixed convection boundary layer flow and heat transfer over a vertical plate embedded in a porous medium filled with a suspension of nano-encapsulated phase change materials. Journal of Molecular Liquids, 293, 111432.

[24] Mehryan, S. A. M., Ghalambaz, M., Chamkha, A. J., & Izadi, M. (2020). Numerical study on natural convection of Ag–MgO hybrid/water nanofluid inside a porous enclosure: A local thermal non-equilibrium model. Powder Technology, 367, 443-455.

[25] Ghalambaz, M., Doostani, A., Izadpanahi, E., & Chamkha, A. J. (2020). Conjugate natural convection flow of Ag–MgO/water hybrid nanofluid in a square cavity. Journal of Thermal Analysis and Calorimetry, 139(3), 2321-2336.

[26] Muhammad, R., Khan, M. I., Khan, N. B., & Jameel, M. (2020). Magnetohydrodynamics (MHD) radiated nanomaterial viscous material flow by a curved surface with second order slip and entropy generation. Computer methods and programs in biomedicine, 189, 105294.

[27] Russell, A. J. (2018). 75th Anniversary of 'Existence of Electromagnetic–Hydrodynamic Waves'. Solar Physics, 293(5), 1-9.

[28] Krishna, M. V., Reddy, M. G., & Chamkha, A. J. (2019). Heat and Mass Transfer on MHD Free Convective Flow over an Infinite Nonconducting Vertical Flat Porous Plate. International Journal of Fluid Mechanics Research, 46(1).

[29] Rasool, G., Shafiq, A., & Durur, H. (2021). Darcy-Forchheimer relation in Magnetohydrodynamic Jeffrey nanofluid flow over stretching surface. Discrete & Continuous Dynamical Systems-S, 14(7), 2497.

[30] Krishna, M. V., Anand, P. V. S., & Chamkha, A. J. (2019). Heat and mass transfer on free convective flow of a micropolar fluid through a porous surface with inclined magnetic field and hall effects. Special Topics & Reviews in Porous Media: An International Journal, 10(3).

[31] Krishna, M. V., Subba Reddy, G., & Chamkha, A. J. (2018). Hall effects on unsteady MHD oscillatory free convective flow of second grade fluid through porous medium between two vertical plates. Physics of fluids, 30(2), 023106.

[32] Krishna, M. V., Jyothi, K., & Chamkha, A. J. (2018). Heat and mass transfer on unsteady, magnetohydrodynamic, oscillatory flow of second-grade fluid through a porous medium between two vertical plates, under the influence of fluctuating heat source/sink, and chemical reaction. International Journal of Fluid Mechanics Research, 45(5).

[33] Von Kármán, T. (1921). Uber laminare und turbulente Reibung. Z. Angew. Math. Mech., 1, 233-252.

[34] Mustafa, M. (2017). MHD nanofluid flow over a rotating disk with partial slip effects: Buongiorno model. International Journal of Heat and Mass Transfer, 108, 1910-1916.

[35] Khan, J. A., Mustafa, M., Hayat, T., & Alsaedi, A. (2018). A revised model to study the MHD nanofluid flow and heat transfer due to rotating disk: numerical solutions. Neural Computing and Applications, 30(3), 957-964.

[36] Turkyilmazoglu, M. (2014). MHD fluid flow and heat transfer due to a shrinking rotating disk. Computers & Fluids, 90, 51-56.

[37] Andrews, J., & Devi, S. A. (2012). Nanofluid Flow over a Rotating Disk with Prescribed Heat Flux. Mapana-Journal of Sciences, 11(3), 77-92.

[38] Krishna, M. V., Ahamad, N. A., & Chamkha, A. J. (2021). Hall and ion slip impacts on unsteady MHD convective rotating flow of heat generating/absorbing second grade fluid. Alexandria Engineering Journal, 60(1), 845-858.

[39] Krishna, M. V., & Chamkha, A. J. (2020). Hall and ion slip effects on MHD rotating flow of elastico-viscous fluid through porous medium. International Communications in Heat and Mass Transfer, 113, 104494.

[40] Krishna, M. V., Ahamad, N. A., & Chamkha, A. J. (2020). Hall and ion slip effects on unsteady MHD free convective rotating flow through a saturated porous medium over an exponential accelerated plate. Alexandria Engineering Journal, 59(2), 565-577.

[41] Krishna, M. V., Swarnalathamma, B. V., & Chamkha, A. J. (2019). Investigations of Soret, Joule and Hall effects on MHD rotating mixed convective flow past an infinite vertical porous plate. Journal of Ocean Engineering and Science, 4(3), 263-275.

[42] Krishna, M. V., & Chamkha, A. J. (2019). MHD peristaltic rotating flow of a couple stress fluid through a porous medium with wass and side effects. Special Topics & Reviews in Porous Media: An International Journal, 10(3).

[43] Motsa, S. S., Sibanda, P., & Shateyi, S. (2011). On a new quasilinearization method for systems of nonlinear boundary value problems. Mathematical Methods in the Applied Sciences, 34(11), 1406-1413.

[44] Krishna, M. V. (2020). Hall and ion slip impacts on unsteady MHD free convective rotating flow of Jeffreys fluid with ramped wall temperature. International Communications in Heat and Mass Transfer, 119, 104927.

[45] Serre, E., Tuliszka-Sznitko, E., & Bontoux, P. (2004). Coupled numerical and theoretical study of the flow transition between a rotating and a stationary disk. Physics of Fluids, 16(3), 688-706.

[46] Lingwood, R. J. (1997). Absolute instability of the Ekman layer and related rotating flows. Journal of Fluid Mechanics, 331, 405-428.

[47] Van Eeten, K. M. P., Van der Schaaf, J., Schouten, J. C., & Van Heijst, G. J. F. (2012). Boundary layer development in the flow field between a rotating and a stationary disk. Physics of Fluids, 24(3), 033601.

[48] Jasmine, H. A., & Gajjar, J. S. (2005). Absolute instability of the von Kármán, Bödewadt and Ekman flows between a rotating disc and a stationary lid. Philosophical Transactions of the Royal Society A: Mathematical, Physical and Engineering Sciences, 363(1830), 1131-1144.

[49] Kumar, S.K., Thacker, W.I., Watson, L.T. (1988). Magnetohydrodynamic flow and heat transfer about a rotating disk with suction and injection at the disk surface." Computers & fluids 16.2 : 183-193.

[50] Turkyilmazoglu, M. (2010). The MHD boundary layer flow due to a rough rotating disk. Journal of Applied Mathematics and Mechanics/Zeitschrift für Angewandte Mathematik und Mechanik: Applied Mathematics and Mechanics, 90(1), 72-82.

[51] Krishna, M. V., Ahamad, N. A., & Chamkha, A. J. (2021). Hall and ion slip impacts on unsteady MHD convective rotating flow of heat generating/absorbing second grade fluid. Alexandria Engineering Journal, 60(1), 845-858.

[52] Sciacovelli, A., Verda, V., & Sciubba, E. (2015). Entropy generation analysis as a design tool. A review. Renewable and Sustainable Energy Reviews, 43, 1167-1181.

[53] Almakki, M., Nandy S.K., Mondal, S., Sibanda, P. & Sibanda., D. (2018). A model for entropy generation in stagnation-point flow of non-Newtonian Jeffrey, Maxwell and Oldroyd-B nanofluids. Heat transfer-Asian Res, 2018, 1-18. https://doi.org/10.1002/htj.21366.

[54] Rashidi, M. M., Mahmud, S., Freidoonimehr, N., & Rostami, B. (2015). Analysis of entropy generation in an MHD flow over a rotating porous disk with variable physical properties. International journal of Exergy, 16(4), 481-503.

[55] Rehman, A. U., Mehmood, R., & Nadeem, S. (2017). Entropy analysis of radioactive rotating nanofluid with thermal slip. Applied Thermal Engineering, 112, 832-840.

[56] Makinde, O. D., & Aziz, A. (2010). Second law analysis for a variable viscosity plane Poiseuille flow with asymmetric convective cooling. Computers & Mathematics with Applications, 60(11), 3012-3019.

[57] Seyyedi, S. M., Dogonchi, A. S., Hashemi-Tilehnoee, M., Ganji, D. D., & Chamkha, A. J. (2020). Second law analysis of magneto-natural convection in a nanofluid filled wavy-hexagonal porous enclosure. International Journal of Numerical Methods for Heat & Fluid Flow.

[58] Pal, D., Mondal, S., & Mondal, H. (2019). Entropy generation on MHD Jeffrey nanofluid over a stretching sheet with nonlinear thermal radiation using spectral quasilinearisation method. International Journal of Ambient Energy, 1-15.

[59] Dalir, N., Dehsara, M., & Nourazar, S. S. (2015). Entropy analysis for magnetohydrodynamic flow and heat transfer of a Jeffrey nanofluid over a stretching sheet. Energy, 79, 351-362.

[60] Goqo, S. P., Oloniiju, S. D., Mondal, H., Sibanda, P., & Motsa, S. S. (2018). Entropy generation in MHD radiative viscous nanofluid flow over a porous wedge using the bivariate spectral quasi-linearization method. Case studies in thermal engineering, 12, 774-788.

[61] Khan, M. I., Khan, S. A., Hayat, T., Javed, M. F., & Waqas, M. (2019). Entropy generation in radiative flow of Ree-Eyring fluid due to due rotating disks. International Journal of Numerical Methods for Heat & Fluid Flow.

[62] Khan, N. S., Shah, Q., Bhaumik, A., Kumam, P., Thounthong, P., & Amiri, I. (2020). Entropy generation in bioconvection nanofluid flow between two stretchable rotating disks. Scientific Reports, 10(1), 1-26.

[63] Rashidi, M. M., Abelman, S., & Mehr, N. F. (2013). Entropy generation in steady MHD flow due to a rotating porous disk in a nanofluid. International Journal of Heat and Mass Transfer, 62, 515-525.

[64] Sahin, A. Z., & Ben-Mansour, R. (2003). Entropy generation in laminar fluid flow through a circular pipe. Entropy, 5(5), 404-416.

[65] Abbas, M. A., Bai, Y., Rashidi, M. M., & Bhatti, M. M. (2016). Analysis of entropy generation in the flow of peristaltic nanofluids in channels with compliant walls. Entropy, 18(3), 90.

[66] Akbar, N. S. (2015). Entropy generation analysis for a CNT suspension nanofluid in plumb ducts with peristalsis. Entropy, 17(3), 1411-1424.

[67] Falade, J. A., Adesanya, S. O., Ukaegbu, J. C., & Osinowo, M. O. (2016). Entropy generation analysis for variable viscous couple stress fluid flow through a channel with non-uniform wall temperature. Alexandria Engineering Journal, 55(1), 69-75.

[68] Ghosh, P., Han, G., De, M., Kim, C. K., & Rotello, V. M. (2008). Gold nanoparticles in delivery applications. Advanced drug delivery reviews, 60(11), 1307-1315.

[69] Pantapasis, K., & Grumezescu, A. M. (2017). Gold nanoparticles: advances in water purification approaches. In Water Purification, 447-477, Academic Press, London.

[70] Qian, H., Pretzer, L. A., Velazquez, J. C., Zhao, Z., & Wong, M. S. (2013). Gold nanoparticles for cleaning contaminated water. Journal of Chemical Technology & Biotechnology, 88(5), 735-741.

[71] Corti, C. W., Holliday, R. J., & Thompson, D. T. (2002). Developing new industrial applications for gold: gold nanotechnology. Gold Bulletin, 35(4), 111-117.

[72] Qureshi, M. Z. A., Rubbab, Q., Irshad, S., Ahmad, S., & Aqeel, M. (2016). Heat and mass transfer analysis of MHD nanofluid flow with radiative heat effects in the presence of spherical Au-metallic nanoparticles. Nanoscale research letters, 11(1), 472.

[73] Rashidi, M. M., Bég, O. A., Mehr, N. F., & Rostami, B. (2013). Second law analysis of hydromagnetic flow from a stretching rotating disk: DTM-Pade simulation of novel nuclear MHD propulsion systems. Front. Aerosp. Eng., 2(1), 29-39.

[74] Motsa, S. S., Dlamini, P. G., & Khumalo, M. (2014). Spectral relaxation method and spectral quasilinearization method for solving unsteady boundary layer flow problems. Advances in Mathematical Physics, 2014, Article ID 341964.

[75] Mishra, S. R., Baag, S., & Mohapatra, D. K. (2016). Chemical reaction and Soret effects on hydromagnetic micropolar fluid along a stretching sheet. Engineering Science and Technology, an International Journal, 19(4), 1919-1928.

[76] Hamid, A., Khan, M., & Khan, U. (2018). Thermal radiation effects on Williamson fluid flow due to an expanding/contracting cylinder with nanomaterials: dual solutions. Physics Letters A, 382(30), 1982-1991.

[77] Krishna, M. V., Jyothi, K., & Chamkha, A. J. (2020). Heat and mass transfer on MHD flow of second-grade fluid through porous medium over a semi-infinite vertical stretching sheet. Journal of Porous Media, 23(8).

[78] Ramana, K. V., Gangadhar, K., Kannan, T., & Chamkha, A. J. (2021). Cattaneo–Christov heat flux theory on transverse MHD Oldroyd-B liquid over nonlinear stretched flow. Journal of Thermal Analysis and Calorimetry, 1-11.

[79] Sithole, H., Mondal, H., Goqo, S., Sibanda, P., & Motsa, S. (2018). Numerical simulation of couple stress nanofluid flow in magneto-porous medium with thermal radiation and a chemical reaction. Applied Mathematics and Computation, 339, 820-836.

[80] Agbaje, T. M., Mondal, S., Makukula, Z. G., Motsa, S. S., & Sibanda, P. (2018). A new numerical approach to MHD stagnation point flow and heat transfer towards a stretching sheet. Ain Shams Engineering Journal, 9(2), 233-243.

[81] Hayat, T., Khan, M. I., Alsaedi, A., & Khan, M. I. (2017). Joule heating and viscous dissipation in flow of nanomaterial by a rotating disk. International Communications in Heat and Mass Transfer, 89, 190-197.

[82] Lingwood, R. J. (1995). Absolute instability of the boundary layer on a rotating disk. Journal of Fluid Mechanics, 299, 17-33.

[83] Fadhilah, S. A., Hidayah, I., Hilwa, M. Z., Faizah, H. N., & Marhamah, R. S. (2013). Thermophysical properties of Copper/Water nanofluid for automotive cooling system. Journal of Mechanical Engineering and Technology (JMET), 5(2).

[84] Makukula, Z., Sibanda, P., & Motsa, S. (2010). A note on the solution of the von Kármán equations using series and Chebyshev spectral methods. Boundary Value Problems, 2010(1), 471793.

[85] Dhlamini, M., Kameswaran, P. K., Sibanda, P., Motsa, S., & Mondal, H. (2019). Activation energy and binary chemical reaction effects in mixed convective nanofluid flow with convective boundary conditions. Journal of Computational Design and Engineering, 6(2), 149-158.

[86] Attia, H. A. (2009). Steady flow over a rotating disk in porous medium with heat transfer. Nonlinear Analysis: Modelling and Control, 14(1), 21-26.

[87] Bellman, R. E., & Kalaba, R. E. (1965). Quasilinearization and nonlinear boundary-value problems.

[88] Canuto, C., Hussaini, M. Y., Quarteroni, A., & Thomas Jr, A. (2012). Spectral methods in fluid dynamics. Springer Science & Business Media.

[89] Magodora, M., Mondal, H., & Sibanda, P. (2019). Dual solutions of a micropolar nanofluid flow with radiative heat mass transfer over stretching/shrinking sheet using spectral quasilinearization method. Multidiscipline Modeling in Materials and Structures.

[90] Trefethen, L. N. (2000). Spectral methods in MATLAB (Vol. 10). Siam, Philadelphia.

[91] Zhou, S. S., Bilal, M., Khan, M. A., & Muhammad, T. (2021). Numerical Analysis of Thermal Radiative Maxwell Nanofluid Flow Over-Stretching Porous Rotating Disk. Micromachines, 12(5), 540.

Summary

In this chapter, we studied nanofluid flow over a rotating disk with suction and a prescribed heat flux condition. The nonlinear system of equations describing the flow was solved using the spectral quasilinearization method. The efficiency and accuracy of the method was shown through a convergence error analysis. Entropy generation analysis showed that an upward variation of the magnetic field the nanoparticle volume fraction tended to increase irreversibility. Entropy generation analysis is important in reducing inefficiencies and losses of scarce energy resources for thermal systems.

Chapter 6

Conclusion

In this study, we have investigated nanofluid flows over a diverse range of solid surfaces, such as a stretching sheet, parallel plates and rotating disks. The coupled equations describing the nanofluid flows are highly nonlinear and complex and finding analytic solutions was not possible. The spectral quasilinearization method was used to solve the model equations. Through comparison with results in the literature for limiting cases and through error and residual error analyses, the results show that the spectral quasilinearization method is accurate, efficient, rapidly convergent, robust and appropriate for solving nanofluid boundary value problems.

In Chapter 2, the micropolar nanofluid flow above a shrinkable/stretchable sheet with thermal radiation, thermophoresis and Brownian motion was investigated. Dual solutions were found to exist depending on whether the surface was stretching or shrinking. The findings are in good agreement, for limiting cases, with results in the literature. It was observed that an increase in the Lewis number leads to increased temperature and reduced concentration. Furthermore, an increase in the Prandtl number led to a drop in temperature distribution and increased concentration.

In Chapter 3, we investigated squeezed flow between parallel plates with Cattaneo-Christov heat flux model for heat conduction. The effects of the homogeneous chemical reaction, radiation and magnetic field were studied. The results show that an increase in the magnetic field is accompanied by a decrease in the mass and heat transfer rates. However, increasing the magnetic field leads to a rise in the skin friction. In addition, increasing the nanoparticle concentration has the effect of reducing the rate of mass transfer. The temperature decreases as a consequence of raising the relaxation parameter. The same trend is observed when the magnetic field strength is increased.

In Chapter 4, we investigated nanofluid flow above a rotating disk with activation energy and binary chemical reaction. A decrease in the radial and tangential velocities and a rise in the axial velocity were realised upon increasing the nanoparticle concentration. An increase in the nanoparticle volume fraction was also accompanied by an elevation of the skin friction and the rates of mass and heat transfer.

In Chapter 5, we studied nanofluid flow past a permeable rotational disk. The impact of prescribed heat flux, magnetic field and suction on the flow were considered. Convergence error analysis showed that convergence was rapid and was attained after a few iterations. This proves the accuracy and suitability of the spectral quasilinearization numerical scheme. Excellent agreement with results in the literature was obtained for limiting cases, and this validated our results. An increase in the nanoparticle concentration yields a fall in velocity but a rise in temperature. The magnetic field enhancement is observed to cause a drop in the radial, tangential and axial velocities. The magnetic field and suction are also observed to positively correlate with the skin friction. Higher values of nanoparticle concentration and magnetic field strength have the effects of reducing the entropy generation.

References

[1] A. Bejan, *Convection Heat Transfer*. John Wiley & Sons, 2013.

[2] J. M. McDonough, "Lectures in Elementary Fluid Dynamics: Physics, Mathematics and Applications," 2009.

[3] S. Patankar, *Numerical Heat Transfer and Fluid Flow*. Taylor & Francis, 2018.

[4] I. Tani, "History of boundary layer theory," *Annual review of fluid mechanics*, vol. 9, no. 1, pp. 87–111, 1977.

[5] R. Fagbenle, O. M. Amoo, A. Falana, and S. Aliu, *Applications of heat, mass and fluid boundary layers*. Woodhead Publishing Limited, 2020.

[6] S. P. Goqo, S. Mondal, P. Sibanda, and S. S. Motsa, "An unsteady magnetohydrodynamic Jeffery nanofluid flow over a shrinking sheet with thermal radiation and convective boundary condition using spectral quasilinearisation method," *Journal of Computational and Theoretical Nanoscience*, vol. 13, no. 10, pp. 7483–7492, 2016.

[7] V. Y. Rudyak, S. Dimov, and V. Kuznetsov, "On the dependence of the viscosity coefficient of nanofluids on particle size and temperature," *Technical Physics Letters*, vol. 39, no. 9, pp. 779–782, 2013.

[8] N. S. Khan, T. Gul, M. A. Khan, E. Bonyah, and S. Islam, "Mixed convection in gravity-driven thin film non-Newtonian nanofluids flow with gyrotactic micro-organisms," *Results in Physics*, vol. 7, pp. 4033–4049, 2017.

[9] H. Qian, L. A. Pretzer, J. C. Velazquez, Z. Zhao, and M. S. Wong, "Gold nanoparticles for cleaning contaminated water," *Journal of Chemical Technology & Biotechnology*, vol. 88, no. 5, pp. 735–741, 2013.

[10] F. White, *Fluid Mechanics*. McGraw-Hill, 1994.

[11] R. P. Chhabra, “Non-Newtonian fluids: An introduction,” in *Rheology of Complex Fluids*, pp. 3–34, Springer, 2010.

[12] F. A. Morrison, *Understanding Rheology*. Oxford University Press, USA, 2001.

[13] O. Enriquez, E. Soto, R. Zenit, and O. Manero, “Rodless Weissenberg Effect,” in *APS Division of Fluid Dynamics Meeting Abstracts*, vol. 61, pp. MT–006, 2008.

[14] J. Bayat, H. Emdad, and O. Abouali, “Numerical investigation of partially liquefied vitreous dynamics as two-phase visco-elastic Newtonian fluid flow in a planar cavity due to oscillatory motion,” *International Journal of Multiphase Flow*, vol. 127, p. 103259, 2020.

[15] A. Shenoy, *Heat Transfer to non-Newtonian Fluids: Fundamentals and Analytical Expressions*. John Wiley & Sons, 2018.

[16] S. Mondal, N. Haroun, S. Nandy, and P. Sibanda, “MHD boundary layer flow and heat transfer of Jeffrey nanofluid over an unsteady shrinking sheet with partial slip,” *Journal of Nanofluids*, vol. 6, no. 2, pp. 343–353, 2017.

[17] A. Tanveer, T. Hayat, A. Alsaedi, and B. Ahmad, “Numerical simulation for peristalsis of Carreau–Yasuda nanofluid in curved channel with mixed convection and porous space,” *PloS One*, vol. 12, no. 2, p. e0170029, 2017.

[18] R. B. Bird, W. E. Stewart, and E. N. Lightfoot, *Transport Phenomena*, vol. 31. John Wiley & Sons, 2007.

[19] Y. Cengel, *Heat and Mass Transfer: Fundamentals and Applications*. McGraw-Hill Higher Education, 2014.

[20] F. P. Incropera, A. S. Lavine, T. L. Bergman, and D. P. DeWitt, *Fundamentals of Heat and Mass Transfer*. Wiley, 2007.

[21] A. Bejan, *Advanced Engineering Thermodynamics*. John Wiley & Sons, 2016.

[22] M. Rashidi, S. Bagheri, E. Momoniat, and N. Freidoonimehr, "Entropy analysis of convective MHD flow of third grade non-Newtonian fluid over a stretching sheet," *Ain Shams Engineering Journal*, vol. 8, no. 1, pp. 77–85, 2017.

[23] J. Gustin, "Runaway reactions, their courses and the methods to establish safe process conditions," *Journal de Physique III*, vol. 1, no. 8, pp. 1401–1419, 1991.

[24] D. W. Hahn and M. N. Özisik, *Heat Conduction*. John Wiley & Sons, 2012.

[25] A. Bejan and A. D. Kraus, *Heat Transfer Handbook*, vol. 1. John Wiley & Sons, 2003.

[26] S. S. Motsa and I. Animasaun, "Unsteady boundary layer flow over a vertical surface due to impulsive and buoyancy in the presence of thermo-diffusion and diffusion-thermo using bivariate spectral relaxation method," *Journal of Applied Fluid Mechanics*, vol. 9, 2016.

[27] H. Mondal, P. De, S. Chatterjee, P. Sibanda, and P. K. Roy, "MHD three-dimensional nanofluid flow on a vertical stretching surface with heat generation/absorption and thermal radiation," *Journal of Nanofluids*, vol. 6, no. 1, pp. 189–195, 2017.

[28] H. Sithole, H. Mondal, S. Goqo, P. Sibanda, and S. Motsa, "Numerical simulation of couple stress nanofluid flow in magneto-porous medium with thermal radiation and a chemical reaction," *Applied Mathematics and Computation*, vol. 339, pp. 820–836, 2018.

[29] A. Noghrehabadi, M. Ghalambaz, E. Izadpanahi, and R. Pourrajab, "Effect of magnetic field on the boundary layer flow, heat, and mass transfer of nanofluids over a stretching cylinder," *Journal of Heat and Mass Transfer Research*, vol. 1, no. 1, pp. 9–16, 2014.

[30] E. Weinan, "Boundary layer theory and the zero-viscosity limit of the Navier-Stokes equation," *Acta Mathematica Sinica*, vol. 16, no. 2, pp. 207–218, 2000.

[31] M. Eckert, *Ludwig Prandtl: A Life for Fluid Mechanics and Aeronautical Research*. Springer, 2019.

[32] H. Schlichting and K. Gersten, *Boundary Layer Theory*. Springer, 2016.

[33] T. R. A. K. P. Burr and C. C. Mei, "Two-dimensional laminar boundary layers," *I-Campus Project School-wide Program on Fluid Mechanics on High Reynolds Number Flows*, vol. 16, no. 2, pp. 1–33, 2016.

[34] C. K. Batchelor and G. Batchelor, *An Introduction to Fluid Dynamics*. Cambridge University Press, 2000.

[35] P. Kameswaran, M. Narayana, P. Sibanda, and P. Murthy, "Hydromagnetic nanofluid flow due to a stretching or shrinking sheet with viscous dissipation and chemical reaction effects," *International Journal of Heat and Mass Transfer*, vol. 55, no. 25-26, pp. 7587–7595, 2012.

[36] S. Dero, A. Mohd Rohni, and A. Saaban, "Effects of the viscous dissipation and chemical reaction on Casson nanofluid flow over the permeable stretching/shrinking sheet," *Heat Transfer*, vol. 49, no. 4, pp. 1736–1755, 2020.

[37] K. Górnicki, R. Winiczenko, and A. Kaleta, "Estimation of the Biot number using genetic algorithms: Application for the drying process," *Energies*, vol. 12, no. 14, p. 2822, 2019.

[38] B. E. Rapp, *Microfluidics: Modeling, Mechanics and Mathematics*. William Andrew, 2016.

[39] A. Malvandi, F. Hedayati, and D. Ganji, "Nanofluid flow on the stagnation point of a permeable non-linearly stretching/shrinking sheet," *Alexandria Engineering Journal*, vol. 57, no. 4, pp. 2199–2208, 2018.

[40] S. Ghosh and S. Mukhopadhyay, "Stability analysis for model-based study of nanofluid flow over an exponentially shrinking permeable sheet in presence of slip," *Neural Computing and Applications*, vol. 32, no. 11, pp. 7201–7211, 2020.

[41] Y. S. Daniel, Z. A. Aziz, Z. Ismail, and F. Salah, "Effects of slip and convective conditions on MHD flow of nanofluid over a porous nonlinear stretching/shrinking sheet," *Australian Journal of Mechanical Engineering*, vol. 16, no. 3, pp. 213–229, 2018.

[42] N. Bachok, A. Ishak, and I. Pop, "Unsteady boundary-layer flow and heat transfer of a nanofluid over a permeable stretching/shrinking sheet," *International Journal of Heat and Mass Transfer*, vol. 55, no. 7-8, pp. 2102–2109, 2012.

[43] S. Nadeem, M. Israr-ur Rehman, S. Saleem, and E. Bonyah, "Dual solutions in MHD stagnation point flow of nanofluid induced by porous stretching/shrinking sheet with anisotropic slip," *AIP Advances*, vol. 10, no. 6, p. 065207, 2020.

[44] M. Stefan, "Versuch uber die scheinbare adhesion, akademie der wissenschaften in wien. mathematisch-naturwwissenschaftliche," 1874.

[45] M. Sobamowo and A. Akinshilo, "On the analysis of squeezing flow of nanofluid between two parallel plates under the influence of magnetic field," *Alexandria Engineering Journal*, vol. 57, no. 3, pp. 1413–1423, 2018.

[46] I. Ullah, M. Waqas, T. Hayat, A. Alsaedi, and M. I. Khan, "Thermally radiated squeezed flow of magneto-nanofluid between two parallel disks with chemical reaction," *Journal of Thermal Analysis and Calorimetry*, vol. 135, no. 2, pp. 1021–1030, 2019.

[47] I. Karatzas and S. E. Shreve, "Brownian motion," in *Brownian Motion and Stochastic Calculus*, pp. 47–127, Springer, 1998.

[48] N. Tarakaramu and P. Satya Narayana, "Chemical reaction effects on bio-convection nanofluid flow between two parallel plates in rotating system with variable viscosity: A numerical study," *Journal of Applied and Computational Mechanics*, vol. 5, no. 4, pp. 791–803, 2019.

[49] M. Atlas, S. Hussain, and M. Sagheer, "Entropy generation and unsteady Casson fluid flow squeezing between two parallel plates subject to Cattaneo-Christov heat and mass flux," *The European Physical Journal Plus*, vol. 134, no. 1, p. 33, 2019.

[50] A. Dogonchi, M. Waqas, S. Afshar, S. M. Seyyedi, M. Hashemi-Tilehnoee, A. J. Chamkha, and D. Ganji, "Investigation of magneto-hydrodynamic fluid squeezed between two parallel

disks by considering Joule heating, thermal radiation, and adding different nanoparticles," *International Journal of Numerical Methods for Heat & Fluid Flow*, 2019.

[51] A. Hussain, S. Akbar, L. Sarwar, and M. Malik, "Numerical investigation of squeezing flow of Walters' B fluid through parallel plates," *Journal of the Brazilian Society of Mechanical Sciences and Engineering*, vol. 41, no. 11, pp. 1–7, 2019.

[52] N. Acharya, K. Das, and P. K. Kundu, "The squeezing flow of Cu-water and Cu-kerosene nanofluids between two parallel plates," *Alexandria Engineering Journal*, vol. 55, no. 2, pp. 1177–1186, 2016.

[53] T. Hayat, R. Sajjad, A. Alsaedi, T. Muhammad, and R. Ellahi, "On squeezed flow of couple stress nanofluid between two parallel plates," *Results in Physics*, vol. 7, pp. 553–561, 2017.

[54] N. A. M. Noor, S. Shafie, and M. A. Admon, "MHD squeezing flow of casson nanofluid with chemical reaction, thermal radiation and heat generation/absorption," *Journal of Advanced Research in Fluid Mechanics and Thermal Sciences*, vol. 68, no. 2, pp. 94–111, 2020.

[55] M. I. Khan, S. Qayyum, S. Kadry, W. Khan, and S. Abbas, "Irreversibility analysis and heat transport in squeezing nanoliquid flow of non-Newtonian second-grade fluid between infinite plates with activation energy," *Arabian Journal for Science and Engineering*, vol. 45, no. 6, pp. 4939–4947, 2020.

[56] T. v. Kármán, "Über laminare und turbulente reibung," *Journal of Applied Mathematics and Mechanics/Zeitschrift für Angewandte Mathematik und Mechanik*, vol. 1, no. 4, pp. 233–252, 1921.

[57] F. Mabood, W. Khan, and O. Makinde, "Hydromagnetic flow of a variable viscosity nanofluid in a rotating permeable channel with hall effects," *Journal of Engineering Thermophysics*, vol. 26, no. 4, pp. 553–566, 2017.

[58] T. Hayat, M. Rashid, M. Imtiaz, and A. Alsaedi, "Nanofluid flow due to rotating disk with variable thickness and homogeneous-heterogeneous reactions," *International Journal of Heat and Mass Transfer*, vol. 113, pp. 96–105, 2017.

[59] M. Awais, S. Bilal, M. Malik, *et al.*, "Numerical analysis of magnetohydrodynamic Navier's slip visco nanofluid flow induced by rotating disk with heat source/sink," *Communications in Theoretical Physics*, vol. 71, no. 9, p. 1075, 2019.

[60] M. Ramzan, J. D. Chung, and N. Ullah, "Partial slip effect in the flow of MHD micropolar nanofluid flow due to a rotating disk: A numerical approach," *Results in Physics*, vol. 7, pp. 3557–3566, 2017.

[61] J. A. Khan, M. Mustafa, T. Hayat, M. Turkyilmazoglu, and A. Alsaedi, "Numerical study of nanofluid flow and heat transfer over a rotating disk using Buongiorno's model," *International Journal of Numerical Methods for Heat & Fluid Flow*, 2017.

[62] M. Alqarni, S. M. R. S. Naqvi, T. Muhammad, and H. M. Kim, "On model for magnetized micropolar-nanofluid flow by a convectively heated rotating disk," *Physica Scripta*, vol. 96, no. 1, p. 015205, 2020.

[63] N. A. Alreshidi, Z. Shah, A. Dawar, P. Kumam, M. Shutaywi, and W. Watthayu, "Brownian motion and thermophoresis effects on MHD three dimensional nanofluid flow with slip conditions and Joule dissipation due to porous rotating disk," *Molecules*, vol. 25, no. 3, p. 729, 2020.

[64] S. U. Choi and J. A. Eastman, "Enhancing thermal conductivity of fluids with nanoparticles," Tech. Rep. 2, Argonne National Lab., IL (United States), 1995.

[65] C. Yin, L. Zheng, C. Zhang, and X. Zhang, "Flow and heat transfer of nanofluids over a rotating disk with uniform stretching rate in the radial direction," *Propulsion and Power Research*, vol. 6, no. 1, pp. 25–30, 2017.

[66] M. Turkyilmazoglu, "Nanofluid flow and heat transfer due to a rotating disk," *Computers & Fluids*, vol. 94, pp. 139–146, 2014.

[67] M. Hojjat, S. G. Etemad, and R. Bagheri, "Laminar heat transfer of non-newtonian nanofluids in a circular tube," *Korean Journal of Chemical Engineering*, vol. 27, no. 5, pp. 1391–1396, 2010.

[68] R. S. R. Gorla and A. Chamkha, "Natural convective boundary layer flow over a nonisothermal vertical plate embedded in a porous medium saturated with a nanofluid," *Nanoscale and Microscale Thermophysical Engineering*, vol. 15, no. 2, pp. 81–94, 2011.

[69] A. K. Hussein and S. H. Hussain, "Heatline visualization of natural convection heat transfer in an inclined wavy cavities filled with nanofluids and subjected to a discrete isoflux heating from its left sidewall," *Alexandria Engineering Journal*, vol. 55, no. 1, pp. 169–186, 2016.

[70] T. Hayat, I. Ullah, A. Alsaedi, and M. Farooq, "MHD flow of Powell-Eyring nanofluid over a non-linear stretching sheet with variable thickness," *Results in Physics*, vol. 7, pp. 189–196, 2017.

[71] N. A. Gamasaee, H. A. Muhammad, E. Tadayon, M. Ale-Ebrahim, M. Mirpour, M. Sharifi, A. Salihi, M. S. Shekha, A. A. Alasady, F. M. Aziz, *et al.*, "The effects of nickel oxide nanoparticles on structural changes, heme degradation, aggregation of hemoglobin and expression of apoptotic genes in lymphocytes," *Journal of Biomolecular Structure and Dynamics*, vol. 38, no. 12, pp. 3676–3686, 2020.

[72] T. Esakkimuthu, D. Sivakumar, and S. Akila, "Application of nanoparticles in wastewater treatment," *Pollut. Res*, vol. 33, no. 03, pp. 567–571, 2014.

[73] A. U. Rehman, R. Mehmood, and S. Nadeem, "Entropy analysis of radioactive rotating nanofluid with thermal slip," *Applied Thermal Engineering*, vol. 112, pp. 832–840, 2017.

[74] R. Saidur, K. Leong, and H. A. Mohammed, "A review on applications and challenges of nanofluids," *Renewable and Sustainable Energy Reviews*, vol. 15, no. 3, pp. 1646–1668, 2011.

[75] V. Trisaksri and S. Wongwises, "Critical review of heat transfer characteristics of nanofluids," *Renewable and sustainable energy reviews*, vol. 11, no. 3, pp. 512–523, 2007.

[76] N. Bachok, A. Ishak, and I. Pop, "Boundary layer flow of nanofluids over a moving surface in a flowing fluid," *International Journal of Thermal Sciences*, vol. 49, no. 9, pp. 1663–1668, 2010.

[77] M. A. M. Noor, R. Nazar, K. Jafar, and I. Pop, "Numerical solutions of flow and heat transfer on a moving plate in a co-flowing nanofluid," in *AIP Conference Proceedings*, vol. 1605, pp. 416–421, American Institute of Physics, 2014.

[78] J. Buongiorno, "Convective transport in nanofluids," *Journal of Heat Transfer*, vol. 128, pp. 2402–250, 2006.

[79] R. K. Tiwari and M. K. Das, "Heat transfer augmentation in a two-sided lid-driven differentially heated square cavity utilizing nanofluids," *International Journal of Heat and Mass transfer*, vol. 50, no. 9-10, pp. 2002–2018, 2007.

[80] S. K. Soid, A. Ishak, and I. Pop, "Boundary layer flow past a continuously moving thin needle in a nanofluid," *Applied Thermal Engineering*, vol. 114, pp. 58–64, 2017.

[81] W. Khan and A. Aziz, "Natural convection flow of a nanofluid over a vertical plate with uniform surface heat flux," *International Journal of Thermal Sciences*, vol. 50, no. 7, pp. 1207–1214, 2011.

[82] A. M. Rohni, S. Ahmad, and I. Pop, "Boundary layer flow over a moving surface in a nanofluid beneath a uniform free stream," *International Journal of Numerical Methods for Heat & Fluid Flow*, 2011.

[83] W. Khan and I. Pop, "Boundary layer flow of a nanofluid past a stretching sheet," *International Journal of Heat and Mass Transfer*, vol. 53, no. 11-12, pp. 2477–2483, 2010.

[84] K. Das, N. Acharya, and P. K. Kundu, "The onset of nanofluid flow past a convectively heated shrinking sheet in presence of heat source/sink: A Lie group approach," *Applied Thermal Engineering*, vol. 103, pp. 38–46, 2016.

[85] N. Bachok, A. Ishak, and I. Pop, "Flow and heat transfer characteristics on a moving plate in a nanofluid," *International Journal of Heat and Mass Transfer*, vol. 55, no. 4, pp. 642–648, 2012.

[86] M. Rahman, M. Al-Lawatia, I. Eltayeb, and N. Al-Salti, "Hydromagnetic slip flow of water based nanofluids past a wedge with convective surface in the presence of heat generation/absorption," *International Journal of Thermal Sciences*, vol. 57, pp. 172–182, 2012.

[87] M. Aghamajidi, M. Yazdi, S. Dinarvand, and I. Pop, "Tiwari-das nanofluid model for MHD natural-convective flow of a nanofluid adjacent to a spinning down-pointing vertical cone," *Propulsion and Power Research*, vol. 7, no. 1, pp. 78–90, 2018.

[88] B. Sun, Y. Qu, and D. Yang, "Heat transfer of single impinging jet with Cu nanofluids," *Applied Thermal Engineering*, vol. 102, pp. 701–707, 2016.

[89] A. V. Minakov, V. Y. Rudyak, and M. I. Pryazhnikov, "About rheology of nanofluids," in *AIP Conference Proceedings*, vol. 2027, p. 030141, AIP Publishing LLC, 2018.

[90] V. Y. Rudyak and A. Minakov, "Modern problems of micro-and nanofluidics," *Science, Novosibirsk*, 2016.

[91] L. G. Leal, *Laminar Flow and Convective Transport Processes*, vol. 251. Elsevier.

[92] B. Weigand, *Analytical Methods for Heat Transfer and Fluid Flow Problems*, vol. 263. Springer, 2004.

[93] S. S. Motsa, "A new spectral local linearization method for nonlinear boundary layer flow problems," *Journal of Applied Mathematics*, vol. 2013, Article ID 423628.

[94] M. Sheikholeslami and D. D. Ganji, *Applications of Semi-Analytical Methods for Nanofluid Flow and Heat Transfer*. Elsevier, 2018.

[95] M. Turkyilmazoglu, "A reliable convergent Adomian decomposition method for heat transfer through extended surfaces," *International Journal of Numerical Methods for Heat & Fluid Flow*, 2018.

[96] H. Shahmohamadi and M. M. Rashidi, “VIM solution of squeezing MHD nanofluid flow in a rotating channel with lower stretching porous surface,” *Advanced Powder Technology*, vol. 27, no. 1, pp. 171–178, 2016.

[97] N. Eldabe and M. Abou-Zeid, “Homotopy perturbation method for MHD pulsatile non-Newtonian nanofluid flow with heat transfer through a non-Darcy porous medium,” *Journal of the Egyptian Mathematical Society*, vol. 25, no. 4, pp. 375–381, 2017.

[98] M. Usman, M. Hamid, U. Khan, S. T. M. Din, M. A. Iqbal, and W. Wang, “Differential transform method for unsteady nanofluid flow and heat transfer,” *Alexandria Engineering Journal*, vol. 57, no. 3, pp. 1867–1875, 2018.

[99] H. Mondal, M. Almakki, and P. Sibanda, “Dual solutions for three-dimensional magnetohydrodynamic nanofluid flow with entropy generation,” *Journal of Computational Design and Engineering*, vol. 6, no. 4, pp. 657–665, 2019.

[100] S. S. Motsa, P. G. Dlamini, and M. Khumalo, “Spectral relaxation method and spectral quasilinearization method for solving unsteady boundary layer flow problems,” *Advances in Mathematical Physics*, vol. 2014, Article ID 341964.

[101] S. S. Motsa, “A new spectral local linearization method for nonlinear boundary layer flow problems,” *Journal of Applied Mathematics*, vol. 2013, Article ID 423628.

[102] W. F. Gray and G. F. Pinder, “On the relationship between the finite element and finite difference methods,” *International Journal for Numerical Methods in Engineering*, vol. 10, no. 4, pp. 893–923, 1976.

[103] K.-J. Bathe, “Finite element method,” *Wiley encyclopedia of computer science and engineering*, pp. 1–12, 2007.

[104] J. P. Boyd, *Chebyshev and Fourier spectral methods*. Courier Corporation, 2001.

[105] C. Canuto, M. Y. Hussaini, A. Quarteroni, and A. Thomas Jr, *Spectral Methods in Fluid Dynamics*. Springer Science & Business Media, 2012.

[106] S. Motsa, V. Magagula, and P. Sibanda, "A bivariate Chebyshev spectral collocation quasilinearization method for nonlinear evolution parabolic equations," *The Scientific World Journal*, vol. 2014, Article ID 581987.

[107] H. Zahed, *Computation of Bifurcations for the Navier-Stokes Equations: PhD Thesis*. The University of Manchester, 2010.

[108] I. Oyelakin, S. Mondal, and P. Sibanda, "Unsteady mixed convection in nanofluid flow through a porous medium with thermal radiation using the bivariate spectral quasilinearization method," *Journal of Nanofluids*, vol. 6, no. 2, pp. 273–281, 2017.

[109] G. Kefayati, "Heat transfer and entropy generation of natural convection on non-Newtonian nanofluids in a porous cavity," *Powder Technology*, vol. 299, pp. 127–149, 2016.

[110] M. Dehghan and F. Fakhar-Izadi, "Pseudospectral methods for Nagumo equation," *International Journal for Numerical Methods in Biomedical Engineering*, vol. 27, no. 4, pp. 553–561, 2011.

[111] M. Javidi, "A numerical solution of the generalized Burger's–Huxley equation by spectral collocation method," *Applied Mathematics and Computation*, vol. 178, no. 2, pp. 338–344, 2006.

[112] Z. Makukula, P. Sibanda, and S. Motsa, "A note on the solution of the von Kármán equations using series and Chebyshev spectral methods," *Boundary Value Problems*, vol. 2010, pp. 1–17, 2010.

[113] L. N. Trefethen, *Spectral Methods in MATLAB*. SIAM, 2000.

[114] C. RamReddy and T. Pradeepa, "Spectral quasilinearization method for homogeneous-heterogeneous reactions on nonlinear convection flow of micropolar fluid saturated porous medium with convective boundary condition," *Open Engineering*, vol. 6, no. 1, 2016.

[115] D. Pal, S. Mondal, and H. Mondal, “Entropy generation on MHD Jeffrey nanofluid over a stretching sheet with nonlinear thermal radiation using spectral quasilinearisation method,” *International Journal of Ambient Energy*, pp. 1–15, 2019.

[116] M. Dhlamini, H. Mondal, P. Sibanda, and S. Motsa, “Activation energy and entropy generation in viscous nanofluid with higher order chemically reacting species,” *International Journal of Ambient Energy*, pp. 1–13, 2020.

[117] S. Goqo, S. Oloniiju, H. Mondal, P. Sibanda, and S. Motsa, “Entropy generation in MHD radiative viscous nanofluid flow over a porous wedge using the bivariate spectral quasilinearization method,” *Case Studies in Thermal Engineering*, vol. 12, pp. 774–788, 2018.

[118] M. Dhlamini, H. Mondal, P. Sibanda, and S. Motsa, “Numerical analysis of couple stress nanofluid in temperature dependent viscosity and thermal conductivity,” *International Journal of Applied and Computational Mathematics*, vol. 7, no. 2, pp. 1–14, 2021.

[119] M. S. Ansari, V. M. Magagula, and M. Trivedi, “Jeffrey nanofluid flow near a Riga plate: Spectral quasilinearization approach,” *Heat Transfer*, vol. 49, no. 3, pp. 1491–1510, 2020.

[120] A. F. Al-Hossainy, M. R. Eid, and M. S. Zoromba, “SQLM for external yield stress effect on 3D MHD nanofluid flow in a porous medium,” *Physica Scripta*, vol. 94, no. 10, p. 105208, 2019.

[121] W. Ibrahim, “Spectral quasilinearization method for solution of convective heating condition,” *Engineering Transactions*, vol. 68, no. 1, pp. 69–87, 2020.

[122] A. C. Eringen, “Simple microfluids,” *International Journal of Engineering Science*, vol. 2, no. 2, pp. 205–217, 1964.

[123] J. Chen, C. Liang, and J. Lee, “Theory and simulation of micropolar fluid dynamics,” *Proceedings of the Institution of Mechanical Engineers, Part N: Journal of Nanoengineering and Nanosystems*, vol. 224, no. 1-2, pp. 31–39, 2010.

[124] A. Tassaddiq, “Impact of Cattaneo-Christov heat flux model on MHD hybrid nano-micropolar fluid flow and heat transfer with viscous and Joule dissipation effects,” *Scientific Reports*, vol. 11, no. 1, pp. 1–14, 2021.

[125] J. P. Kumar, J. C. Umavathi, A. J. Chamkha, and I. Pop, “Fully-developed free-convective flow of micropolar and viscous fluids in a vertical channel,” *Applied Mathematical Modelling*, vol. 34, no. 5, pp. 1175–1186, 2010.

[126] S. Muhammad, S. I. A. Shah, G. Ali, M. Ishaq, S. A. Hussain, and H. Ullah, “Squeezing nanofluid flow between two parallel plates under the influence of MHD and thermal radiation,” *Asian Research Journal of Mathematics*, pp. 1–20, 2018.

[127] S. Salehi, A. Nori, K. Hosseinzadeh, and D. Ganji, “Hydrothermal analysis of MHD squeezing mixture fluid suspended by hybrid nanoparticles between two parallel plates,” *Case Studies in Thermal Engineering*, vol. 21, p. 100650, 2020.

[128] M. Sheikholeslami and D. Ganji, “Heat transfer of Cu-water nanofluid flow between parallel plates,” *Powder Technology*, vol. 235, pp. 873–879, 2013.

[129] G. Domairry and M. Hatami, “Squeezing Cu-water nanofluid flow analysis between parallel plates by DTM-Padé method,” *Journal of Molecular Liquids*, vol. 193, pp. 37–44, 2014.

[130] M. I. Khan, M. ur Rahman, S. A. Khan, T. Hayat, and M. I. Khan, “Evaluation of entropy generation in cubic autocatalytic unsteady squeezing flow of nanofluid between two parallel plates,” *Computer Methods and Programs in Biomedicine*, vol. 185, p. 105149, 2020.

[131] M. Sheikholeslami, D. Ganji, and H. Ashorynejad, “Investigation of squeezing unsteady nanofluid flow using ADM,” *Powder Technology*, vol. 239, pp. 259–265, 2013.

[132] M. Zubair, Z. Shah, S. Islam, W. Khan, and A. Dawar, “Study of three-dimensional Darcy–Forchheimer squeezing nanofluid flow with Cattaneo–Christov heat flux based on four different types of nanoparticles through entropy generation analysis,” *Advances in Mechanical Engineering*, vol. 11, no. 5, p. 1687814019851308, 2019.

[133] U. Khan, S. Ahmad, M. Ramzan, M. Suleman, D. Lu, S. Inam, *et al.*, "Numerical simulation of Darcy–Forchheimer 3D unsteady nanofluid flow comprising carbon nanotubes with Cattaneo–Christov heat flux and velocity and thermal slip conditions," *Processes*, vol. 7, no. 10, p. 687, 2019.

[134] M. Dhlamini, P. K. Kameswaran, P. Sibanda, S. Motsa, and H. Mondal, "Activation energy and binary chemical reaction effects in mixed convective nanofluid flow with convective boundary conditions," *Journal of Computational Design and Engineering*, vol. 6, no. 2, pp. 149–158, 2019.

[135] M. Ijaz Khan and F. Alzahrani, "Activation energy and binary chemical reaction effect in nonlinear thermal radiative stagnation point flow of Walter-B nanofluid: Numerical computations," *International Journal of Modern Physics*, vol. 34, no. 13, p. 2050132, 2020.

[136] M. Ijaz, M. Ayub, and H. Khan, "Entropy generation and activation energy mechanism in nonlinear radiative flow of Sisko nanofluid: Rotating disk," *Heliyon*, vol. 5, no. 6, p. e01863, 2019.

[137] M. Asma, W. Othman, and T. Muhammad, "Numerical study for Darcy–Forchheimer flow of nanofluid due to a rotating disk with binary chemical reaction and arrhenius activation energy," *Mathematics*, vol. 7, no. 10, p. 921, 2019.

[138] M. Alghamdi, "Significance of Arrhenius activation energy and binary chemical reaction in mixed convection flow of nanofluid due to a rotating disk," *Coatings*, vol. 10, no. 1, p. 86, 2020.

[139] K. Maleque *et al.*, "Effects of binary chemical reaction and activation energy on MHD boundary layer heat and mass transfer flow with viscous dissipation and heat generation/absorption," *International Scholarly Research Notices*, vol. 2013, 2013.

[140] M. Ramzan, N. Ullah, J. D. Chung, D. Lu, and U. Farooq, "Buoyancy effects on the radiative magneto micropolar nanofluid flow with double stratification, activation energy and binary chemical reaction," *Scientific Reports*, vol. 7, no. 1, pp. 1–15, 2017.

[141] S. Ahmad, K. M. Ijaz, A. K. M. Waleed, T. A. Khan, T. Hayat, and A. Alsaedi, "Impact of Arrhenius activation energy in visco-elastic nanomaterial flow subject to binary chemical reaction and non-linear mixed convection," *Thermal Science*, vol. 24, no. 2 Part B, pp. 1143–1155, 2020.

[142] A. Sciacovelli, V. Verda, and E. Sciubba, "Entropy generation analysis as a design too-A review," *Renewable and Sustainable Energy Reviews*, vol. 43, pp. 1167–1181, 2015.

[143] M. M. Rashidi, S. Mahmud, N. Freidoonimehr, and B. Rostami, "Analysis of entropy generation in an MHD flow over a rotating porous disk with variable physical properties," *International Journal of Exergy*, vol. 16, no. 4, pp. 481–503, 2015.

[144] M. Rashidi, S. Abelman, and N. F. Mehr, "Entropy generation in steady MHD flow due to a rotating porous disk in a nanofluid," *International Journal of Heat and Mass Transfer*, vol. 62, pp. 515–525, 2013.

[145] K. Hosseinzadeh, A. Mogharrebi, A. Asadi, M. Sheikhshahrokhdehkordi, S. Mousavisani, and D. Ganji, "Entropy generation analysis of mixture nanofluid $H_2O/C_2H_6O_2 - Fe_3O_4$ flow between two stretching rotating disks under the effect of MHD and nonlinear thermal radiation," *International Journal of Ambient Energy*, pp. 1–13, 2019.

[146] M. I. Khan, S. A. Khan, T. Hayat, M. F. Javed, and M. Waqas, "Entropy generation in radiative flow of Ree-Eyring fluid due to due rotating disks," *International Journal of Numerical Methods for Heat & Fluid Flow*, 2019.

[147] M. Nayak, S. Shaw, M. I. Khan, V. Pandey, and M. Nazeer, "Flow and thermal analysis on Darcy-Forchheimer flow of copper-water nanofluid due to a rotating disk: A static and dynamic approach," *Journal of Materials Research and Technology*, vol. 9, no. 4, pp. 7387–7408, 2020.